Multiple Pages Intentionally Left Blank

STRATIGRAPHY AND TECTONICS OF SOUTHEASTERN SERENITATIS

by

Theodore Allen Maxwell

A dissertation submitted to the faculty of the
University of Utah in partial fulfillment of the requirements
for the degree of

Doctor of Philosophy

in

Geology

Department of Geology and Geophysics

University of Utah

December 1976

STRATIGRAPHY AND TECTONICS OF SOUTHEASTERN SERENITATIS

by

Theodore Allen Maxwell

A dissertation submitted to the faculty of the
University of Utah in partial fulfillment of the requirements
for the degree of

Doctor of Philosophy

in

Geology

Department of Geology and Geophysics

University of Utah

December 1976

ABSTRACT

Results of investigations of returned Apollo 17 samples, and Apollo 15 and 17 photographs have provided a broad data base on which to interpret the southeastern Serenitatis region of the moon. Although many of the pre-Apollo 17 mission interpretations remain valid, detailed mapping of this region and correlation with earth-based and orbital remote-sensing data have resulted in a revision of the local mare stratigraphy.

Two major pre-Imbrian highland units ring the southern Serenitatis basin: steep, smooth-sloped massifs of the Taurus-Littrow region; and less rugged, hummocky terra (the sculptured hills). Both units have a high Al/Si ratio, appear red on color difference photographs, and are composed of anorthositic breccias. Both units apparently resulted from the impact that produced the southern Serenitatis basin. Light plains material has a lower visual albedo and Al/Si ratio than the hummocky highlands, but not as low as Imbrian mare material. The plains may have formed either by volcanism or by deposition of fine secondary ejecta from nearby highlands.

Mare materials of southeastern Serenitatis are characterized by a lower Al/Si ratio, blue appearance on color difference photographs (different shades), and higher radar reflectivity than the highlands. Imbrian mare materials are present as valley and basin fill. The oldest mare (3.8-3.9b.y.), the dark mantle of the Apollo 17 site, contains

abundant dark glassy spheres, and is composed of a very incoherent regolith. Younger (3.7-3.8 b.y.) Imbrian mare basalt occurs as a prominent dark annulus surrounding central Mare Serenitatis. Four mare units form the dark annulus; three Imbrian in age, and one Eratosthenian-to-Imbrian in age. Both orbital X-ray and Apollo Lunar Sounder data indicate that in the southeastern Serenitatis region, the total thickness of the dark annulus units is 600-800 m. As determined from Apollo orbital investigations, there is a progressive decrease in Ti content from the basin edges to the central mare. The youngest (Eratosthenian-Imbrian) dark annulus unit is lower in Ti than the Imbrian mare materials, and occurs as a discontinuous ring basinward of the Imbrian-age dark annulus. On the basis of crater age-dating of both this unit and the crater Eratosthenes, this material is most likely 3.2-3.3 b.y. old, approximately the same age as the central mare.

The orientation and morphology of small volcanic rilles is consistent with the hypothesis that early, high-Ti basaltic flooding occurred circumferential to the Serenitatis basin, and flowed basinward. Wrinkle ridges of the Taurus-Littrow area that formed after the initial basaltic flooding are divided into three types based on morphology: surficial folds and faults of thin basalt layers over deeper fractures, small extrusive flows, and probable flow fronts in the dark mantle material. Those in the younger, central mare may be related to deep fractures of the Serenitatis ring structure and a possible smaller impact in the pre-mare floor of the basin.

Analysis of the structural features of southeastern Serenitatis supports a revised ring structure for the basin with the Apollo 17 site

located on the third ring. However, the analogous rings of the Orientale basin are topographically higher than the southern Serenitatis basin rings, which indicates post basin-formation downdropping of the inner basin. Additional uplift of the massifs continued through the Imbrian Period, and was characterized by the massifs acting as rigid crustal blocks. The hummocky highlands near the crater Littrow were subject to more regional uplift than the massifs. The location of arcuate rilles only in the early Imbrian dark annulus units, and their absence in later mare materials indicates that downdropping of the central part of the basin was accomplished primarily in Imbrian time. The Eratosthenian-Imbrian mare was therefore deposited on a more rigid crust of older basalts.

Consequently, detailed mapping and analysis of age relations among the various mare units have shown that the geologic history of the southeastern Serenitatis region is more complex than a single impact basin model. The morphology and timing of structural relationships indicate that most of the highland features can be related to Serenitatis basin formation, while those of the mare resulted from post-basin adjustment of the lunar crust to later basalt emplacement and highland uplift.

"Page missing from available version"

CONTENTS

ILLUSTRATIONS

CHAPTER 1

INTRODUCTION

The Serenitatis basin is a multi-ringed, circular basin 680 km in diameter. It is located in the northeastern quadrant of the moon's near side. Previous geologic investigations have shown that the Serenitatis basin formed during a period of high impact flux at an early stage in the moon's development (Hartmann, 1972; Stuart-Alexander and Howard, 1970; Hartmann and Wood, 1971). As shown by Wilhelms and McCauley (1971), Imbrium basin rings and ejecta are superposed on the western part of Serenitatis, indicating a pre-Imbrian age for the Serenitatis basin-forming events.

The study area encompasses the southeastern part of the Serenitatis basin, including both the relatively smooth mare units and the more rugged massifs and highland materials (Fig. 1). Consequently, the area contains many structural features characteristic of lunar maria (rilles, arches and ridges) and of the highlands (rilles and basin-controlles lineaments). Local stratigraphy is dominated by both basin-related highlands and several units of basaltic mare material of different ages. A mare unit that locally embays the highlands is one of the darkest units on the moon's near side (Pohn and others, 1970). The Apollo 17 site in the Taurus-Littrow valley was thus chosen in order to sample both this dark mare unit and the nearby highlands.

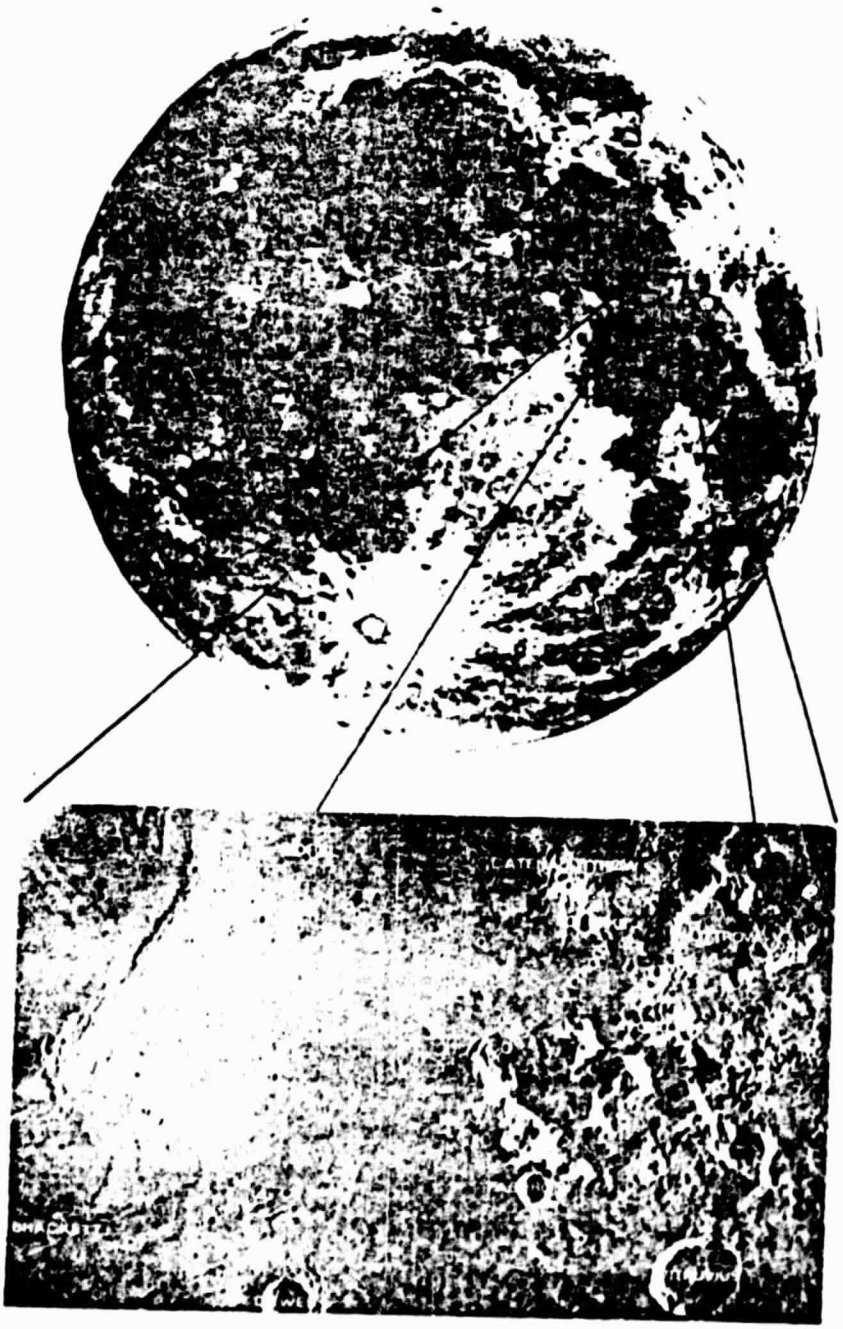

Figure 1. Earth-based photograph of full-moon from Kuiper and others (1967) showing area mapped. Mosaic below (Apollo 17 metric Fr. 0447 and 0450) indicates names of features discussed in text. Names used are consistent with those on NASA's 1:250,000 scale Lunar Topographic Orthophotomaps 42C1 through 42C4 (1974).

Throughout this report, the terms "central mare", "dark annulus" and "dark mantle" will be used informally to designate surface units of approximately the same age. It must be noted, however, that the dark annulus that is delineated by visual albedo is made up of geologic units spanning Imbrian through early Eratosthenian periods.

Southeastern Serenitatis is suitable for this detailed geologic study for the following reasons:

1) Pre-Apollo 17 photogeologic mapping resulted in a stratigraphic interpretation of mare units that is inconsistent with the results of Apollo 17 sample investigations.
2) The region is covered by metric an panoramic photographs at various sun elevations from both Apollo 15 and 17 missions (Appendix I).
3) The high quality Defense Mapping Agency's 1:250,000 scale Lunar Topographic Orthophotomaps provides a suitable base for geologic mapping of the area. Also, five large scale (1:10,000 and 1:50,000) Topophotomaps are available for features of special interest within the area.
4) Ground-truth control (both lithology and ages of samples from the Taurus-Littrow valley) is available for orbital geochemical and geophysical experiments.
5) A limited amount of subsurface information is available for the Taurus-Littrow valley and the mare in the southeastern part of the basin as a result of the Apollo Lunar Surface Experiments package (ALSEP) and the Apollo Lunar Sounder Experiment (ALSE).

6) Doppler line-of-sight gravity information has been compiled for the area, and is presently subject to various interpretations.

The intent of this study is to explain both stratigraphic and structural relationships in southeastern Serenitatis. The region allows the study of a sequence of basin formation and modification, basaltic volcanism, and deformation effects on this part of the lunar crust. As an aid to the interpretation of geological and geophysical results from Apollo missions 15 and 17, part of the study is designed to synthesize all pertinent earth-based and orbital data for the region.

Previous Work

Stratigraphy.

Numerous maps of early astronomers included portrayals of geologically significant features. In 1645, Anton de Rheita recognized the massifs that bound the southeastern edge of the Serenitatis basin. In the same year, Johannes Hevelius published a map (reproduced in Kopal and Carder, 1974; p. 12-15) in which the visual albedo of Serenitatis mare units can be distinguished.

Recent geologic mapping of the area began with the work of Carr (1966), who mapped Mare Serenitatis at a scale of 1:1,000,000 (Table 1). On the basis of visual observations and earth-based photographs, Carr (1966) divided the mare in southeastern Serenitatis into four units of Imbrian age (Im_1 - Im_4) defined by means of visual albedo. One additional unit, the dark mantle, was assigned an Eratosthenian age on the basis of its extremely low albedo. The highland massifs in the area were grouped as pre-Imbrian undifferentiated materials of unknown origin (Carr, 1966). Crater deposits were mapped in accordance with

TABLE 1. PREVIOUS MAPPING OF SOUTHEASTERN SERENITATIS

AUTHORS	DATE PUBLISHED	SCALE	COMMENTS
de Rheita	1645	——	Recognized Haemus and Taurus Mountains.
Hevelius	1645	——	Recognized albedo boundaries in mare units.
Carr	1966	1:1,000,000	Geologic map of LAC 42 area; mapped on the basis of visual observations and earth-based photographs; dark mantle interpreted as final stage filling of Serenitatis basin.
Scott and Pohn	1972	1:1,000,000	Geologic map of LAC 43 area; mapped on the basis of Lunar Orbiter and Apollo 15 photography. Stratigraphic interpretation similar to Scott and others (1972).
Carr	1972	——	Geologic sketch map on the basis of Apollo 15 photographs.
Scott, Lucchitta and Carr	1972	1:250,000 and 1:50,000	Pre-Apollo 17 geologic maps of lansite; dark mantle interpreted as possible Copernican-age pyroclastics.
Howard, Head and Muehlberger	1973	——	Geologic sketch map of southern Mare Serenitatis; revised stratigraphy based on Apollo 17 results.

principles proposed by Shoemaker and Hackman (1962). Scott and Pohn (1972) mapped the eastern portion of the study area, and recognized that the massifs were most likely the result of the Serenitatis impact. In that map, the dark mantle material was thought to be Imbrian in age.

With the designation of the Taurus-Littrow valley as the Apollo 17 landing site, two pre-mission geologic maps were prepared by the U. S. Geological Survey. The 1:250,000 map sheet of Scott and Carr (in Scott and others, 1972) shows two mare units of Imbrian and Eratosthenian ages, and an additional Imbrian unit of either mare or plains material. Terra materials were divided by the same authors into three major groups: massif and hilly terra material were thought to represent the ejecta deposits of large basins, especially the Serenitatis basin. Terra material that is morphologically intermediate between plains and hilly terra was interpreted as either ejecta, mass-wasted material or volcanics. The 1:50,000 map of Lucchitta (in Scott and others, 1972) generally followed the stratigraphy of the 1:250,000 map, except that the plains materials were further subdivided into two units.

On the basis of Apollo 17 returned samples (Muehlberger and others, 1973) and visual observations (El-Baz and Evans, 1973), Howard and others (1973) revised the stratigraphy of mare units in the southern Serenitatis basin. In their sketch map, the dark annulus material surrounding the Serenitatis basin was assigned an Imbrian age, and the lighter central mare fill was interpreted as Eratosthenian, on the basis of possible superposition relations with ejecta from the crater Plinius (Howard and others, 1973). Most recently, Wilhelms (writ-

ten communication, 1976) is mapping the central mare unit as Imbrian. However, crater age studies by Boyce and Dial (1973), Boyce and others (1974), Boyce (1975; 1976) and data obtained during the course of this study support an Eratosthenian-Imbrian age.

Structure.

As shown by Wilhelms and McCauley (1971), the second ring of the Serenitatis basin passes through the massifs just west of the Apollo 17 landing site (Fig. 2). Recently, Scott (1974) and Reed and Wolfe (1975) have revised the ring structure of Serenitatis in a manner consistent with both the gravity data and a theory of multiple impact origin (Fig. 2). According to Reed and Wolfe (1975), there are three rings of the southern Serenitatis basin in the study area. The first ring is represented by a circular wrinkle ridge system 400 km in diameter. The second is the extension of the arc of the Haemus Mountains using the center of a best-fit, surface-disc model for the Serenitatis mascon as the center of the ring (Wolfe and Reed, 1976). The Apollo 17 site, therefore, is located on the third ring of the southern Serenitatis basin. The similar morphology of the outer Rook Mountains (third ring of the Orientale basin) and the Taurus-Littrow massifs was additional support for the revised ring structure (Reed and Wolfe, 1975). The rest of this third ring in Serenitatis, however, is more subdued than the outer Rook Mountains, which may be a result of additional uplift of the Serenitatis rim after formation of the basin.

Photogeologic mapping of the Serenitatis basin suggests an origin by multiple impacts, as revealed by the irregular northern part of the basin (Carr, 1966; Scott, 1972). Recent reductions of low altitude gravity data have supported these interpretations (Scott, 1974). Also,

Figure 2. Low sun elevation earth-based photograph (from Kuiper and others, 1967) of southeastern Serenitatis showing location of best-fit surface disc model for the Serenitatis mascon (white; Phillips and others, 1972); ring structure as defined by Wilhelms and McCauley (1971; black); and revised ring structure (black and white; Reed and Wolfe, 1975).

mapping of the Serenitatis mare ridge systems has suggested the possibility of additional impacts on the basin floor (Maxwell and others, 1975). Consequently, the pre-mare basin floor and highland fractures must be more complex than in the case of the simple impact model of the Orientale basin.

Scott and others (1972) recognized that the major highland structrual patterns in the Taurus-Littrow area were part of both the lunar grid system (Strom, 1964) and reactivated fractures radial to both the Serenitatis and Imbrium basins. The high elevation of the Taurus-Littrow massifs (highest single mountains of the Serenitatis rim except for those adjacent to Imbrium) may be the result of relatively recent (post-mare) uplift (Scott and others, 1972).

Major post-basin structural features include highland lineaments, highland and mare rilles, and ridge systems in the mare. Head (1974a) classified the grabens (arcuate rilles) of the Taurus-Littrow area as belonging to two types; those related to pre-existing structural trends and those that are basin concentric. The northeast-trending grabens (Fossae Littrow) were interpreted as having been developed during and immediately following basin formation. Muehlberger (1974) recognized the same orientation of these grabens, but instead assigned them an age following the emplacement of the Taurus-Littrow basalts. Later grabens, recognized by both Head (1974a) and Muehlberger (1974) as being related to the downdropping of the inner Serenitatis basin, are most prominent in the dark annulus material northwest of Dawes and near the crater Clerke (Fig. 1).

Theories for the origin of mare ridges in the southeastern Serenitatis area are dominated by two main themes. Both a tectonic mode of

origin by compression and thrust faulting of near-surface materials (Howard and Muehlberger, 1973; Muehlberger, 1974) and an origin by lava intrusion and extrusion (Hodges, 1973) have been proposed. These hypotheses have been summarized by Mutch (1972, p. 196), Muehlberger (1974) and Maxwell and others (1975). It is possible that some of the ridge systems in Mare Serenitatis are localized by pre-mare impacts on the floor of the basin (Fig. 3). Scott and others (1975) recently completed a map of mare ridges on the lunar near side and concluded that both ridges and rilles have a common structural origin arising from tensile stresses. In that model, hydrostatic position and hence, elevation determined whether the fractures were intruded by lava (Scott and others, 1975). It is difficult to reconcile that mode of origin with both photogeology and topography of the southeastern Serenitatis area. Most recently, Lucchitta (1976) has studied the ridges in the Taurus-Littrow area and concluded that they are the surface expression of high angle faulting at depth.

Small-scale structural and volcanic features of the Taurus-Littrow area have been reported on extensively in the Apollo 17 Preliminary Science Report (1973). With the exception of Howard and others (1973), no attempt was made to correlate these features with the regional geology of southeastern Serenitatis. Consequently, since accurate timing of structural events is inevitably related to the relative ages of surface units, it is necessary to accurately define the stratigraphy in order to understand the tectonic episodes.

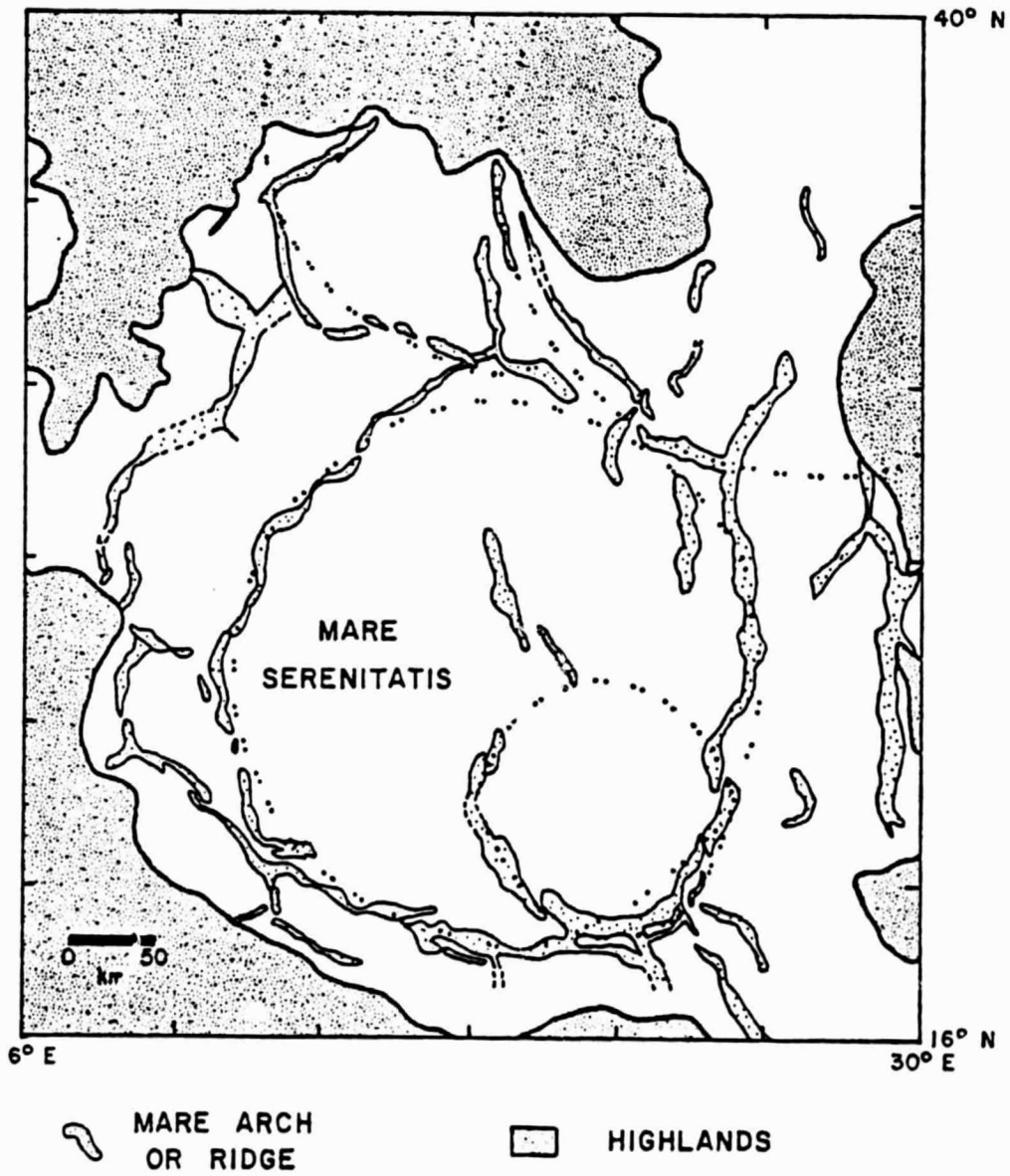

Figure 3. Distribution of major ridge systems in Mare Serenitatis (modified from Maxwell and others, 1975).

CHAPTER 2

REMOTE SENSING DATA

Spectral Reflectance

Recent measurements of lunar spectral reflectivity (McCord and others, 1976) from 0.3 to 1.1 μm have improved on earlier measurements of only a few wavelengths (Soderblom, 1970) by providing better resolution (about 20 km) for surface units. In a crystalline material certain regions of the optical spectrum are absorbed preferentially depending on the energy levels of the orbiting electrons that are affected by a photon (McCord and Adams, 1973). The location of these absorption bands can therefore be used to characterize the chemistry of the material on the surface. The addition of glasses and agglutinates in the lunar soil complicates this simplified model, however, and masks the true chemical composition of the soil (Pieters and McCord, 1975). Assuming that the amount of these two constituents is relatively constant throughout the mare regolith, the spectral reflectivity can be normalized to provide estimates of the TiO_2 content (Charette and others, 1976). The results of FeO composition are still preliminary, however, and data have not yet been reported for Mare Serenitatis.

Southeastern Serenitatis and the Serenitatis-Tranquillitatis boundary have been the targets of many spectral determinations. One area in Mare Serenitatis (MS-2) is the standard reference for observations of other areas on the lunar surface (McCord and others, 1972; McCord

and Adams, 1973; Pieters and others, 1974). For this reason, there have been many attempts at correlating spectral reflectance with other remote sensing studies and stratigraphic units (Howard and others, 1973), resulting in a variety of named surface types.

Spectral reflectance data in southeastern Serenitatis are consistent with observations made on color difference photographs (Whitaker, 1972a). Pieters and others (1973) show that the dark mantle material of the Apollo 17 site has only a small absorption near 0.95μm, which is consistent with the high glass content of the soil found at the site (LSPET, 1973). In addition, the gradual slope of the reflectance curve (from 0.38 to 1.1μm) supports a relatively blue color, which is indicative of high Ti and Fe. Data for the central mare and dark annulus are provided by Johnson and others (1975). Dark annulus materials are also blue (unit TQB of Johnson and others, 1975), and are inferred to have a TiO_2 content of 7-8%. The central mare, however, has low TiO_2 (2-3%; based on normalization procedures of Charette and others, 1974), but may also have a higher rock to glass ratio than materials of the dark annulus.

Color Difference Photographs

Using earth-based, full-moon photographs taken with two different color filters (UV and IR), the albedo differences of the lunar surface are suppressed, and the resulting composite print enhances relative color differences in the lunar maria (Whitaker, 1966; 1972a). The correlation of color difference photographs with mare surfaces of different ages has been successfully used to define the extent of the relatively young (Eratosthenian) lava flows in Mare Imbrium (Schaber, 1973a; Whitaker, 1972b).

As observed on high sun elevation photographs of southeastern Serenitatis, the color difference photograph of the area primarily helps to define the contact between the Tranquillitatis "blue" basalts of the dark annulus, and the Serenitatis "red" basalts of the central mare (Fig. 4). The cause of the different colors (as in the case of spectral reflectance) can be related to differing amounts of iron and titanium in the regolith; the higher the Ti and Fe, the bluer the unit (Whitaker, 1972a).

There are three major contributions of the color composite photographs to the identification and interpretation of mare units in southeastern Serenitatis. 1) The blue mare of the dark annulus extends farther north than the contact visible on low sun elevation photographs. 2) To the west of Dawes, an arc of reddish material about 5-8 km wide extends to the north. Full-moon photographs also indicate a higher visual albedo in the same area. 3) One of the younger dark annulus units (Im_2, Plate 1; and 28° E, 20°N, Fig. 4) is slightly less blue than the surrounding Imbrian-age mare.

X-Ray Fluorescence

The Apollo 15 X-ray fluorescence (XRF) experiment was operated on several revolutions that overflew part of southeastern Mare Serenitatis (Adler and others, 1972). Using trend-surface analysis, Podwysocki and others (1974) have shown that residuals from the trend surface correlate with specific geologic features (Podwysocki and others, 1974). The data have more recently been used in comparison with albedo measurements, color-difference photographs and spectral information in order to explain the relatively high Al/Si values near

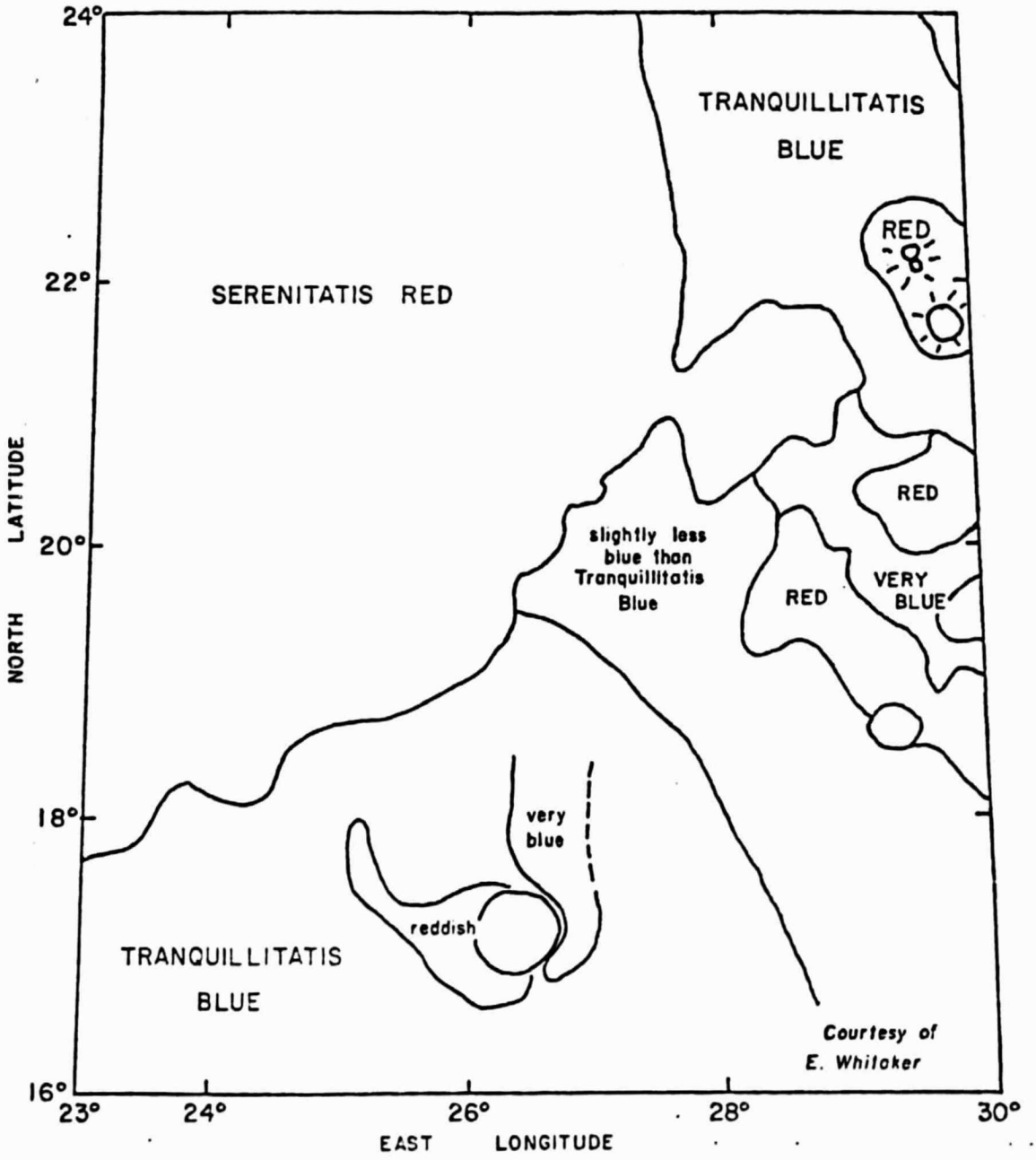

Figure 4. Sketch map of mare colors from UV-IR color composite. Data courtesy of E. Whitaker (see also Whitaker, 1972a).

Catena Littrow (Andre and others, 1975). Although Mg/Si data are also available from the experiment, values are subject to large variations on different orbits, and at present, results are not generally correlable with small surface features (Podwysocki and others, 1974).

In southeastern Serenitatis, there are several Al/Si trend-surface anomalies that aid in both structural and stratigraphic interpretations (Areas 4 through 10, Fig. 2, in Podwysocki and others, 1974). The background intensity value for mare in this region averages about 0.68, corresponding to an Al/Si concentration ratio of about 0.28; somewhat higher than Apollo 11 high K rocks (0.23) and lower than Apollo 15 soil (0.33; Adler and others, 1973). Average intensity ratios for the highlands in this region range from 0.80 near the edge of the mare, to about 1.00 northeast of Littrow. These values alone would suggest a composition intermediate between Apollo 15 soils and anorthositic gabbro. However, since most of the signal was returned from areas 38 km in diameter (Andre and others, 1975), values in the Taurus-Littrow area are most likely the result of a combination of highland and mare units.

Al/Si data show negative residual values on either side of the crater Plinius (0.62-0.65 intensity ratios), and a higher positive value for the crater itself, thus suggesting that the crater has excavated highland type material (Podwysocki and others, 1974). This interpretation is supported by color composite photographs that show a reddish color surrounding the crater (Whitaker, 1972a).

The eastern portion of the inner-ring ridge system (Fig. 3) also has a relatively high Al/Si intensity value associated with it (0.87). Podwysocki and others (1974) interpret this anomaly as indicating two

different types of mare basalt, possibly the result of a later differentiation product enriched in Al forming the ridge. However, full-moon photographs indicate that there is a slightly subdued ray that is coincident with the ridge in this area. It is more likely, therefore, that the Al/Si data, with an effective depth of only 10μm (Andre and others, 1975) indicates the small amount of highland material that forms the ray.

The Al/Si values of highland areas near the crater Littrow and east of Vitruvius show positive residuals with intensity values of 1.12 and 1.02. The similarity of these positive values with those of the Haemus Mountains (0.99) was used by Podwysocki and others (1974) to suggest that a thin amount of Imbrium ejecta is present in the Taurus-Littrow highlands. The corresponding concentration ratios (0.44-0.49; Adler and others, 1973) are too low for compositions of anorthositic gabbros (about 0.63). However, they may represent a mixture of anorthositic breccias from the upper part of North Massif (sample 76230; Al/Si conc. ratio = 0.606; LSPET, 1973) and noritic breccias from South Massif (sample 72215; Al/Si conc. ratio = 0.36; LSPET, 1973). Since no distinct suite of Apollo 17 samples has yet been found to correlate with Imbrium impact ages (Reed and Wolfe, 1975), it is more likely that the similar Al/Si values represent similar rock types formed by the same process, but excavated by different impacts.

Andre and others (1975) have shown that there is no major geochemical difference between Al/Si measurements of the "central mare" (east of 28°E) and intensity ratios of the dark mantle units. Instead, concentration ratios over the Taurus-Littrow area were higher than

those predicted by measured basalt samples. This was attributed to the possible contribution of highland material to the site (Andre and others, 1975). According to color difference photographs and geologic mapping of the area (Plate 1), the color boundary between the central mare (Eim) and the dark annulus (Eimb) is at about 28°E in this area. Consequently, the geochemical boundary reflecting the lower Ti basalts of the central mare region has not yet been defined by the XRF experiment.

In the vicinity of Catena Littrow, the high Al/Si value associated with the bright ejecta has been used as evidence that the craters have excavated highlands-type material (Andre and others, 1975). If this is the case, then it places a maximum thickness of about 0.5 km for the dark annulus materials in this area. As will be shown, this supports the interpretation of data obtained by the Lunar Sounder Experiment.

Gamma-Ray Spectrometry

The Apollo 15 and 16 gamma ray experiment has been used primarily to show net lunar radioactivity and therefore concentrations of U, Th and K in the overflown lunar materials (Trombka and others, 1973, Plate II, Proc. Fourth Lunar Science Conf.). Maps of the net lunar radioactivity show that the western half of Mare Serenitatis is slightly higher in radioactivity than the eastern half. This is most likely due to the proximity of the Imbrium basin (and hence KREEP basalts), however, no major anomalies in radioactivity are apparent in the southeastern Serenitatis area. Recently, the data have been normalized to allow comparisons of the concentrations of Fe, Mg, Ti, Th and K (Metzger and others, 1974; Reedy and others, 1975). Two regions of the Apollo 15 orbital coverage; from 6° to 21°E in Mare Tranquillitatis have been studied. However,

normalization procedures to Apollo 11 soil samples make preliminary observations of Ti flux in Serenitatis and Tranquillitatis difficult to interpret (Reedy and others, 1975).

In Mare Serenitatis, the relative flux values have been calculated for the dark annulus and central mare (Reedy and others, 1975). These data indicate that Fe, Th and K are relatively higher in dark annulus materials, whereas Mg is slightly lower. Although the data have not yet been converted to elemental concentrations, the higher value for Fe in the dark annulus materials is consistent with other orbital observations that suggest a slightly more mafic composition. High values of Th and K may be related to the area of observation (just north of the Haemus Mountains), which is closer to an anorthositic (highland) region.

Ultraviolet Spectrometry

Variations in the far UV albedo of the moon as measured by the UV spectrometer on Apollo 17 can be related to the relative refractive index of the surface at 1200-1650 Å wavelength (Fastie and others, 1973). The field of view of the spectrometer (a square roughly 30 km on a side) allows gross comparisons of highlands and maria (Lucke and others, 1974), however, more refined resolution has not yet been reported. In southeastern Serenitatis, the central mare has a relatively high UV reflectance; the dark annulus and areas of northern Tranquillitatis are intermediate, and the highlands are low (Plate 9, Proc. Fifth Lunar Science Conf.). These values are the opposite of optical albedo, but are consistent with the general trend of the UV data for high reflectivity of the maria and low for the highlands.

A small area north of Plinius shows a lower UV albedo than the surrounding mare, which may be additional evidence that Plinius has excavated highland materials. The relatively high UV albedo south and east of Dawes, however, is more difficult to interpret. Sensitivity of these data to only a very thin surface layer, possibly only a grain coating (Lucke and others, 1974), obviates any clear correlation with rock type.

Earth-based Radar

Reflections of 3.8 and 70 cm earth-based radar have been measured in both polarized and depolarized modes and provide information on blockiness and relative roughness of near-surface materials (Thompson and others, 1974). As shown by Burns (1969) and Thompson (1974), the difference in reflectivity between polarized and depolarized reflections can be explained by the relative proportion of quasi-specular versus diffuse returns, although there is some controversy over the mechanism of depolarization (Pieters and others, 1973). Since quasi-specular returns are the result of wavelength-size facets facing the radar on the surface and in the near surface, the polarized returns can be used to estimate relative blockiness (assuming a relatively constant Ke). Similarly, the depolarized echo can be used to measure the sub-wavelength size roughness of the surface materials (Thompson, 1974).

The correlation of 3.8 and 70 cm radar with mare types defined by color difference photographs supports the contention that the surface types are discrete lithologic units more than a few meters in thickness (Thompson and others, 1973). However, the enhanced radar return associated with ray material, particularly a NE-trending patch south of

Dawes (Fig. 5) suggests that the reflectivity may be influenced more by surface roughness than subsurface factors. In southeastern Serenitatis, dark mantling material has the lowest polarized and depolarized reflection at both 3.8 and 70 cm wavelength. On this basis, Pieters and others (1973) accurately predicted a smooth, relatively rock-free surface for the Apollo 17 site. Dark annulus materials also show a relatively low radar backscatter north of Plinius, but elsewhere are obscured by the brighter reflection of Dawes ejecta. The central mare is a stronger 3.8 cm reflector than the annulus, and faint traces of the inner-ring ridge system are enhanced relative to the smoother mare (Fig. 5). The correlation of radar enhancement and the ridge system does not hold throughout the basin, and is also not apparent on the 70 cm radar. As shown by visual albedo and Al/Si data, the enhancement of the southeastern part of the ridge system is most likely due to a ray that is coincident with the ridge. Highlands units are the strongest reflectors at both 3.8 and 70 cm, but the massifs in the Taurus-Littrow area are no different than less rugged units.

Radar reflectivity of mare units shows a gross correlation with the age of the surface in this area; the older the mare, the fewer centimeter and meter size blocks on the surface and the lower the reflectance. However, this generalization does not hold for cratered areas and highlands. The chronology of individual craters may be deduced from reflectivity (Thompson and others, 1974), but the influence of ejecta blankets, rays and mantling materials make detailed correlation with mare surfaces in the study area uncertain.

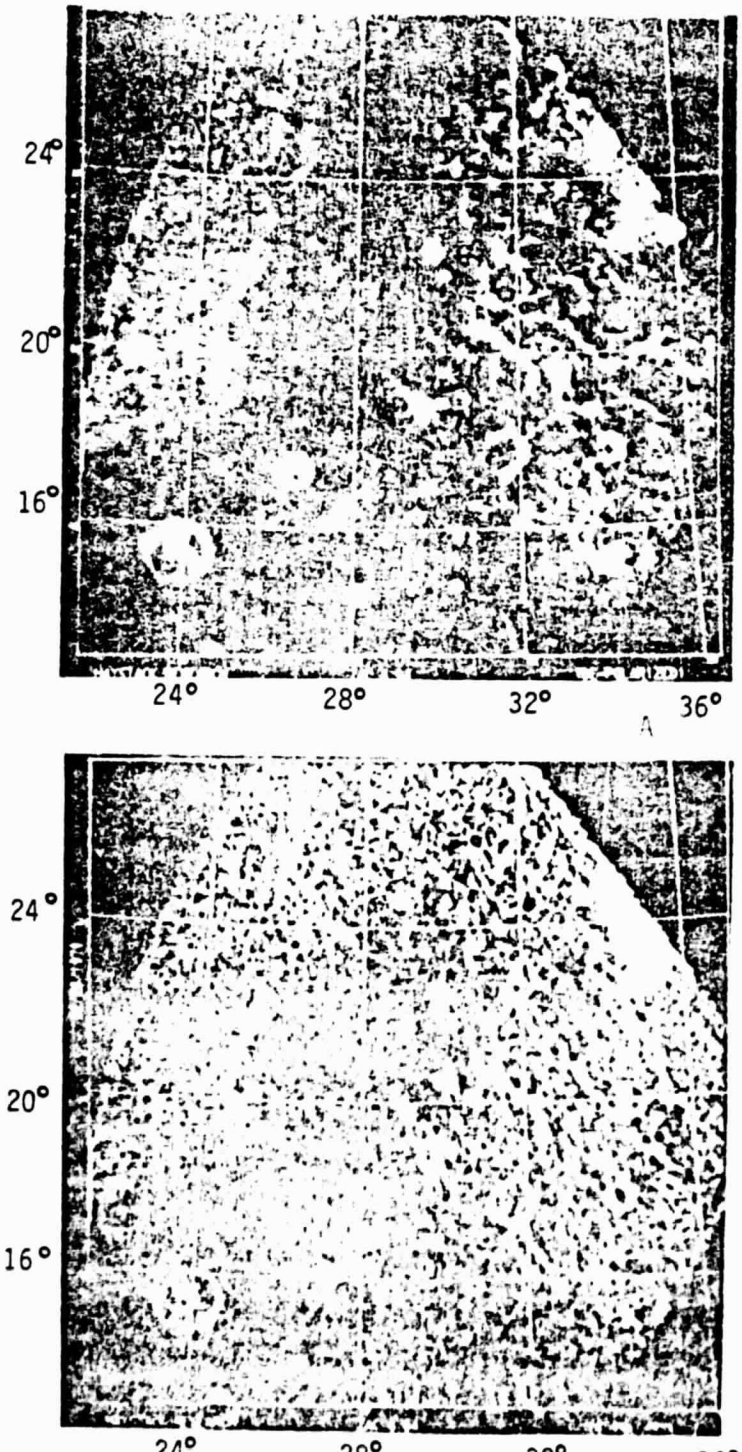

Figure 5. 3.8 cm radar images of southeastern Mare Serenitatis. A) Depolarized image indicates topography and surface roughness smaller than 3.8 cm. B) Ratio of depolarized/polarized data, which removes effects of topography (from Zisk, 1970).

Apollo Lunar Sounder

The Apollo Lunar Sounder Experiment (ALSE) flown on Apollo 17 was a coherent synthetic aperature radar system designed to probe the subsurface of the moon and detect variations in electrical properties of surficial materials (Brown, 1972; Phillips and others, 1973; Porcello and others, 1974). Of the three frequencies used in the system, the 5 MHz (HF_1) and 150 MHz (VHF) have provided data that are useful for geologic interpretation of southeastern Serenitatis. Because the Apollo 17 groundtracks were constrained by the landing site, revolutions 16 through 18 (HF_1) and 25 to 26 (VHF) have the same groundtracks at approximately 20° N latitude in the area of study.

VHF.

The VHF imagery is best suited for topographic profiling, and enlarged prints of the imagery correlate well with data obtained from the Apollo 17 laser altimeter. However, the effect of surface scattering in highland regions restricts the effective use of ALSE topographic profiling to mare and plains regions. At the southeastern edge of Serenitatis, elevations of plains and mare units can be measured from the imagery, but profiles of Mons Argaeus are hindered by the lack of a distinct nadir return (Fig. 6).

One of the unique characteristics of this part of Serenitatis is the lack of an elevated shelf region at the edge of the mare such as the one in Mare Crisium and western Mare Serenitatis (Ward and others, 1973). According to studies of ALSE topography by Kobrick (1976), the

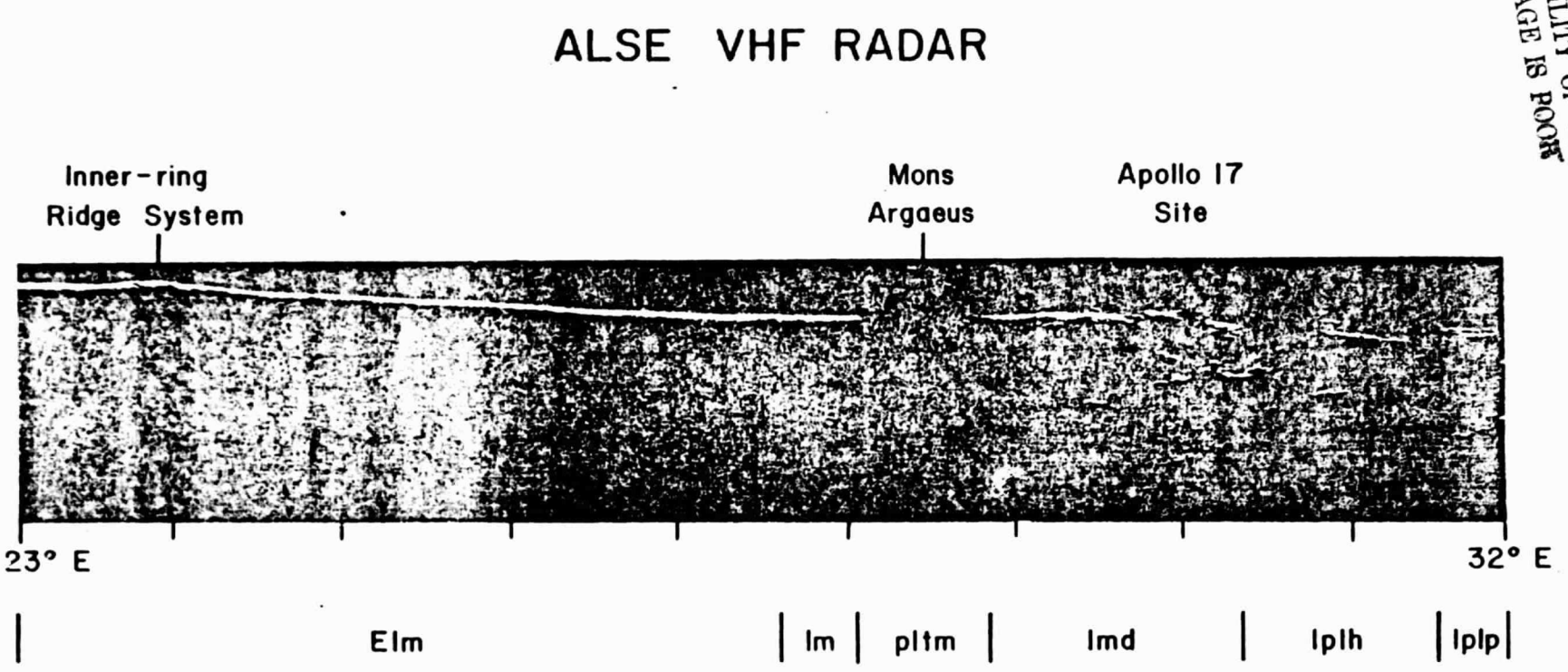

Figure 6. ALSE VHF radar imagery of southeastern Mare Serenitatis region along 20°N Latitude. Topographic profile correlates well with laser altimeter data. Note decrease of echo strength over highlands, particularly Mons Argaeus.

outer 50-100 km of Maria Serenitatis and Crisium are raised about 500 m above the general mare level. This generalization does not hold true for southeastern Serenitatis (Fig. 6), however, where there are more complex stratigraphic and structural relations. The topographic "doming" of the centers of Serenitatis and Crisium mentioned by Kobrick (1976) is really the returns from mare arches and ridges in the centers of both basins.

The reflection coefficient for VHF radar is primarily a function of the dielectric constant of the surface, while the specular flash will also be affected by surface roughness characteristics at 2 m wavelength. It is these two factors that enable the distinction of geologic units by radar. In mare regions, no qualitative correlation was found between ALSE radar "albedo" and visual albedo, however, there is a distinction between mare and plains materials (Fig. 6). In general, plains units on the VHF imagery have a lower radar albedo than do mare units. This is most likely due to both a lower dielectric constant for the plains-forming materials (lower Ti and Fe than mare basalts) and a rougher surface resulting in a greater scatter of the energy.

Although the VHF mode of the Lunar Sounder was also designed for shallow (less than 100 m) subsurface sounding, no reflections from the subsurface have been defined from either the imagery or the holography. The lack of recognition of subsurface returns is attributable to several causes: 1) There is extreme surface clutter at 2 m wavelength that effectively masks any possible returns. 2) The shallow subsurface may not have sufficient dielectric contrast to return the signal. Since the dielectric constant is primarily dependent on density and rock type (Peeples and others, 1976), lack of an abrupt density contrast

in the upper 100 m will prohibit reflection. Studies of both the near-surface electrical properties (Olhoeft and Strangway, 1975) and seismic velocities (Cooper and others, 1974) support a gradual increase in density and dielectric constant with depth. 3) If a possible interface did exist, it is likely that the surface would be rough, resulting in sporadic reflections that would be difficult to recognize against the background surface imagery. 4) Finally, signal weighting procedures were such that any layering in the first 10 m would be included in the specular flash.

HF_1.

The lowest frequency used on the Lunar Sounder has produced topographic profiles (Brown and others, 1974) which have been related to the moon's center of figure, but these profiles are not of value to the present study because of the limited resolution (wavelength = 60 m). However, sounding data (May and others, 1976) and the specular power monitor (SPM) data (Killpack, 1975) are useful for studies of southeastern Serenitatis.

During the mission, averaged returned power was transmitted to earth for real-time observations of the data (Phillips and others, 1973). The specular power monitor data are capable of distinguishing highlands and mare units on a gross scale, but only generalized observations can be made (Fig. 7). The data show a relative decrease in power over dominantly highland regions and a higher power level over the maria. As is the case with the VHF data, variations in surface roughness on the scale of the wavelength and topography are the major factors contributing to the returned power (T. Killpack, oral communication, 1976).

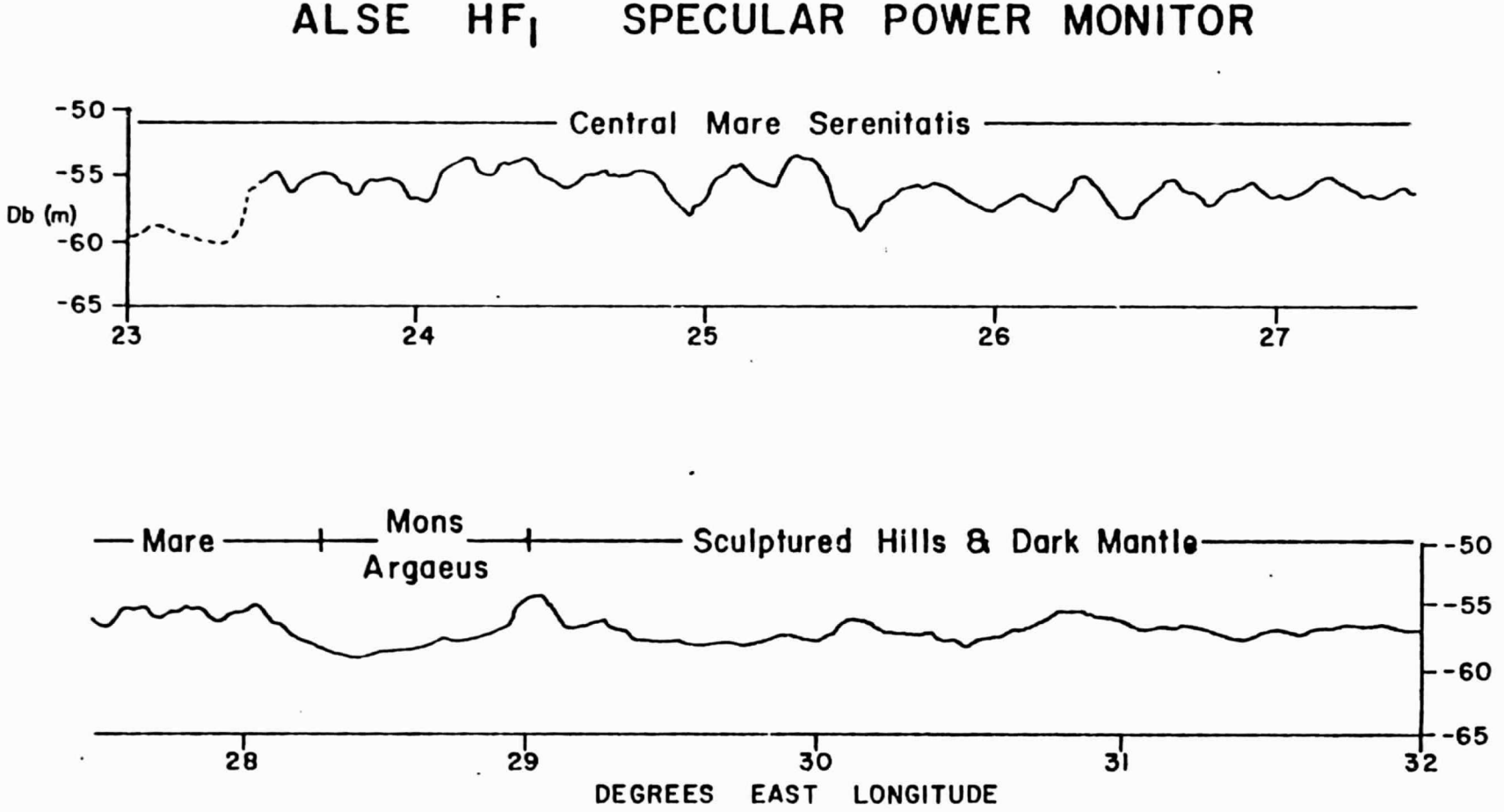

Figure 7. Specular power monitor data from ALSE HF_1 on rev. 17. Loss of returned power in highland regions is primarily due to extreme surface scattering. Power levels of the 60 m wavelength radar do, however, distinguish between dominantly highlands versus mare regions.

Two subsurface reflectors have been detected in southern Mare Serenitatis from the HF_1 data at average depths of 900 and 1600 m. The shallowest reflector dips toward the center of the basin at both the eastern and western margins of the central mare fill. In the eastern part of the basin, the linear projection of the shallowest reflector to the lunar surface coincides with the contact between the dark annulus and the lighter mare of the central part of the basin (Fig. 8). In the western part of the basin, the projection of the first reflector coincides with the concentric ridge system within the mare. It is difficult to map the exact contact of the dark annulus with the lighter mare in this area, but the projection is only slightly west of the contact as drawn by Howard and others (1973). The shallowest reflector is thus interpreted as an interface between the dark annulus material (Im_1) and the younger, lighter mare fill (EIm). Unfortunately, details of this interface beneath the wrinkle ridges are not resolvable because of the great amount of surface clutter from the ridges (Peeples and others, 1976)

As a test of the interpretation, profiles of the present surface topography were constructed from Lunar Topographic Orthophotomaps 42C3 and 42C4. Extending the topographic slope of the adjacent dark annulus northward into the basin, it was found that the dark annulus should be at a depth of 900 m. The depth of the shallowest reflector detected by ALSE was calculated to be 850 m in the same area.

In southeastern Mare Serenitatis, the first reflector forms a trough between the concentric ridge system and the edge of the basin. The topography from LTOs 42C2 and 42C3 shows a depression in the present mare surface that coincides with this subsurface trough (Fig. 9).

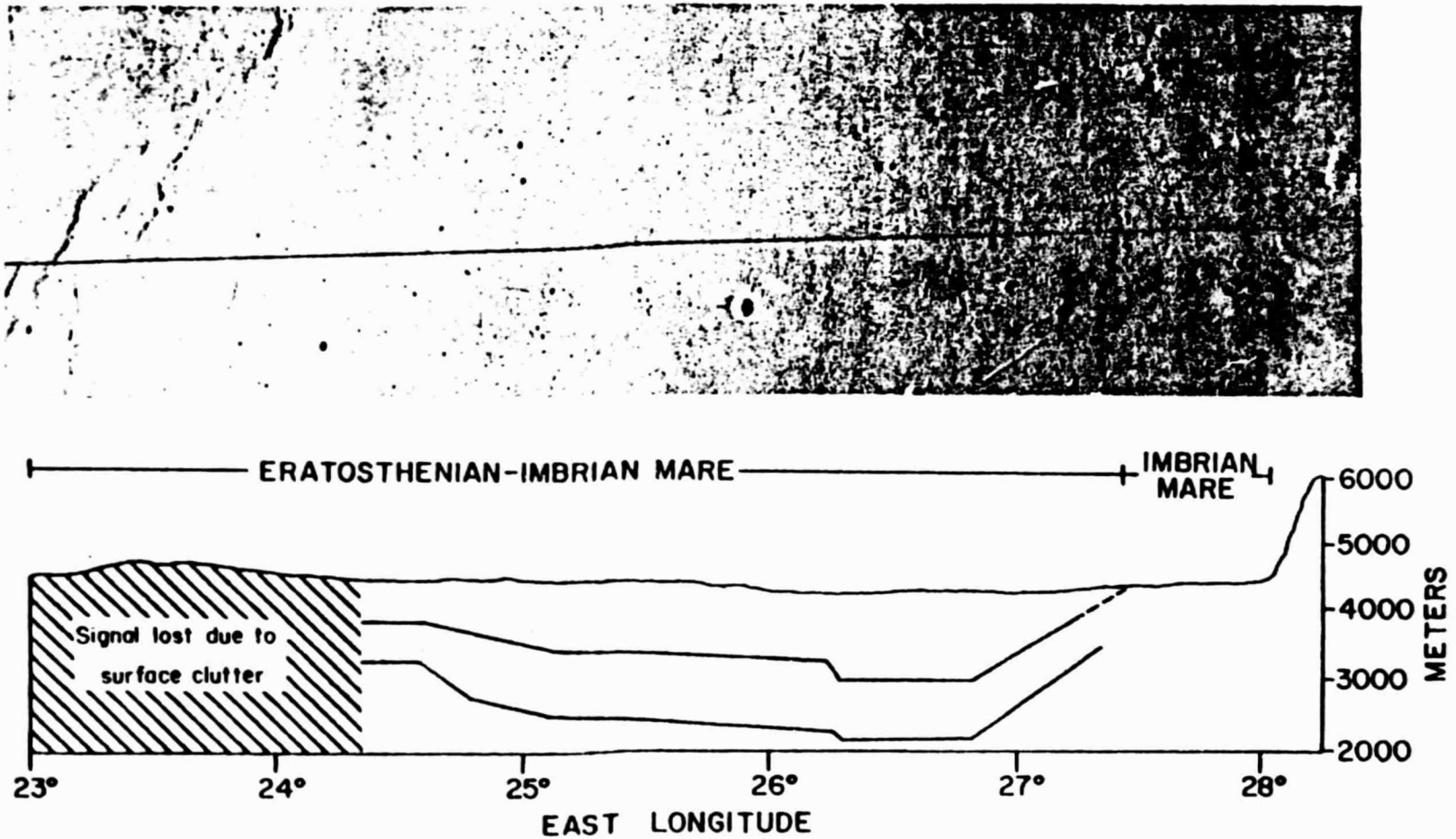

Figure 8. Subsurface reflections detected holographically from ALSE HF_1 data. Trough between 26° and 27°E corresponds with lowest present-day mare surface elevation (Fig. 9). Ground track shown above is on Apollo 17 metric Fr. 1222.

Figure 9. Topography of present-day mare surface compiled from Lunar Topographic Orthophotomaps 42C2 and 42C3. Lowest area of the mare corresponds to trough seen by ALSE HF_1 sounding. Line A-A' is cross-section shown in Figure 8. Elevations are in kms relative to a 1730 km mean lunar radius.

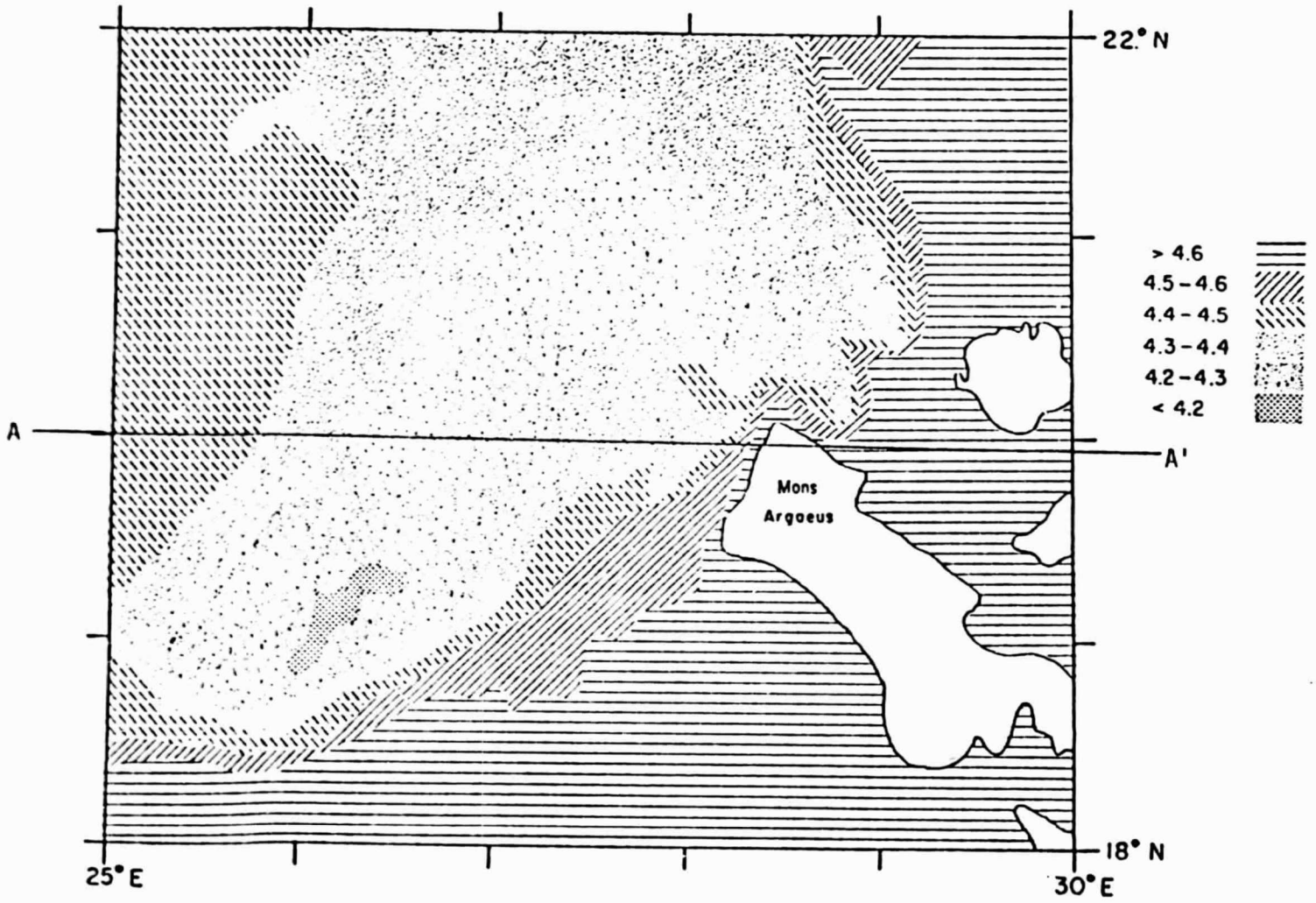
22° N
18° N
25° E
30° E
A
A'
Mons
Argaeus
> 4.6
4.5 - 4.6
4.4 - 4.5
4.3 - 4.4
4.2 - 4.3
< 4.2

The second reflector is more difficult to interpret because its eastern margin does not project to any distinct topographic or geologic feature.

There are two possibilities for a density contrast that would produce a sufficient dielectric contrast to be visible to the HF_1 radar. While a layer of regolith may satisfy the first reflector seen in this region, either a regolith layer, or a layer of relatively low density pyroclastics could be responsible for the second reflector.

Regolith layer. A thick layer of regolith has been postulated to lie beneath the thick mare basin volcanic fill (Hartmann, 1973; Short and Forman, 1972). However, it should be emphasized that if the subsurface reflectors are discrete low density layers, they need be only a few meters thick (Peeples and others, 1976).

The correlation of the first reflector in Mare Serenitatis with the dark annulus at the eastern margin of the basin suggests that the contact between the darker annulus material continues across the basin as postulated by Howard and others (1973). Apparently, the cratering on the annulus material was sufficient to produce a regolith visible at radar wavelengths before it was covered by younger mare units. Using the same argument, the second reflector may be another regolith layer within the Imbrian (dark annulus) material. The thickness of the second layer (700 m) correlates well with DeHon's (1976) estimate of mare thickness on the eastern edge of Mare Serenitatis (about 550 m). In addition, Andre and others (1975) suggest a maximum of 550 m for mare material on the shelf region of Serenitatis near the crater Clerke.

Pyroclastics. The dark material at the Apollo 17 site has been interpreted by many workers as consisting totally or partially of pyroclastics (Carr, 1966; Scott and others, 1972; El-Baz, 1972; Heiken and others, 1974; Lucchitta and Schmitt, 1974); and it has been proposed recently that the pyroclastic material is really a dark stratigraphic layer at the base of the regolith. The unit has been incorporated into the regolith by repeated cratering (Lucchitta and Sanchez, 1975). It is possible that even without a significant regolith above the dark unit, the second reflector might consist solely of a relatively low density layer of pyroclastic material.

Lucchitta (1975a) suggested that the orange and black glass spheres found at Shorty crater near the Apollo 17 site are concentrated deposits of the dark mantle unit. Since similar orange material has been noted at the southwestern edge of Mare Serenitatis (El-Baz and Evans, 1973; Lucchitta and Schmitt, 1974), it is likely that this unit continues across the basin beneath the more recent mare basalts.

Consequently, the first reflector is herein interpreted as the contact between the central mare fill (EIm) and dark annulus materials (Im_1). The second reflector is most likely a regolith layer between the dark annulus and deeper basalts, with a possible contribution by low density pyroclastics. Lunar Sounder data thus indicate a thickness of about 800 m for the central mare, and 600 to 800 m for the dark annulus materials.

Gravity

Doppler tracking of Lunar Orbiter satellites, the Apollo 15 CSM and subsatellite, and the Apollo 17 CSM have provided repeated measurements of the magnitude and geometry of the Serenitatis mascon (Muller and Sjogren, 1968; Sjogren and others, 1972; 1973). Repeated orbits of Apollo's 15 and 17 at different latitudes over the Serenitatis basin indicate that the anomaly is greater than 200 milligals in the central part of the basin (Sjogren and others, 1973). Although the boundaries of the basin are delineated by the gravity data, line-of-sight geometrical effects inhibit exact correspondence of the mascon boundaries with surface features. By using both the high altitude Lunar Orbiter data and lower altitude data from Apollo 15 subsatellites, however, it is possible to define the surface extent of the anomalies.

The surface disc model of Sjogren and others (1972) has a radius of 245 km, coinciding fairly well with a 200 km radius of the inner-ring ridge system (Maxwell and others, 1975). Later analysis, however, has decreased this radius to 221 km (Sjogren and others, 1974), and has shown that there is an irregularity in the mascon resulting in a gravity saddle at 27.5°N in the center of the basin. Scott (1974) used this data in support of a double basin model for the pre-mare floor of Serenitatis. According to his arguments, two mascons are required to explain variations in the gravity data.

Details of the edges of the Serenitatis mascon, particularly in the southeastern part of the basin are dependent on whether one uses

higher altitude Lunar Orbiter and CSM data, or the Apollo 15 subsatellite data. Both Apollo 15 and 17 show a slight shoulder at the eastern edge of the Serenitatis gravity anomaly (Sjogren and others, 1973, Figure 14-3). In addition, the data from both Apollo 17 revolution 5 (20°N) and Apollo 15 revolution 4 (27°N) show a peak anomaly at 200-240 milligals in the central part of the basin. Predictions of the Apollo 17 data based on the best-fit model from Apollo 15 had indicated that the basin would become shallower to the south. However, the data have shown that the anomaly remains relatively constant (Sjogren and others, 1973). On the basis of these characteristics, it is now probable that the Serenitatis mascon is a relatively thin (less than 5 km) surface disc that is influenced by irregularities in the subsurface structure (May and others, 1976).

Head (1974) found that the mass of basalt filling in the Orientale basin would not satisfy the gravity data, and invoked a model of early mantle rebound for isostatic adjustment of the impact crater such as that proposed by Wise and Yates (1970). Analysis of high and low altitude gravity data for Serenitatis support this model and further suggest that the later filling of basalt was supported as a superisostatic load. Dating of subsurface layers derived from ALSE data (May and others, 1976) puts additional constraints on early basin formation, which will be discussed in Chapter 5.

The existence of negative gravity rings surrounding major mascon basins has been subject to various interpretations. It is possible that these features are mass deficiencies as a result of extrusion of mare filling lavas from the periphery of the basin (Arkani-Hamed, 1974a). Depending on the reference altitude and the wavelength of the gravity

anomaly, however, the negative values may be an artifact of the gravity reduction (R. J. Phillips; oral communication, 1975). Bowin and others (1975) have suggested a model that accounts for the central mascon. In that model, the negative rings were assumed to be the expression of a thicker crust, and were not included. According to them, the negative anomalies do not completely encircle the Serenitatis basin. Instead, the minimum values follow the third ring of the basin (second ring of Wilhelms and McCauley, 1971), but then deviate into Tranquillitatis south of the crater Vitruvius. The arc of these minimum values coincides with the highest albedo faces on the massifs (Fig. 10). If these values really indicate negative anomalies, then it is most likely that the massifs of the Taurus-Littrow area have been isostatically aided in uplift following the initial basin-forming event.

Independent support for isostatic rebound of the massifs and surrounding terrain comes from two sources. 1) According to the Traverse Gravimeter Experiment on Apollo 17, the massifs are the sites of negative Bouguer anomalies relative to the rest of the landing site. 2) Topography of the dark mantle material near the Apollo 17 site and light plains unit north of the site both show an eastern dip of the surface (east of the arc of the massifs) of about 1.5°. If it is assumed that these units were deposited horizontally in Imbrian time (less doubtful for the mare than the plains), then the topographic slope suggests a regional differential uplift of at least 200-300 m along the arc. Since the dark mantle post-dates the formation of the Imbrium basin, this mechanism of uplift is independent of seismic effects of that impact as proposed by Scott and others (1972).

A

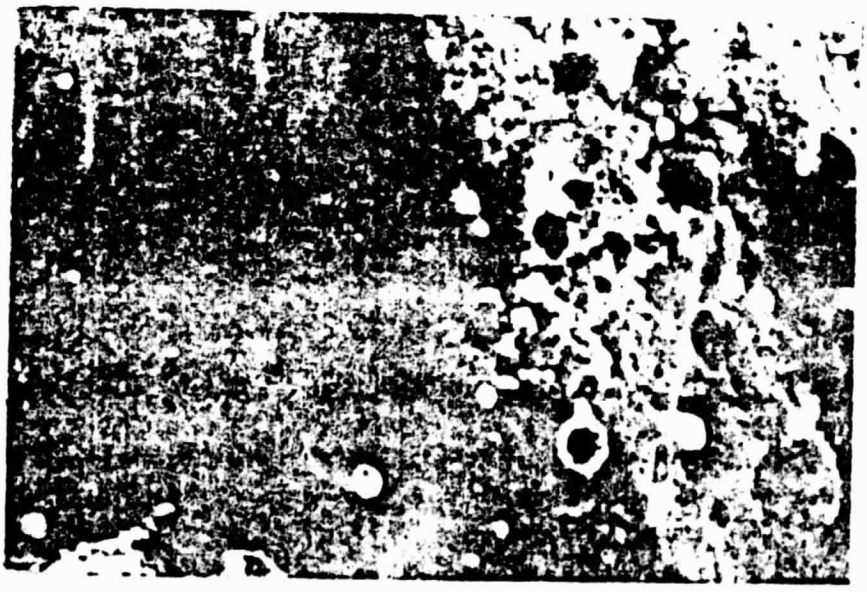

B

Figure 10. A) Location of free-air gravity maxima (pluses) and minima (dashes) from Apollo 15 CSM data (from Bowin and others, 1975). B) High sun photograph of southeastern Serenitatis from Kuiper and others (1967). Note correspondence of gravity minima with bright areas on massifs.

CHAPTER 3

SYNTHESIS: REMOTE SENSING AND STRATIGRAPHY

Highland Materials

Both highland massifs (pItm) and hummocky highland materials (IpIh) are spectrally red and have a distinctly higher Al/Si ratio than mare materials. However, Apollo 15 X-ray data at present only distinguish mare and highland terrain, and do not differentiate among the highland units. Radar albedo at 3.8 cm is much higher for highlands than maria, which is more likely the result of near-surface blockiness rather than the minor change in dielectric constant between basalt and anorthosite (Olhoeft and Strangway, 1975). Consequently, the most useful information on lithologic type and mode of formation of highland units comes from returned samples. Two major highland units were sampled on the Apollo 17 mission, the massifs (pItm) at stations 2 and 6, and the lower slopes of the sculptured hills (IpIh) at station 8 (Lunar Photomap 43D1S2; NASA, 1975).

Massifs.

Two of the steep-sloped, large (20-30 km diameter) mountains in the Taurus-Littrow area were sampled on Apollo 17. Both the North and South Massifs are composed of coarse, fragmental boulders and fine regolith. Indistinct clumps and possible layering have been noted for blue-gray and greenish-gray rocks (Reed and Wolfe, 1975). Returned samples indicate a noritic to anorthositic breccia composition of mas-

sif rocks (LSPET, 1973). The lack of a distinct chemical difference between rocks of the North and South Massifs suggests that both were formed from a single parent material (Reed and Wolfe, 1975). Both the structural orientation of the massifs and the majority of dated highland samples indicate that they were formed as a result of the impact that produced the southern Serenitatis basin. The lunar-wide occurrence of massif-type highland units at the second rings of multi-ringed basins is additional support that the massifs were formed from thick layers of Serenitatis basin ejecta. The morphologic evidence of Head (1974a) and the present study suggests that younger basin ejecta (e.g. Imbrium) if present, constitutes only a minor component. On the basis of petrologic information, Simonds (1975) has interpreted a station 6 boulder as formed within a 14 m thick melt sheet of Serenitatis ejecta.

Radiometric dating of Apollo 17 highland samples is by no means consistent with a single event resetting the isotopic clocks. On the basis of age dating of anorthositic rock fragments, breccias, and matrix material, the Serenitatis basin excavation event has been dated at 3.95-4.1 b.y. (Nyquist and others, 1974; Kirsten and others, 1973; Kirsten and Horn, 1974; Hinthorne and Conrad, 1976); older than 4.25 b.y. (Schaeffer and Husain, 1974); and as old as 4.45 b.y. (Nunes and others, 1974). Dating of unshocked clasts within the breccias however, may yield ages unrelated to the Serenitatis impact event, which may not have completely degassed the radiogenic Ar or Sr. Most recently, Jessberger and others (1976) have interpreted South Massif sample 73215 as a breccia deposited by a single event. Although ages of clasts within the breccia range from 4.1 to 4.3 b.y., basin excavation (from the matrix) is suggested to be 4.05 b.y from Pb and Rb loss

(Jessberger and others, 1976). An age of 4.05 b.y. is consistent with most Rb/Sr dating, and extends the hypothesis of the "lunar cataclysmic" bombardment by 50 m.y. (Tera and others, 1974a;1974b).

Consequently, the massifs in the Littrow area are interpreted as having been initially formed of thick layers of Serenitatis anorthositic ejecta, and elevated as a result of both inward collapse of the basin (Stuart-Alexander and Howard, 1970) and later uplift as massive structural blocks.

Hilly and Smooth Terra.

Although spectrally similar to massif materials, the hilly and smooth terra materials are morphologically quite distinct. These units (IpIhs and IpIh) are composed of low, hummocky hills 2-5 km in diameter, and intervening patches of smooth, intermediate albedo material that appears to blanket and subdue local topography. A distinct "corn-on-the-cob" texture is displayed by the hilly unit (IpIh) that includes the sculptured hills near the Apollo 17 site. Locally, the material is subdued by the dark mantle (Imd) material.

Returned samples from Apollo 17 station 8 were described as friable feldspathic breccias (Muehlberger and others, 1973), and are less coherent than breccias of the massifs. Lithologically, the prevailing rock type is anorthositic gabbro, and soil samples from the North Massif and sculptured hills have a higher anorthosite content than those from the South Massif (Rhodes and others, 1974). On the basis of the smallest blocky-rimmed craters, the regolith thickness of the sculptured hills was estimated to be about 10 m (Muehlberger and others, 1973) although this value may be a minimum depth since the unit is partially covered by dark mantle material. The low slopes and smoother

areas between the hills indicate that considerable mass wastage has taken place, and soil samples taken from station 8 are a mixture of highland breccias and abundant mare basalts (Bence and others, 1974). Dating of the highland components indicates no significantly different age from the massifs.

Hilly and smooth terra materials are therefore interpreted to be less coherent ejecta deposits dominantly from the southern Serenitatis and possibly the Tranquillitatis impacts. The ejecta was not deposited as discrete cooling units, and it was later mixed with local highland ejecta and mare materials to form the present smooth-sloped morphology. Unlike the massifs, the material did not act as crustal blocks during immediate post-basin tectonic deformation.

Plains Materials

Smooth, highly cratered plains (unit IpIp) occur as valley fill between more rugged terra materials, and as floor-fill in pre-Imbrian craters (particularly Littrow). The unit is intermediate in earth-based 3.8 cm radar reflectance, and is slightly less red than the highlands in color difference photographs. As in the case of the hilly terra material, plains units are too small to allow definition on the basis of Al/Si data, where there is no apparent difference between plains and neighboring highlands. Orbital geochemical data in the Taurus-Littrow area, however, were not obtained directly over the crater Littrow, so additional inferences cannot be made. Oberbeck and others (1975) have correlated lunar-wide smooth plains units and orbital geochemical data and found that the Al/Si and Mg/Si ratios of plains units in different areas show more similarities to neighboring high-

land units than to each other. Plains units near the crater Littrow are locally subdued and blanketed by dark mantle material, further masking their chemical characteristics.

The origin of smooth, or Cayley-type plains has been reviewed extensively by Howard and others (1974) and diverse origins ranging from locally derived secondary ejecta to primary basin ejecta have been proposed. Results of both geochemical experiments and small impact modeling studies by Oberbeck and others (1975) and Oberbeck (1975) favor a secondary ejecta origin for smooth plains units. This mode of formation is consistent with the morphology of plains in the southeastern Serenitatis area. Units in Littrow and surrounding areas are more highly cratered than mare materials, thus suggesting an older age than the mare materials. The plains units do not contain any of the small-scale volcanic or structural features that are characteristic of mare units. However, Imbrium ejecta may form a significant component of the plains materials in this area (Short and Forman, 1972; McGetchin and others, 1973), and therefore, the unit has been assigned an Imbrian to pre-Imbrian age.

Mare Materials

Relative Ages.

Where superposition relationships are not available to deduce relative ages of mare units, three general methods of dating based on crater density and morphology may be used. 1) Assuming a known flux rate of impacts on the lunar surface, the absolute crater frequency will be proportional to the age of the surface (Shoemaker and Hackman, 1962; Shoemaker and others, 1962). 2) Considering the morpholo-

gically oldest superposed crater on a mare surface, a sequence of basin flooding has been deduced by Pohn and Offield (1970). 3) Using the method of Soderblom (1970) for mare units of more local extent has also proved valuable for geologic mapping. This method involves the determination of the maximum diameter of craters that have been eroded such that the interior slope angles are less than the sun angle. The maximum crater diameters are converted to an equivalent diameter (D_L) of a crater eroded to an interior slope of one degree by the net accumulated flux. Values of D_L are therefore proportional to the total number of craters accumulated on the lunar surface (Soderblom and Lebofsky, 1972).

Recently, this last method has been modified slightly so that craters that are half-shadowed for a given sun angle may be used to estimate D_L values (Boyce and Dial, 1975). Although the method has the advantage that it does not necessitate finding a size boundary between unshadowed and shadowed craters, it does require a sufficient population of larger craters (200 m - 2 km) to find the necessary size range. For the present study, photographs were of sufficient scale and sun elevation to allow the use of the D_L method to determine relative ages for mare units.

Methods. Visual estimates of the D_L range were made on a 1° X 1° grid (approximately 750 km^2) from Apollo 17 panoramic frames 2311 to 2329, with sun elevation angles varying from 10° to 16°. In cases where pan frames overlapped within the same degree of longitude, craters were measured from both frames and the results averaged. Since this method requires a large enough sample of shadowed craters (greater

than 10) to be present, no less than 5 (and usually 10) of the largest unshadowed and smallest shadowed craters were measured, and their diameters averaged (see Soderblom and Lebofsky, 1972, for a more detailed explanation of the method).

As a check on the results, detailed crater size frequency information was gathered for four areas in southeastern Serenitatis using a Zeiss TGZ 3 Particle Size Analyzer as described by Greeley and Gault (1970). Three of the areas (Im(d), Im(f) and Im(c)) are within dark annulus units Im_1 and Im_2 (Appendix 2), and the fourth counting area is in the central mare (EIm; Fig. 11). Using Apollo 17 rectified 2X prints as a base, all shadowed craters were counted first, and then all unshadowed craters. The Particle Size Analyzer was operated in the logarithmic mode to give detailed information on craters less than 300 m in diameter. In addition, since the age of the mare in the central part of Serenitatis has been interpreted as both Imbrian and Eratosthenian, crater size-frequency data were gathered for the hummocky and radial ejecta blanket of the crater Eratosthenes. Because the areas of the different units counted ranges from 70 to 2100 km^2, it is also possible to compare the effect of counting area on D_L estimates.

Results. Visual D_L estimates for southeastern Serenitatis are summarized in Figures 12 and 13. The average values of D_L found for the central mare (230 m), dark annulus (300 m) and dark mantle (380 m) are in agreement with previous studies on a more regional basis (Boyce and Dial, 1973; Boyce and others, 1974). They also support the revised stratigraphic interpretation of the area by Howard and others,

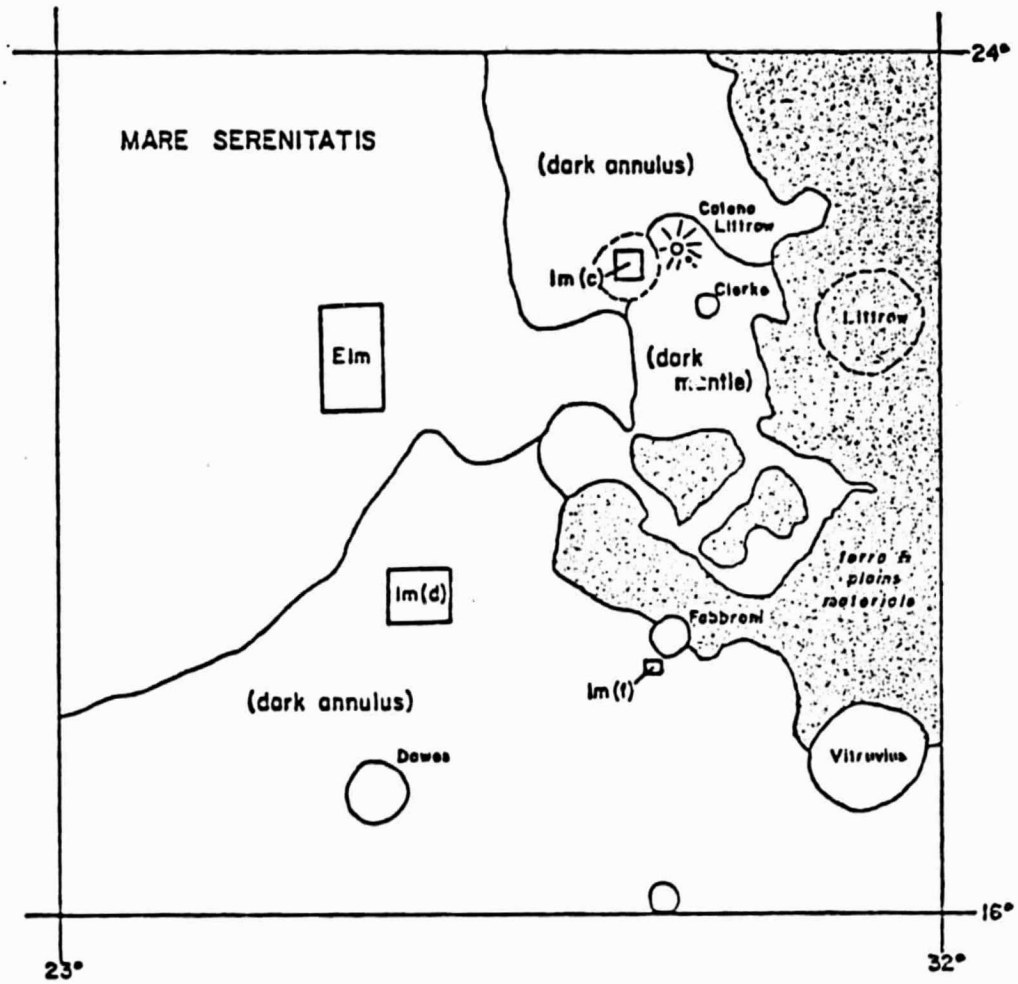

Figure 11. Sketch map of southeastern Mare Serenitatis showing areas studied for detailed crater size-frequency distributions. Three areas (Im(c), Im(f) and Im(d)) are in dark annulus materials, and one area (Elm) is in the central mare.

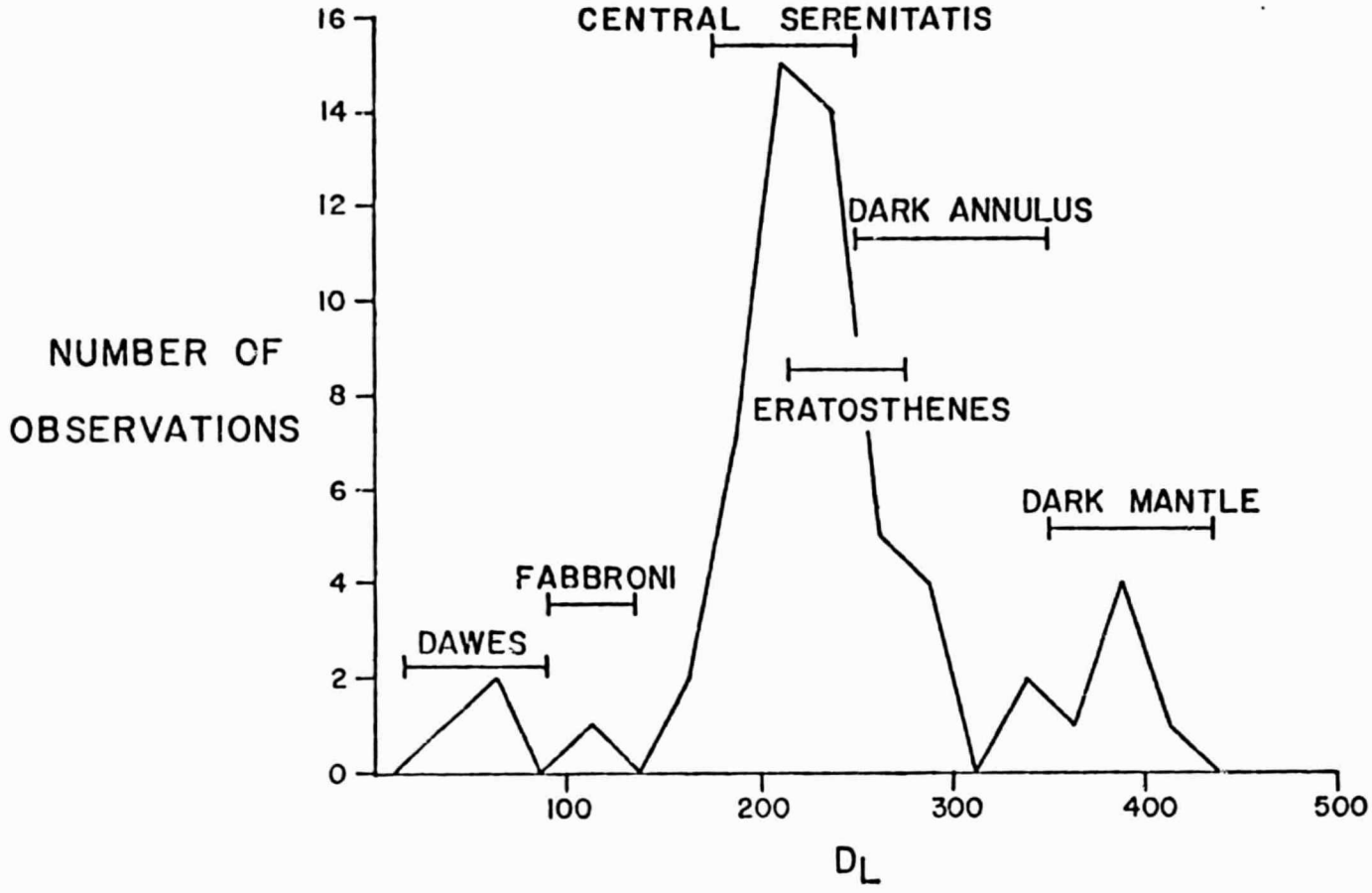

Figure 12. Histogram of D_L values of mare units in study area; each value estimated from an area of 750 km^2.

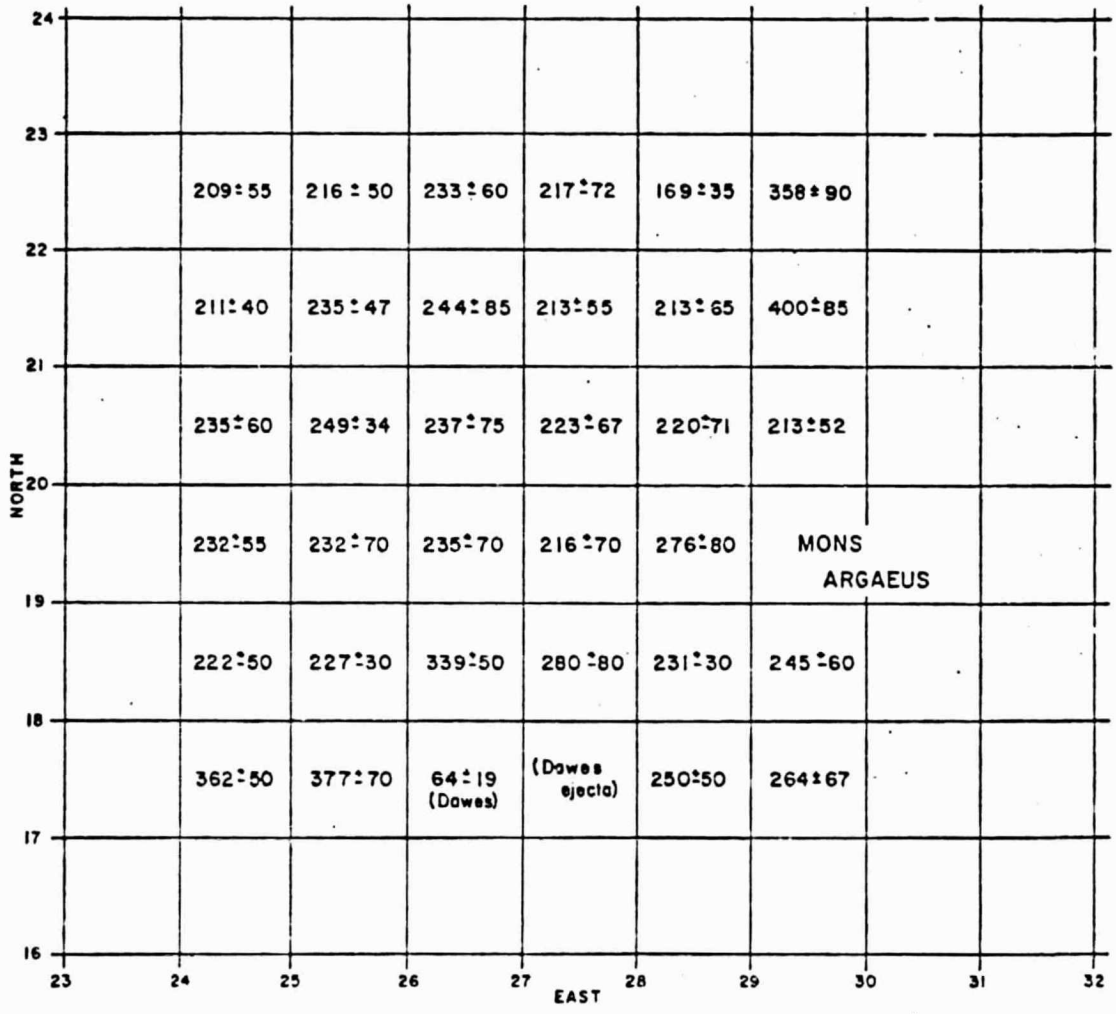

Figure 13. D_L values for southeastern Serenitatis; data from Apollo 17 panoramic photographs 2311-2330 (sun elevation varies from 10° to 16°).

(1973). Material of the dark annulus is intermediate in age between the central mare and the dark mantle. In addition, visual estimates of D_L for the crater Eratosthenes summarized in Figure 12 indicate that the central mare is approximately equal to or slightly younger than the crater Eratosthenes.

By defining the size-frequency distribution for shadowed and unshadowed craters on the same unit, it is possible to more accurately define the D_L value of the unit. For the floor, rim and radial ejecta of Eratosthenes, the distributions are shown in Figures 14 and 15. Because of the possibility of using pre-Eratosthenian unshadowed craters that were covered by ejecta (hence yielding an anomalously large D_L value and older age), the 98% level on the cumulative curve was chosen for an upper limit. D_L values for Eratosthenes range from 200 to 280 m and average 245 m.

Similar plots for the central mare (EIm) and the dark annulus north of Dawes (Im(d)) are consistent with D_L estimates based on visual observations (Fig. 16). The area for which these distributions were defined is greater than 200 km^2, which therefore probably represents a valid size distribution for the estimation of D_L. Two other counts on the dark annulus, however, come from areas less than 100 km^2 (Fig. 17). As predicted by Soderblom and Lebofsky (1972), the small counting area resulted in underestimates of the size distribution of shadowed craters and therefore of D_L. This effect can be demonstrated by plotting cumulative percent unshadowed craters against D_L (to negate sun elevation effects) as shown in Figure 18. The smallest areas counted (Im(c) and Im(f)) have the smallest size distributions, and there is a trend towards increasing crater size with area counted.

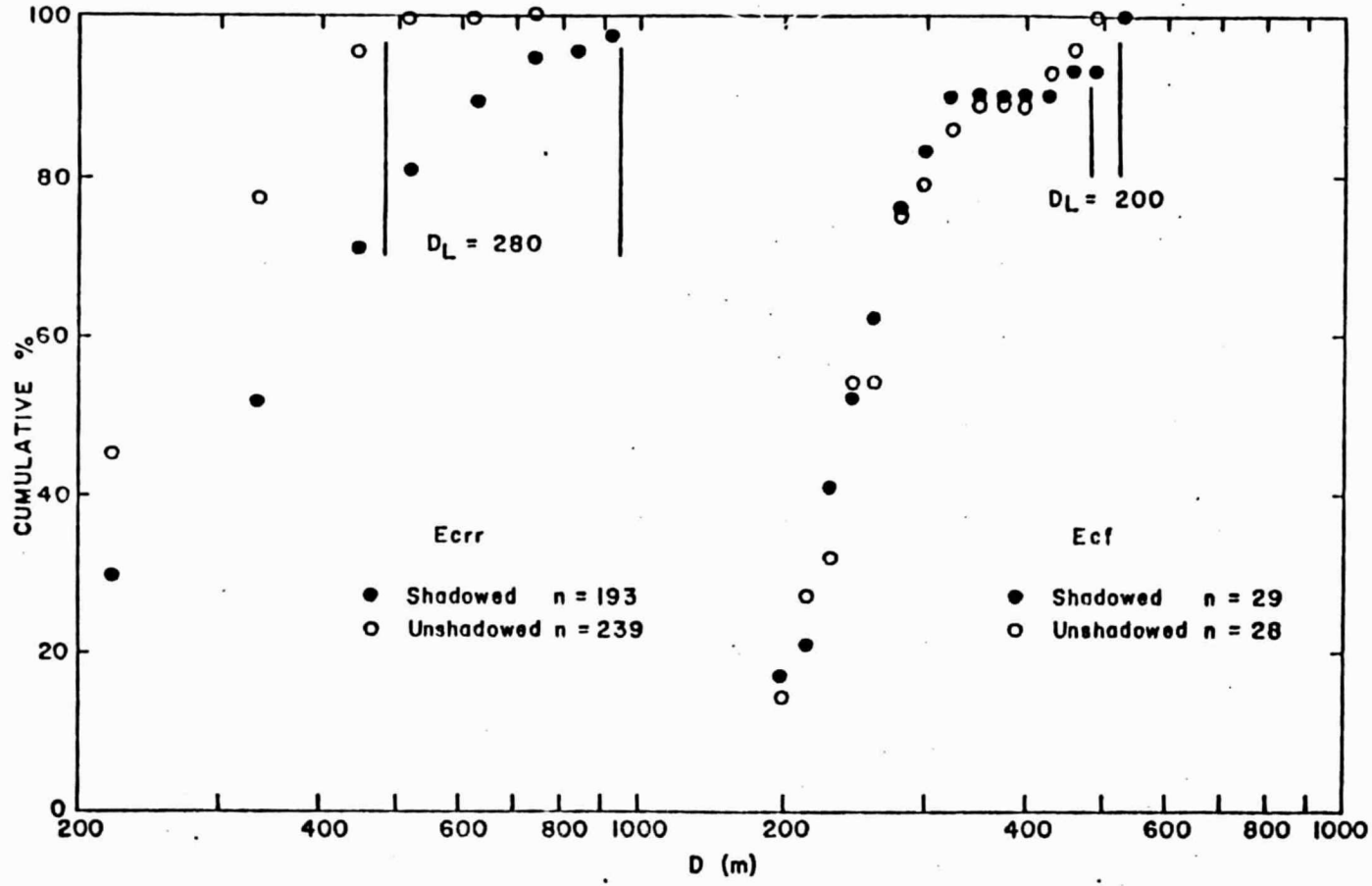

Figure 14. Cumulative crater-frequency diagrams for shadowed and unshadowed craters on radial ejecta (Ecrr) and floor (Ecf) of Eratosthenes. Craters were counted on Lunar Orbiter V Fr. 135M.

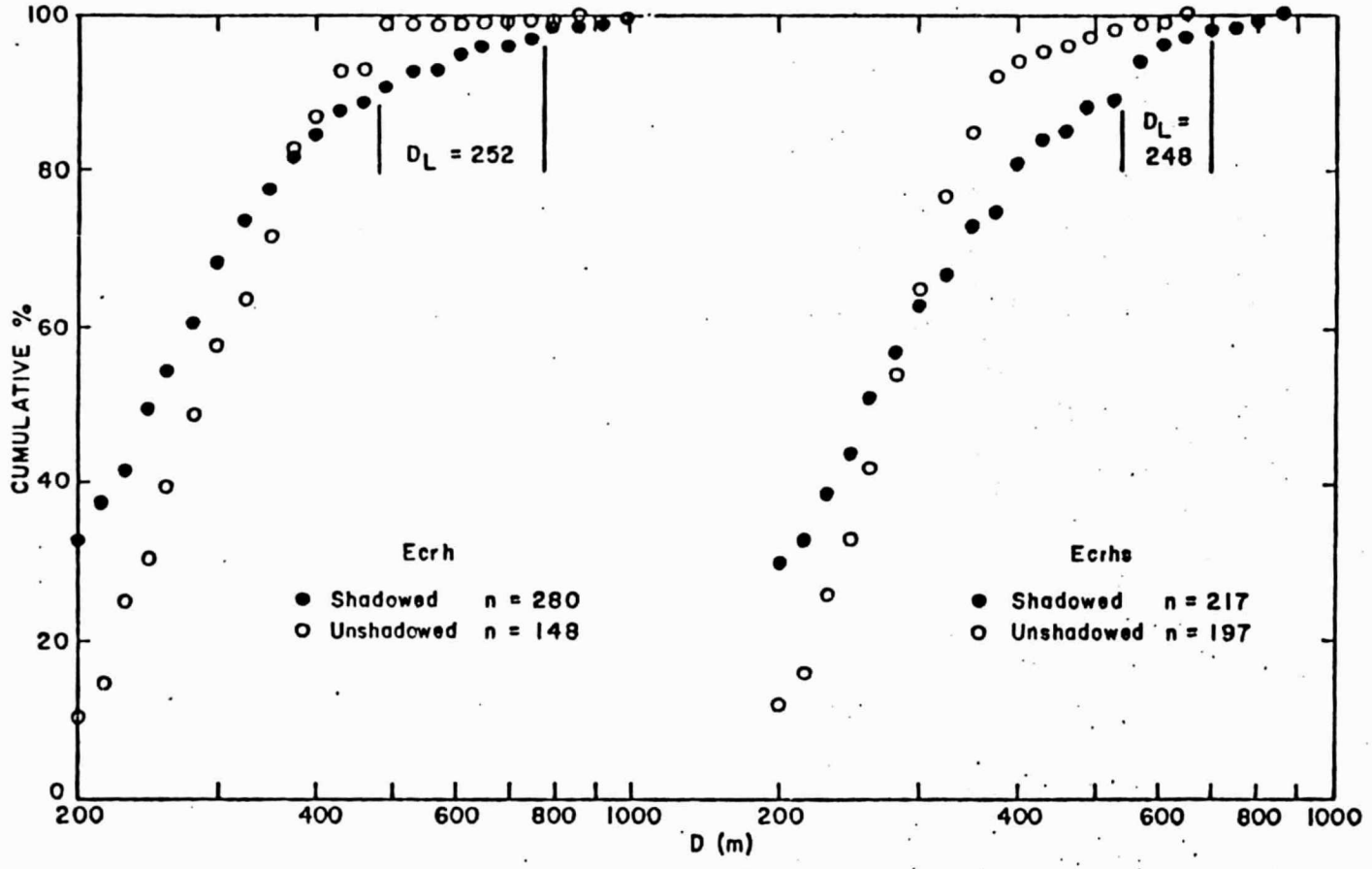

Figure 15. Cumulative crater-frequency diagrams for shadowed and unshadowed craters on hummocky ejecta east (Ecrh) and south (Ecrhs) of Eratosthenes. On Ecrhs, Copernicus secondaries and rays were excluded from counting area

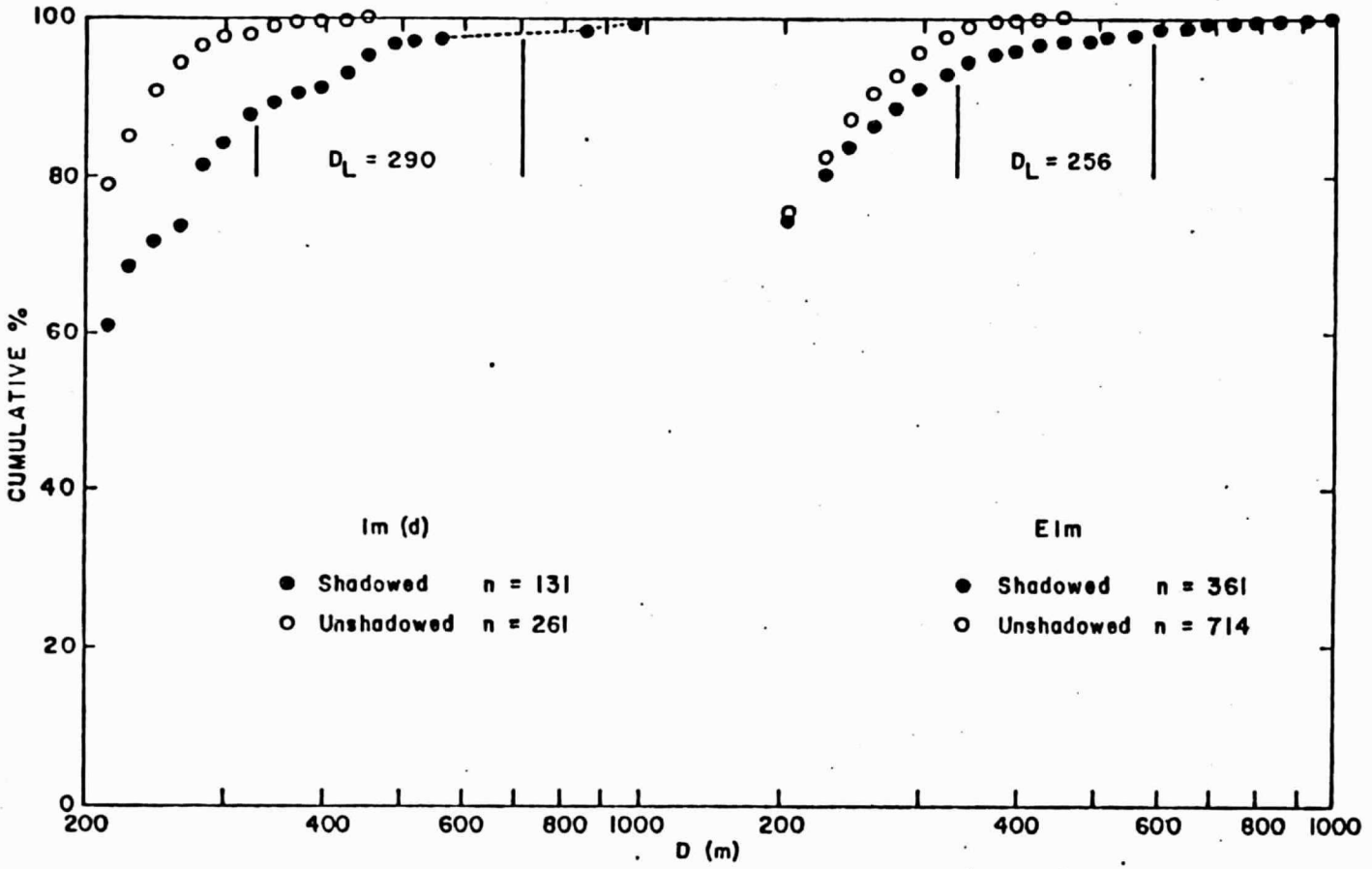

Figure 16. Cumulative crater-frequency diagrams for shadowed and unshadowed craters on Imbrian mare near Dawes (Im(d)) and Eratosthenian-Imbrian mare of central Serenitatis (EIm).

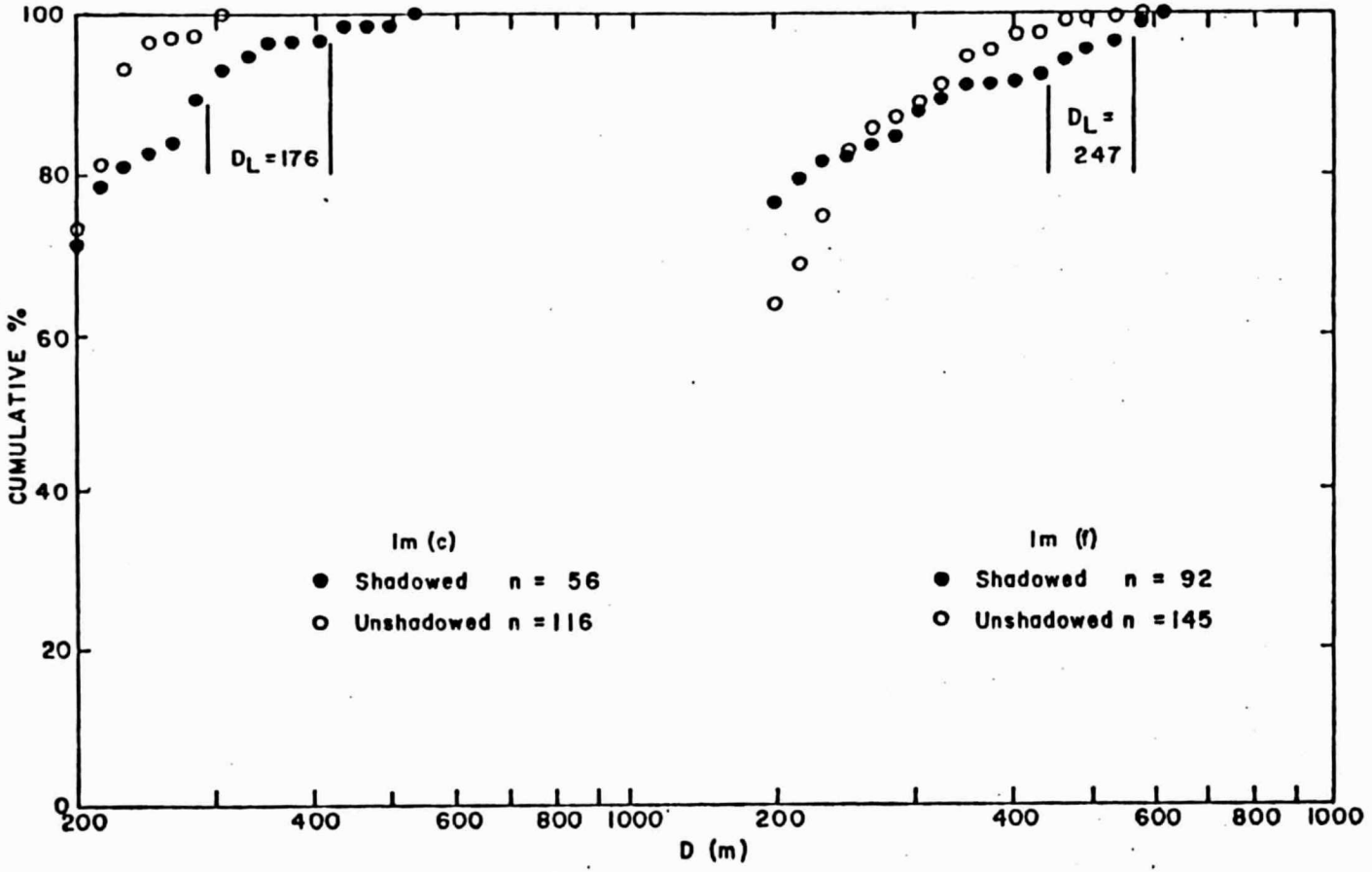

Figure 17. Cumulative crater-frequency diagrams for shadowed and unshadowed craters on Imbrian mare near Clerke (Im(c)) and Fabbroni (Im(f)).

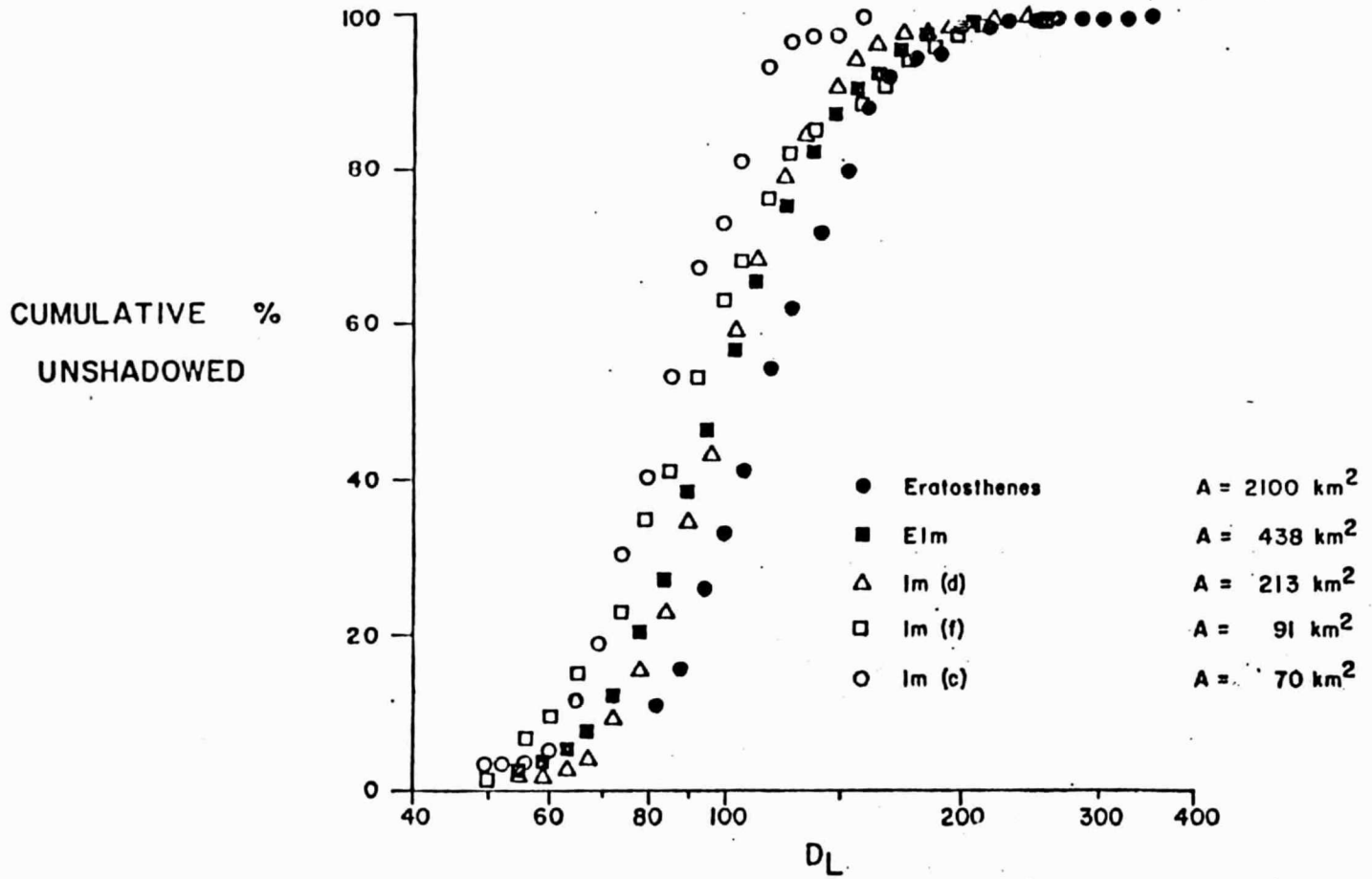

Figure 18. Cumulative percent unshadowed craters plotted as a function of D_L (to remove sun elevation effects). Changes in size of counting area overrides differences in crater populations due to age of surface.

The age of a mare surface may also be dated by comparison of the absolute crater frequency of those craters larger than the minimum saturation diameter (Young, 1975). This method is complicated, however, by varying regolith thickness, blanketing effects of ejecta, secondary impacts and differences in impacted materials. Consequently, the reliability of absolute crater counts may be more indicative of the surficial materials than of the age of the surface (Young and others, 1974). Crater data for the four areas in Serenitatis and Eratosthenes ejecta were normalized to absolute frequency of all craters per 200 km^2 in order to compare the central mare with the crater Eratosthenes. Eratosthenes has a greater number of craters above 400-500 m than the central mare, while below that diameter, the central mare has a larger frequency (Fig. 19). Although this relationship may suggest that the central mare is younger than Eratosthenes (assuming that secondaries produced the high crater frequency in the 200-400 m size range), similar relationships with the dark annulus units that are obviously older do not support that theory (Fig. 19). Young (1975) concluded that impacts producing craters less than 300 m contributed to regolith development, and that older surfaces may actually have fewer small craters as a result of seismic modification, regolith formation and mantling deposits. Consequently, it is difficult to use the absolute crater frequency in the size ranges studied to determine relative age.

Correlation with Absolute Age. Using ages of basalts at Apollo landing sites in conjunction with crater age determinations of the surfaces, the D_L values can be used to estimate the absolute age of the surface

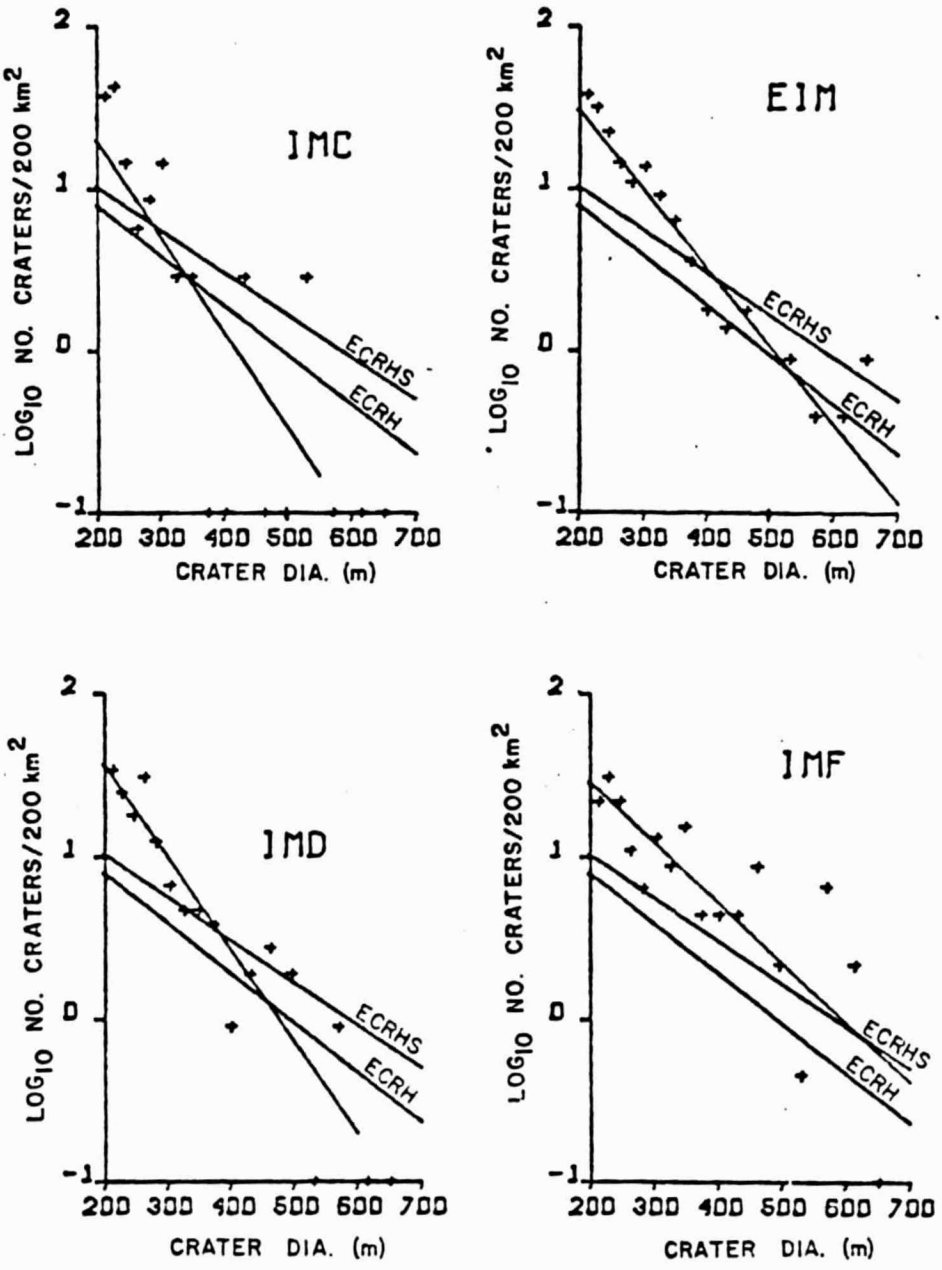

Figure 19. Absolute crater frequency normalized to 200 km^2 areas. Data for best-fit curves of Eratosthenes ejecta blanket not shown.

(Soderblom, 1970; Soderblom and Lebofsky, 1972). Because of uncertainties in both the isotopic dating and D_L estimates, the absolute age is subject to about 0.5 b.y. error. The curves shown in Figure 20 use Rb/Sr ages of the Apollo samples from Papanastassiou and Wasserburg (1976), and D_L values of the Apollo 11, 12, and 15 sites from Boyce and others (1974). The range of D_L values for Eratosthenes determined in the present study indicates an age of 3.2 ± 0.2 b.y., which correlates with the Eratosthenian ages of Apollo 12 and 15 mare (Pohn, 1971; Carr and others, 1971). These data also indicate an age of 3.7-3.8 b.y. for the dark mantle (ages of Apollo 17 mare samples range from 3.6-3.9 b.y.; Tera and others, 1974a), 3.6 b.y. for the dark annulus units, and 3.2-3.3 b.y. for the central mare.

Imbrian Mare.

Imbrian-age mare units in the southeastern Serenitatis area consist of the dark mantle, three dark annulus units, two units in northern Tranquillitatis, and three small patches of domical mare at the Serenitatis-Tranquillitatis border. Earth-based and orbital remote sensing data are summarized in Table 2. In general, the older mare units in this area are darker and more Ti rich, while the younger units are lighter and have a smaller percent Ti.

Dark Mantle. The oldest mare unit in the area is the dark mantle of the Taurus-Littrow area. Apollo 17 samples indicate a mixture of high Ti mare basalts similar to those of the Apollo 11 site (dominantly olivine normative basalts; Wolfe and others, 1975), and abundant orange and black glassy spheres in the regolith. Seismic investigations at the site (Cooper and others, 1974) and the few number of

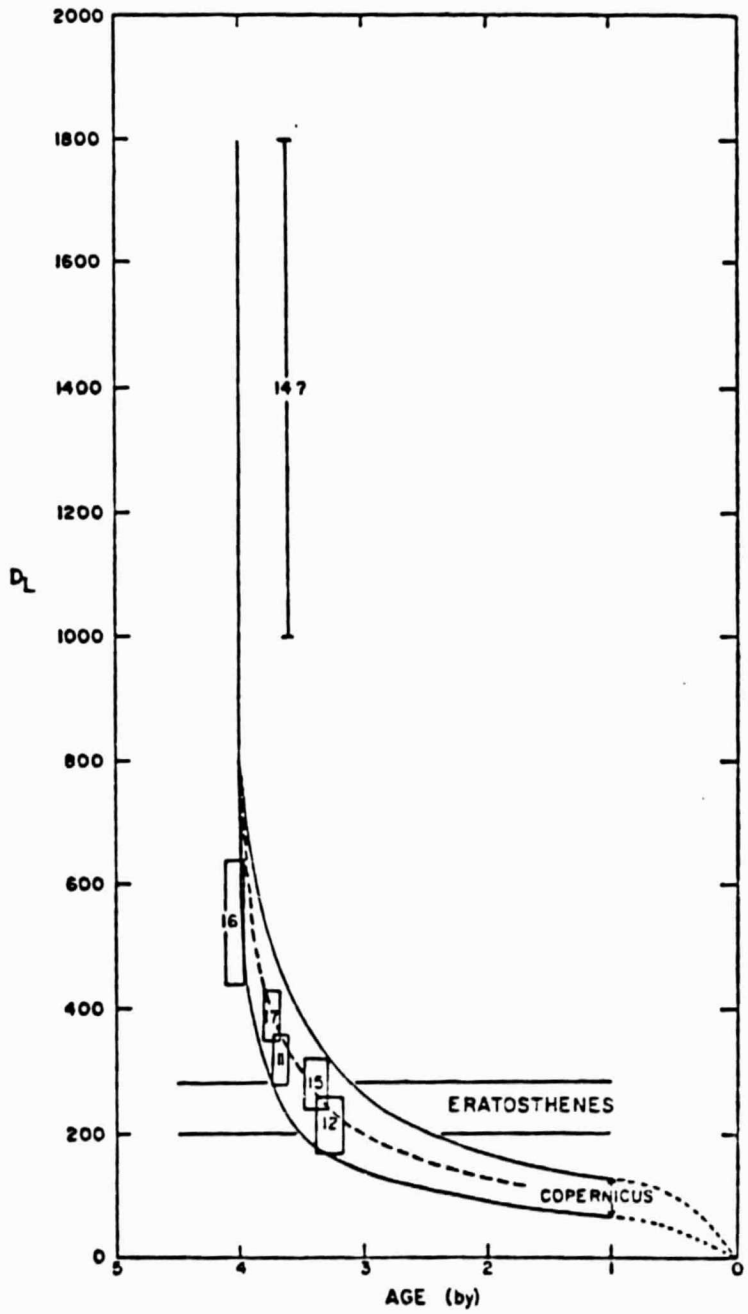

Figure 20. Correlation of D_L values with ages of Apollo samples (modified from Boyce and others, 1974).

TABLE 2. CORRELATION OF REMOTE SENSING INFORMATION

	GEOLOGIC UNITS	Earth-based radar Reflectance 3.8 & 70cm*	Spectral Reflectance 0.3-1.1μm*	Color Difference Photographs 0.38-0.78μm*	UV Reflectance 0.12-0.165μm*	Visual Color	Al/Si Ratio
central mare	EIm	I	R;2-3% Ti	R	H	lTG	L
dark annulus	EImb Im	W	B;7-8% Ti	b B	I	dBG	L
dark mantle	Imd	W	B;9-10% Ti	B	—	dBG	I
Tranquillitatis basalts	Imt	W	B;7-8% Ti	B	I	—	L
plains	IpIp	I	—	r	L	—	H
highlands	IpIh pItm	S	—	R	L	lG —	H
		S-strong I-intermediate W-weak	R-red B-blue	R-red r-reddish b-bluish B-blue	H-high I-intermediate L-low	G-gray TG-tan gray BG-blue gray d-dark l-light	H-high I-intermediate L-low

* wavelength.

small, blocky-rimmed craters (Wolfe and others, 1975) show that the valley is underlain by about 15 m of regolith and 1400 m of basaltic material. Lucchitta and Sanchez (1975) have suggested the possibility that the dark mantle may actually consist of regolith overlying a concentrated layer of glassy spheres. Although the majority of dated mare basalts fall in the range from 3.65 to 3.9 b.y., Pb/Pb dating of glassy spheres from the regolith indicate an age of 3.48 b.y. (Tera and Wasserburg, 1976). If these dates are supported by further investigation, then it is possible that the deposition of the dark glass occurred over 200-400 m.y. The relatively thick regolith of the dark mantle would therefore be composed of alternating layers of concentrated glassy spheres and mixtures of glass and basalt. The extension of ages of the glass also rules out the possibility of their origin by impact into liquid lava (Roedder and Weiblen, 1973). Many of the stratigraphic relationships at the dark mantle-central mare contact are obscure, and the dark mantle in places appears to overlie younger mare (Lucchitta, 1973). These features may be caused by impact redistribution of concentrated dark glass, or by a truly younger age in some localities.

The similarity of small sinuous rilles in the dark mantle to those in mare materials within the Rook Mountains of Orientale suggest that the earliest mare materials originated peripheral to the basin and then flowed towards the basin. The oldest mare materials in both Orientale and Serenitatis are therefore at the edges of the basins, a conclusion borne out by crater studies of Boyce (1975).

Dark Annulus. Dark annulus materials at the Serenitatis-Tranquilli-

tatis boundary and along the eastern edge of Mare Serenitatis (Im_1-Im_3) are spectrally less blue than the dark mantle, and have a slightly higher visual albedo than the dark mantle (Pohn and Wildey, 1970). Earth-based spectral data indicate a Ti content of 7-8% (Pieters and others, 1973), and the relatively weak radar reflectance at 3.8 cm is indicative of a rock-free surface. All of the Imbrian dark annulus units are topographically higher than the mare of central Serenitatis, and the small sinuous rilles in one of the units (Im_2) trend downslope towards the basin.

Both X-ray data (Andre and others, 1975) and ALSE subsurface profiles indicate that the total thickness of the three major dark annulus units is 600-800 m. According to the gravity data, the topographic slope (1.8°) of the dark annulus towards the central basin is relatively constant up to 20°N Latitude, but at that point, the subsurface contact between the dark annulus and the central mare becomes nearly horizontal (Sjogren and others, 1974). The continuation of that dip would imply more mass of basalt than is predicted by a surface disc model of the Serenitatis mascon (Phillips and others, 1972).

Consequently, the dark annulus is composed of several thin basaltic flows (layering can be seen in the interior rim of Dawes) that most likely originated at or near the basin rim at 3.7-3.8 b.y. One of the last flows (Im_2) may have originated in Tranquillitatis, and the source area for the youngest unit (Im_3) is obscured by Dawes. Three small patches of finely textured mare and domes (Id) formed subsequent to deposition of unit Im_2, but may have formed before or after emplacement of unit Im_3.

Tranquillitatis Mare. Two units of Imbrian-age mare in northern Tranquillitatis (Imt_1 and Imt_2) are similar spectrally to dark annulus materials, suggesting a Ti content of 7-8%. Superposition relations suggest that unit Imt_1 is younger than unit Im_2, although crater morphology dating by Boyce and others (1974) indicates a similar age. Unit Imt_2 is limited in extent, occurring only near Vitruvius, and has a lower visual albedo than Imt_1. Morphologically, it is somewhat similar to the dark mantle material, and has relatively few 100-400 m craters. Both of the Tranquillitatis mare units originated as low viscosity basaltic flows, however, source regions for these units have not been identified in the map area.

Eratosthenian-Imbrian Mare

On the basis of crater age dating, the interior of Mare Serenitatis is Eratosthenian to Imbrian in age (3.2-3.3 b.y.). Two units are defined primarily on the basis of spectral information.

Bluish Mare. The bluish color of the dark annulus extends inwards in a band about 30 km wide, but is embayed by the redder material of the central mare (EIm) northwest of Mons Argaeus. Unit EImb is unique in that it is composed of fairly high Ti basalt (6-7%?) but is younger than the other dark annulus units. The contact of this unit with the central mare is indistinct, and does not correspond to any topographic boundary. The limited extent and location of this unit thus suggest a compositional mixture of reddish basalt of the central mare, and blue, dark-annulus basalt. It is possible that deposition of the central mare produced only a thin cover of basalt in this area, and subsequent vertical mixing by impact has produced a regolith composed of both types

of basalt. An alternative hypothesis, however, is that the unit formed as one of the succession of Serenitatis basin-filling lavas. Although distinctly younger than the other dark annulus units, unit EImb may be compositionally the precursor the the later, low-Ti basin fill.

Central Mare. The light tan-gray (El-Baz and Evans, 1973; Schmitt, 1974) basalt of central Mare Serenitatis (EIm) appears reddish on color composite photographs (Whitaker, 1972a), and vidicon imagery, thus indicating a low Ti (2-3%) basaltic regolith with a lower glass content than dark annulus or dark mantle materials (Johnson and others, 1975). Layering seen in the interior rim of Bessel (Young, 1976) suggests that the unit may be made up of numerous thin flow units, although no flow fronts are visible on the surface. ALSE data suggest a total thickness of 800 m for the central mare in the map area, with the subsurface contact being fairly horizontal although a trough exists at 27° to 28°E. This later flooding, therefore originated in the interior of the basin, and took place on a relatively undeformed layer of mare basalt. The depth of the trough in the subsurface is less than that of the present topography, so that it is likely that most of the subsidence took place in Imbrian time. This conclusion is supported by the fact that arcuate rilles in early dark annulus basalt (Im_1) are filled in by later Imbrian basalt (Im_2 and Im_3), and the scarcity of rilles in both the bluish (EImb) and tan-gray (EIm) mare units.

CHAPTER 4

STRUCTURAL AND VOLCANIC FEATURES

Basin Structure

Rings.

As shown by Hartmann and Wood (1971), placement of basin rings follows a relationship of $\sqrt{2}$ radius with increasing ring size, although the exact mechanical reason is unknown. Mechanisms of ring formation have been ascribed to frozen shock waves or "tsunamis" (Baldwin, 1963) and inward collapse along deep fractures (Hartmann and Wood, 1971). Both of these theories have been extensively reviewed by Howard and others (1974). In the present study, the location of basin rings and their influence on structures of southeastern Serenitatis is of importance in differentiating between basin-related features, and those resulting from later tectonic stresses.

On the basis of morphological comparisons with the Rook Mountains of the Orientale basin, Wolfe and Reed (1976) have recently shown that the Taurus-Littrow area lies approximately on the third ring of the southern Serenitatis basin (Fig. 21) rather than on the second ring as depicted by Wilhelms and McCauley (1971). In both the Orientale and southern Serenitatis basins, massifs are aligned roughly radial to the center of the basin (Wolfe and Reed, 1976). There is an additional morphological similarity between the sculptured hills (unit Ipih, Appendix 2) and the knobby basin material (Moore and others, 1974) or

Figure 21. Revised ring structure of southern Serenitatis basin (Reed and Wolfe, 1975) is shown in black lines. Third ring is composed of segments of the second and third rings of Wilhelms and McCauley (1971). A possible smaller ring structure in the southeastern quadrant of the basin is outlined in white (Orbiter IV Fr. 102M).

Figure 22. Lineated highland terrain north of the crater Littrow (oblique view; Apollo 17 panoramic Fr. 2310). Note offset of Fossa Littrow (arrow). Rille is 2.5 km wide in this area.

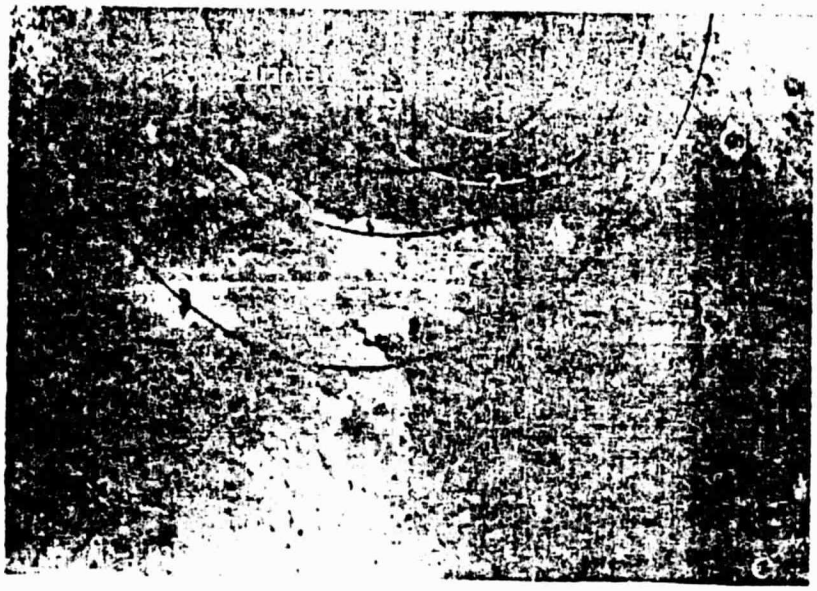

domical facies (Head, 1974b) separating the outer Rook from the Cordillera Mountains of the Orientale basin. Knobby basin material near the Rook Mountains, however, is topographically lower than the massifs, and is composed of sharper appearing hills and troughs than the more subdued sculptured hills. Mare flooded valleys in both the Rook and Taurus Mountains are characterized by small sinuous rilles oriented approximately radial to the basin.

North of Littrow, distinctly lineated highland terrain similar to the Fra Mauro Formation is present (Fig. 22), unlike the corresponding Rook Mountains of Orientale. The orientation of the lineaments and grooves is radial to neither Crisium or Imbrium (Wolfe and Reed, 1976) nor to the southern Serenitatis basin. It is possible that this sculpturing may be related to one of many pre-Imbrian basins in the northern Serenitatis area (Scott, 1972; Maxwell and others, 1975).

Although these morphological arguments support the revised placement of southern Serenitatis basin rings, there are some topographic discrepancies between the rings of the Orientale and Serenitatis basins. Both the inner and outer Rook Mountains (second and third rings) are roughly 1.5 to 2.5 km above the surrounding plains (Figure 3 in Head, 1974). The major topographic offset of the Orientale basin is at the Cordillera scarp (fourth ring). There, the crests of the mountains are 4 to 8 km above the central basin, and 2 to 5 km above the surrounding terrain (Figure 5 in Howard and others, 1974). Consequently, the 2.5 km height of the Taurus-Littrow massifs, if analogous to the Orientale third ring, suggests that the second Serenitatis ring would have had mountain peaks at approximately the same elevation as the massifs before mare deposition. At present, the mare material at the continua-

tion of the second (Haemus Mountains) ring lies at 4200 to 4300 m (relative to a 1730 km mean lunar radius), while peaks of the massifs reach elevations of 6500 to 7000 m. Thus, any topographic analogy would indicate a minimum of 2.2 to 3.8 km downdropping of the interior basin (or uplift of the massifs) before mare deposition. Apollo Lunar Sounder data indicate a minimum mare basalt thickness of 2 km in this area, which increases the amount of offset even more. However, the steep faces, high albedo, and rocky surfaces of the massifs lend support to the conclusion that they have undergone post-basin uplift (Scott and others, 1972). Most of the highlands north of Littrow reach elevations equal to those of the massifs, but the smoother appearance and lack of distinct tectonic lineaments support a broader, more regional uplift of the northern region rather than differential movement.

This analogy with topography is subject to two difficulties. The relative elevations of the Orientale rings were obtained by shadow measurements (Head, 1974b) and a combination of laser altimeter profiles on the north side of the basin (Howard and others, 1974). Consequently, extrapolating these few profiles to the rest of the basin may be dangerous. In addition, the heights of the rings are measured relative to the neighboring plains or mare surfaces. The relatively minor amount of volcanic filling of Orientale may cause overestimates of the heights of the rings; but assuming a constant base level, the relative peak heights should be fairly consistent. Consequently, although pre-mare differential uplift of the massifs is almost a certainty, the amount of post-mare uplift is difficult to quantify by comparisons with the Orientale basin.

Both gravity models of the Serenitatis basin and results of the Apollo Lunar Sounder subsurface profiles support the placement of the rings as proposed by Wolfe and Reed (1976). As shown by Bowin and others (1975), the gravity minimum on the eastern side of Serenitatis coincides with the third ring of the basin, and with the brightest slopes of the massifs (Fig. 10). The negative gravity ring surrounding the Orientale basin is likewise located at the third ring of the outer Rook Mountains (Sjogren and others, 1974). Two subsurface profiles from the Lunar Sounder indicate a trough in the mare materials in the southeastern part of the basin. The 300 m offset at the western edge of this trough (Fig. 8) coincides with the placement of the second ring of the basin, and indicates downdropping of the area between the second and third rings during the periods of mare deposition.

Mapping of ridges and arches in Mare Serenitatis has suggested an additional impact on the pre-mare floor of the southeastern quadrant of the basin (Maxwell and others, 1975). Although evidence for rings of this impact is not as distinct as that of Serenitatis, a possible second ring (1.4 times the inner-basin diameter) of the smaller basin coincides with both the subsurface trough as detected by ALSE and an arcuate rille on the southern rim of Brackett. As in the case of the ridge systems in the southeastern part of the basin, however, it is difficult to separate the effects of the southern Serenitatis basin from those of the smaller impact on a purely morphological basis. The proposed impact does, however, help to explain the relatively small radius of curvature of the rille adjacent to Brackett.

Lineaments.

Basin-related lineaments in highland units are both radial and concentric to the southern Serenitatis basin. Modification of this area by early impacts was overshadowed by the later Serenitatis events, and no morphologic evidence for structural deformation caused by either Tranquillitatis or Crisium has been recognized.

The radial and concentric trends formed by the massifs (Fig. 23) have been interpreted by Head (1974a) as grabens resulting from the Serenitatis impact. However, concentric lineaments surrounding other lunar basins have been interpreted as the result of inward collapse and readjustment of the crust immediately following excavation (Stuart-Alexander and Howard, 1970; Hartmann and Wood, 1971; Howard and others, 1974). Because of this probability and the relationship with the Serenitatis basin, it is doubtful that the discontinuous northeast-trending valleys in the Taurus-Littrow area are true grabens (bounded on <u>both</u> sides by normal faults). The term may be more justifiable for the radial valleys, where both the north and south sides are delineated by the bright faces of the massifs.

One of the northeast-trending highland lineaments continues as a low scarp in mare units south of Fabbroni (Plate 1), where it is paralleled in part by small linear rilles. The northeast trend parallels that of Fossa Littrow and one of the orientations of the lunar grid (Strom, 1964; Casella, 1976), and indicates NE-SW extension of the area during Imbrian time. Faulting may have been the last stage of movement related to earlier stretching across the Serenitatis-Tranquillitatis boundary.

Figure 23. Orbiter IV Frames 78H2 and 78H3 showing basin controlled orientation of massifs. Most surficial volcanic features (Rima Carmen and small wrinkle ridges) occur between the southernmost two radial lineaments. The extension of the second concentric lineament coincides with a scarp in the mare to the southwest (compare Fig. 18 in Head, 1974a).

Linear and Arcuate Rilles

Linear and arcuate rilles in southeastern Serenitatis are primarily confined to the dark annulus and dark mantle materials surrounding the central mare basin. As would be expected, most rilles are concentric with the southern Serenitatis basin rings, however, the exception is Fossae Littrow, a system of arcuate rilles trending northeast, and exhibiting very little curvature in this area (Fig. 24). North of the map area, the major rille (Fossa Littrow) curves to the north and northwest, and is concentric to the entire Serenitatis basin. In addition, there are numerous more subdued rilles in the dark mantle that trend north-south. The relatively straight walls, cross-cutting relations with various surface materials, and basin-controlled orientation of these features are all consistent with a graben origin, and the rilles are interpreted as such here. Head (1974a) proposed two groups of grabens for the Taurus-Littrow area; Type I grabens are bounded by the large blocks forming the massifs, and are dominantly radial to the basin. Type II grabens are those that are described in the present study as linear and arcuate rilles in dark mantle material. The orientation and morphology of these rilles are similar to rilles in the dark annulus materials, and hence are considered as the result of the same stress system.

On the basis of morphology, rilles may be divided into two types. Sharp, well-defined rilles occur at the western edge of the dark mantle, on the dark annulus northwest of Catena Littrow, and in the cen-

Figure 24. Circumferential grabens in dark mantle and dark annulus materials (black and white dashed lines) and fresh-appearing north-trending rilles (white). Solid black lines are locations of cross-sections for dip estimates of Fossa Littrow (Apollo 17 metric Fr. 0448).

Figure 25. Forked rille northwest of Catena Littrow; rille has sharper appearance than rilles in dark mantle material. Arrow shows area where rille turns into ridge adjacent to crater (Apollo 17 panoramic Fr. 2313).

tral mare. With the exception of one northwest-trending rille in northern Mare Tranquillitatis, these rilles are oriented north-south. More abundant, relatively subdued arcuate to straight rilles occur in the dark mantle and dark annulus, where they are concentric with the basin.

A few of the wider arcuate rilles (Fossa Littrow) cross-cut both the dark mantle material and highland units, but southwest of Mons Argaeus, they are truncated by Imbrian basalt (Im_2, Plate I). Thus, the major basin-controlled tensional faulting is confined to early Imbrian time. Because of the mantling characteristics of the dark regolith at the Apollo 17 site, it is difficult to establish whether rille formation took place before or after pyroclastic activity. Any faulting that took place before dark mantle deposition would be subdued by the deposits, but post-mantle faulting would likewise be subdued by the incoherent, fine-grained nature of the regolith (Lucchitta and Sanchez, 1975). South of Clerke, some small scarps cross-cut and fill portions of the rilles, which suggests that some faulting took place on the subfloor basalt and was obscured by the latest flows of the Taurus-Littrow area. On the basis of cross-cutting relations among the rilles, there is no clearly defined change in trend that would indicate a changing stress orientation. North-trending rilles may crosscut or be crosscut by northeast-trending rilles.

The sharper, fresh-appearing rilles in dark annulus and central mare materials appear to have formed from late Imbrian to early Eratosthenian time (possibly in response to the same stress system responsible for the uplift of the massifs and highlands near Littrow). North-

west of Catena Littrow, one such rille has a distinct forked pattern, and is a complex system made up of numerous smaller rille segments.

At the southern end of this complex system, one rille is distinctive in that it abruptly changes into a ridge in the vicinity of a small (2.5 km) crater (Fig. 25). Although this feature and other examples of ridges having the same orientation as grabens have been cited as evidence that a tensile stress may be compatible with ridges and rilles (Hodges, 1973; Scott and others, 1975), coincidence of the ridge with ejecta from the nearby crater suggests another mode of origin. Superposition of crater ejecta on the rille indicates that the rille predated the crater. It may be possible that a horizontal pressure gradient caused by the impact (Melosh, 1976) could effectively revive pre-existing fractures causing uplift of the central part of the graben. This mechanism is dependent on a thin layer of basalt effectively transmitting horizontal stress, and the center of the graben acting as a coherent block. Nonetheless, it removes the necessity of volcanic extrusion for such a local feature.

Using a simple geometric method proposed by McGill (1971), it is possible to estimate the dip of faults bounding graben rilles. Fossa Littrow is the only rille in the area that encompasses sufficient elevation change to make the method valid. Using rille widths measured from 24X metric transparencies and topographic data from Lunar Topographic Orthophotomaps, the dip angle (α) may be estimated from the following formula:

$$\alpha = \arctan \frac{2\,\Delta h}{\Delta W} \qquad (1)$$

in which Δh is the change in elevation of the rim of the rille, and

Δw is the change in rille width (slightly modified from McGill, 1971). The cross sections for the four areas chosen (Fig. 24) indicate a fault dip averaging 61°, consistent with model studies (Hubbert, 1951) and lunar studies (McGill, 1971) on normal faulting. It is tempting to apply this technique to smaller and more subdued rilles in the area, but slumping of the edges of the rilles and blanketing effects of the dark mantle decrease the reliability of the method.

Arcuate rilles near Dawes also allow an estimate of stretching and failure of the Imbrian mare in this region. Assuming that the arcuate rilles are formed by basinward stretching of the mare crust, and that they are bounded by 60° dipping faults, the amount of stretching can be calculated. Depths of six rilles in this area were calculated from sun angle measurements on a 24X metric frame (Apollo 17 Fr. 0446; Fig. 26). Results indicate that in this 42 km wide area, about 620 m of extension could produce these features. This estimate should, however, be regarded as a minimum because of post-faulting degradation.

Ridges and Arches

Mare ridge systems in southeastern Serenitatis can be separated into three categories. 1) The southeastern portion of the inner-ring system (Fig. 3; Maxwell and others, 1975) forms an arc concentric to the basin, and is composed of discontinuous ridges and arches. At the southern margin, a ridge radial to the basin extends from the inner-ring ridge system into mare material of the dark annulus. 2) The southernmost part of a north-trending system of ridges occurs at the boundary between the dark annulus (Im_1) and the bluish annulus (EImb)

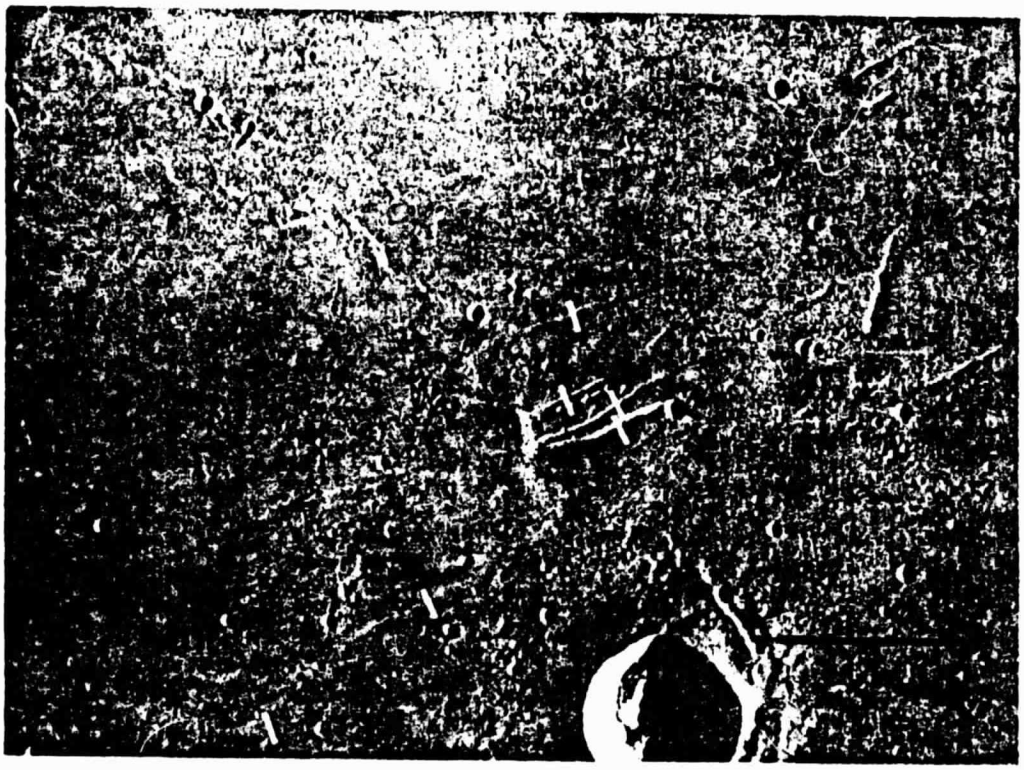

Figure 26. Northeast extension of Fossae Plinius showing cross-sections used to estimate amount of extension across Tranquillitatis-Serenitatis boundary (white lines). Crater at bottom center is Dawes (Apollo 17 panoramic Fr. 0449).

west of the crater Littrow. 3) Smaller, more localized segments of ridges occur locally in valleys between the massifs and to a lesser extent, in the central mare units. These ridges generally trend northwest to north, but locally vary greatly in orientation, and may be continuous with scarps in highland materials ("Scarp" of the Apollo 17 site).

Viewed at Lunar Orbiter scale, the essential lunar-wide similarity of wrinkle ridges suggests that a single explanation should account for the major features of the ridges. However, detailed studies of ridges have resulted in a variety of explanations for their origin. Baldwin (1963) postulated a thin veneer of lava on a dominantly pre-mare surface, and Bryan (1973) preferred a tectonic origin resulting from isostatic subsidence of mare lava flows. Both intrusive (Whitaker, 1966; Strom, 1972) and extrusive (Young and others, 1973; Hodges, 1973; Scott and others, 1975) volcanism have also been invoked to explain wrinkle ridges. Mapping of ridges and arches in Mare Serenitatis has suggested that their origin is related to isostatic adjustments of pre-mare fractures and thin mare basalt units (Maxwell and others, 1975).

The association of the inner-ring ridge system with a surface disc model for the Serenitatis mascon (Phillips and others, 1972), and the coincidence of the north-trending ridge system with a discontinuity in mare thickness (DeHon, 1975) both indicate that subsurface, pre-mare topography and fractures are responsible for the location of these major ridge systems. Ridges of the inner-ring ridge system mark the location of the first ring of the Serenitatis basin, and in the study area, may also be the result of a smaller impact in the south-

eastern Serenitatis basin floor (Fig. 21). The north-trending ridge system at the EImb-Im_1 boundary (Plate I) coincides with neither the Serenitatis ring structure drawn by Wilhelms and McCauley (1971) nor that of Wolfe and Reed (1976). On the basis of flooded craters, DeHon (1975) has shown that this ridge marks the boundary between relatively shallow and deep mare fill, although the area has very few craters on which to base thickness estimates (DeHon, personal communication, 1975). The 300 m topographic downdropping of the central mare relative to the mare east of the ridge system is quite similar to the ring of ridges in Mare Crisium (Ward and others, 1973). Consequently, both the inner-ring and north-trending systems can best be explained by surficial folding and faulting above pre-mare faults.

The fact that both the inner-ring and radial ridge systems are continuous in the central mare (EIm) and dark annulus (EImb; Im_1) units indicates that formation occurred after deposition of the central mare. On Apollo 17 photographs, the low sun angle accentuates the "freshness" of some ridges, however, crater studies in other areas of the moon (Oceanus Procellarum) have shown that the surfaces of the ridges are not appreciably younger than the surrounding mare (Soderblom and Lebofsky, 1972). Formation of these ridge systems may have continued to the present (Muehlberger, 1974), although their subdued appearance on the surface (at least at the Apollo 17 site) suggests that no major recent activity has occurred (Fig. 27).

Small ridges in the Taurus-Littrow valley and in neighboring valleys exhibit a variety of features that are suggestive of different modes of origin. Thrust-faulting (Howard and Muehlberger, 1973), autointrusion (Hodges, 1973), extrusion (Scott, 1973), and high angle

Figure 27. A) Low sun elevation Apollo panoramic Fr. 2309 showing "Lee-Lincoln" Scarp in the vicinity of the Apollo 17 site. Note the smoother morphology where scarp cuts the North Massif.

B) View looking north along Scarp from area of light mantle. The ridge is much more subdued and lobate when seen from the surface (Apollo 17 Hasselblad Fr. 138-21119).

A

B

faulting (Lucchitta, 1976) have all been suggested, and there is ample photogeologic support for all of these modes of origin. It is difficult to decide on a single mechanism that would produce the variety of structural and volcanic morphologic features. On the basis of morphology, small ridges and highland continuations of ridges can be divided into three groups; faults, flow fronts, and extrusive ridges.

Faults.

The Scarp at the Apollo 17 site (Fig. 27) is the best documented example of a highland fault that continues as a mare ridge. It has been interpreted as an eastward-dipping normal fault or a high angle fault (Head, 1974; Lucchitta, 1976). The fault cross-cuts and therefore is younger than Fossa Littrow, indicating that it did not form in response to the same stress system that produced the arcuate rilles, as proposed by Scott and others (1975). During the Apollo 17 mission, the Scarp was investigated by E. A. Cernan and H. H. Schmitt on EVA 2. According to Schmitt (in Bailey and Ulrich, 1975; p. 103):

> . . . Scarp is just about what I think we all expected it to be. It's very rolling and relatively smooth. I don't really see any outcrops exposed anywhere out here to the south.

and later (in Bailey and Ulrich, 1975; p. 135):

> See the lobes coming out - looks like lobes out from the scarp. The scarp rather than being a line in there on the plain, appears to be lobes. I got a couple of shots of that, Whereas when it gets up on the massif, it's fairly continuous curve; although it does appear to be younger, at least there's less relief on it for the first few kilometers of that bend there . . . the scarp, so-called scarp, impresses me as less of a scarp than a series of lobes which roughly have a north-south trend. And we've been driving over various hummocks within those lobes.

Cross-cutting relations with massifs and hummocky highlands, and the smoother nature of the scarp in the highlands suggest that the

actual fault plane is buried beneath mare regolith and slumped highland material (Fig. 28A). The surface expression of this fault, as noted, is much more hummocky and lobate in the mare than in the highlands. Faulting and folding of thin surficial basalt layers and slumping of regolith most likely accounts for its appearance.

Flow Fronts.

Ridges that are formed on the edges of gentle topographic breaks are roughly aligned in a northwest trend. As noted by Scott (1973), one of these possible flow fronts that obscures arcuate rilles on the south side of the ridge (Fig. 29) suggests a flow direction opposite to the present-day slope. In terrestrial basaltic flows, terminal ridges (pressure ridges) will form when a flow front is continuously pushed against some obstacle and the surface buckles into an anticline, which sometimes may overturn and form thrust faults (Fig. 28B). According to Macdonald (1972; p. 78), ". . .the continued movement has resulted in overturning of the fold with a gentle slope of the surface on the side towards the source of the lava and a steep slope on the side away from it." Consequently, the asymmetric profile, lobate front, tendency to fill rilles on one side of the ridge, and occurrence in a single geologic unit are herein used as criteria for interpreting some of the ridges as flow fronts.

The side of the ridge with the more gentle slope should indicate the direction of flow, but later dark mantle material has obscured any source vents in this area. In general, however, the source of the lava lies in a 40 km wide northwest-trending band (Fig. 30). Included in this band are two sinuous rilles which were most likely developed

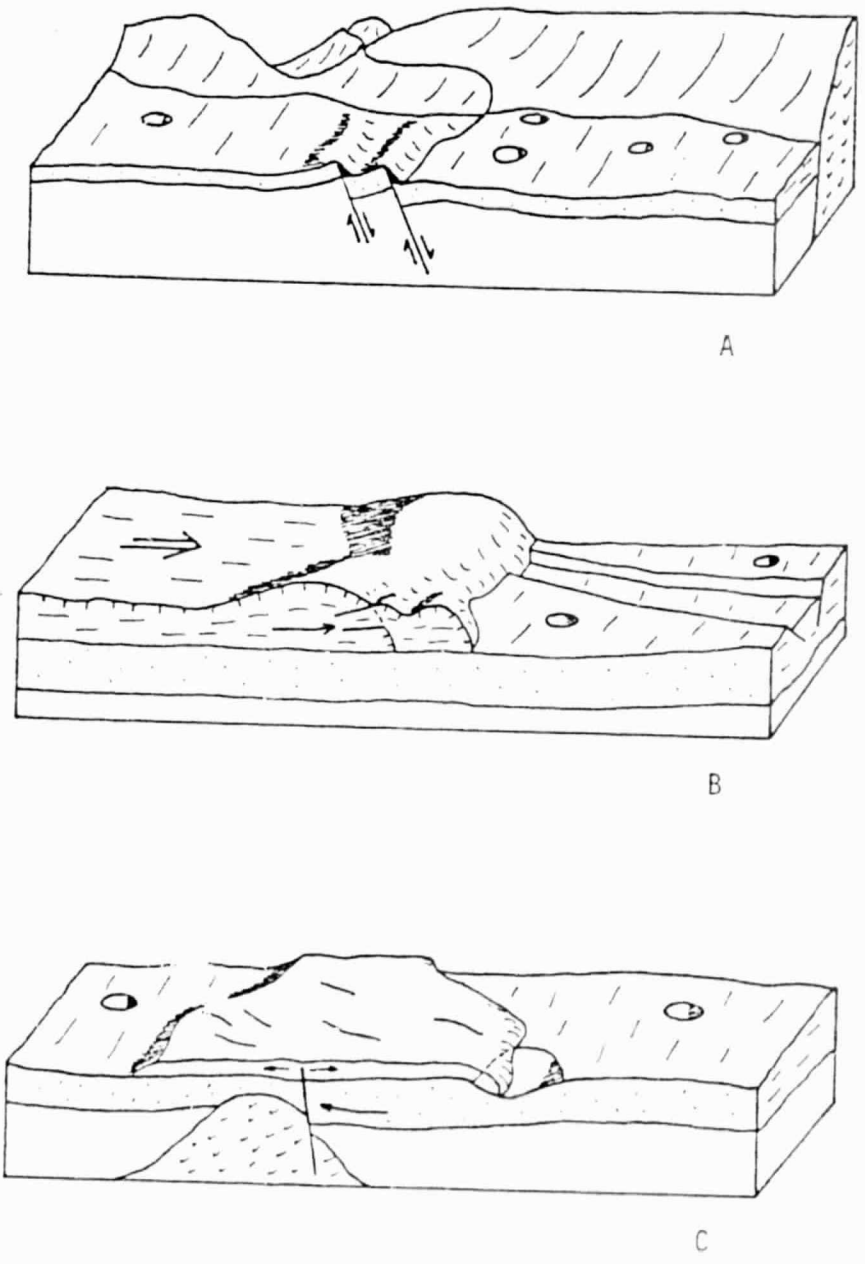

Figure 28. Three modes of ridge formation: A) High-angle normal faulting for "Lee-Lincoln" Scarp is consistent with abrupt change in strike. B) Local blanketing of rilles and morphology of scarps south of Clerke are evidence for flow fronts. C) Near Vitruvius, flooding of craters and lobate margins on both sides of ridges suggest small fissure extrusions (see Fig. 31).

Figure 29. Fossae Littrow south of Clerke; southern parts of rilles are more subdued, and numerous low scarps (probable flow fronts) cross-cut the rilles (Apollo 17 panoramic Fr. 2313).

Figure 30. Rima Carmen; a small sinuous rille that trends basinward (upper left) between the massifs. Another smaller sinuous rille is present on the northern edge of Mons Argaeus (Apollo 17 metric Fr. 1219).

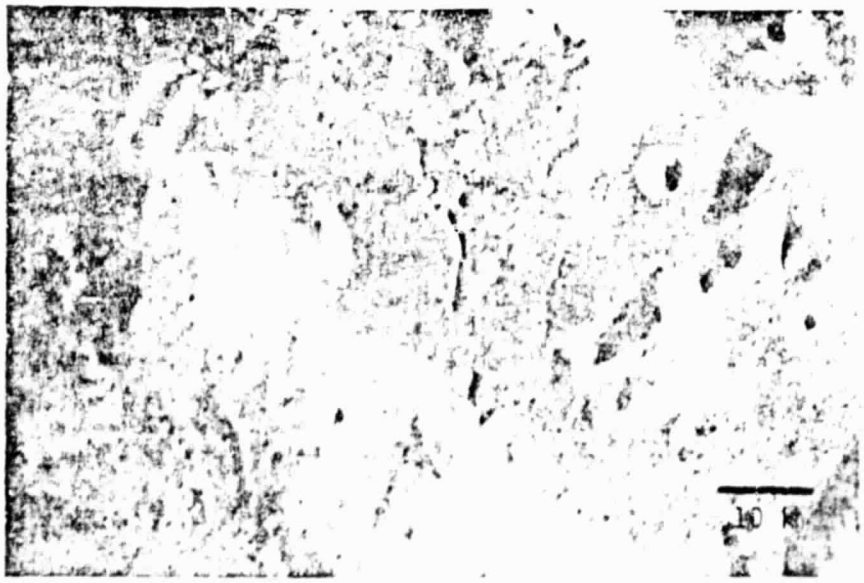

as lava channels on these latest flow units.

Extrusive Ridges.

South of the Taurus-Littrow valley, a northwest trending ridge (Fig. 31) with lobate edges and small (about 20 m wide) north to northeast trending cracks on the surface is similar to autointrusive "squeeze-up" structures (Fig. 28C) of terrestrial lava lakes (Hodges, 1973). Such an autointrusive origin is appealing for this ridge and similar northwest-trending ridges northwest of Vitruvius because it accounts for both the morphology and their location along continuations of highland boundaries (Fig. 30). It should be noted, however, that the extrusions were most likely concurrent with the latest flows in the Littrow area and were localized by faulting during formation.

Volcanic Features

Sinuous Rilles.

Two sinuous rilles occur in dark mantle material of the Taurus-Littrow area; Rima Carmen and a smaller, less distinct rille bordering a highland massif to the south (Fig. 30). Rima Carmen crosses both mare and highland units, and is strikingly similar to sinuous rilles in the outer Rook Mountains of Orientale (where rilles in mare-covered valleys between massifs indicate basinward tilting and flow during early stages of mare flooding). In the case of Rima Carmen, however, the gradient of the rille changes from 0.007 to 0.018 (Fig. 32) where the rille enters the highlands, and the rille is generally deeper in the mare than in the highlands. The gradient is compatible with that of sinuous rilles in the Prinz and Angstrom provinces (Strain and El-Baz, 1975), where gradients average 0.007 (P. Strain, oral communi-

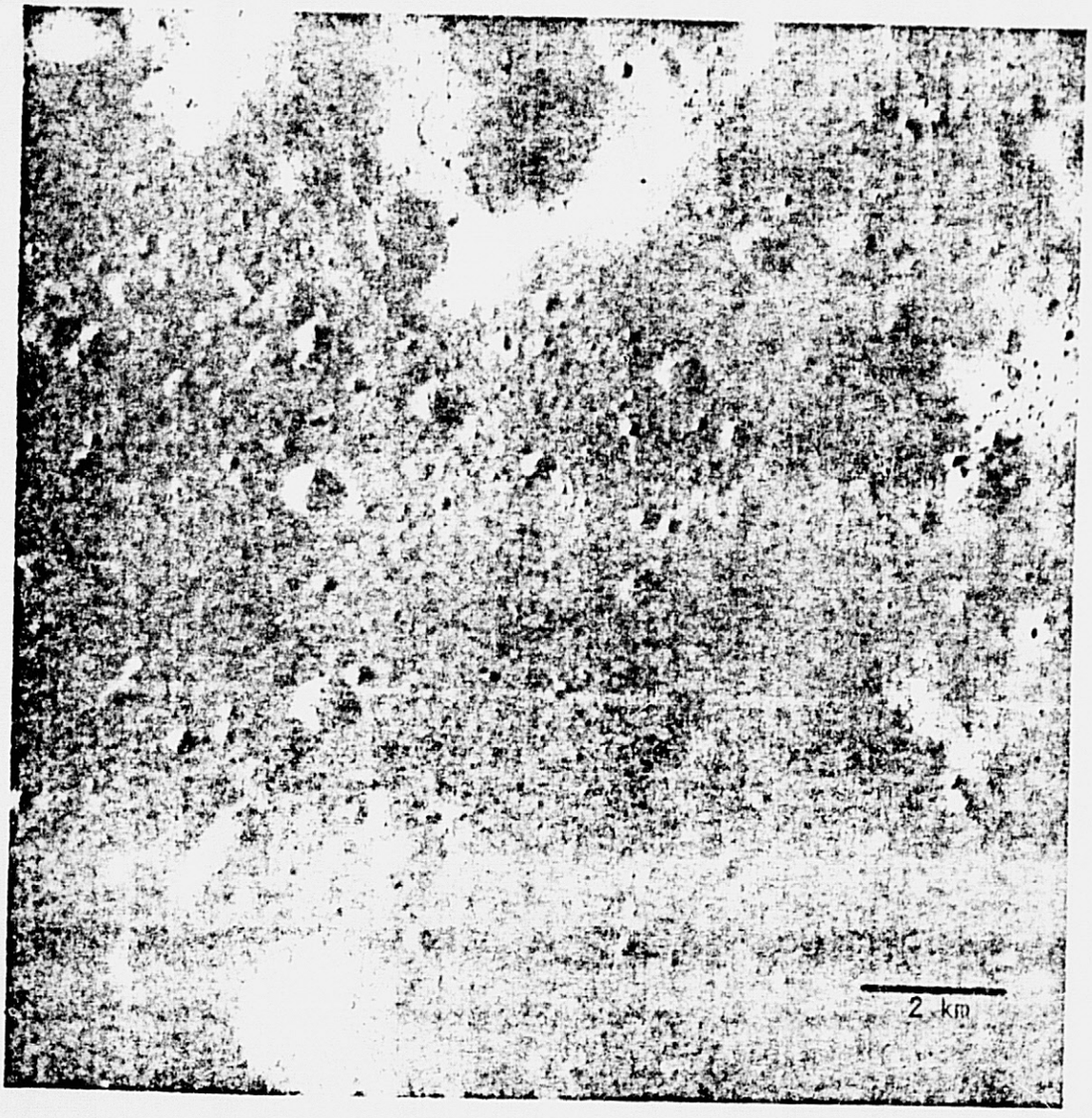

Figure 31. Small ridge west of Vitruvius bounded on both sides by lobate margins. Small cracks in mare at right of photo are concentric towards the northern Tranquillitatis basin (Apollo 17 panoramic Fr. 2309).

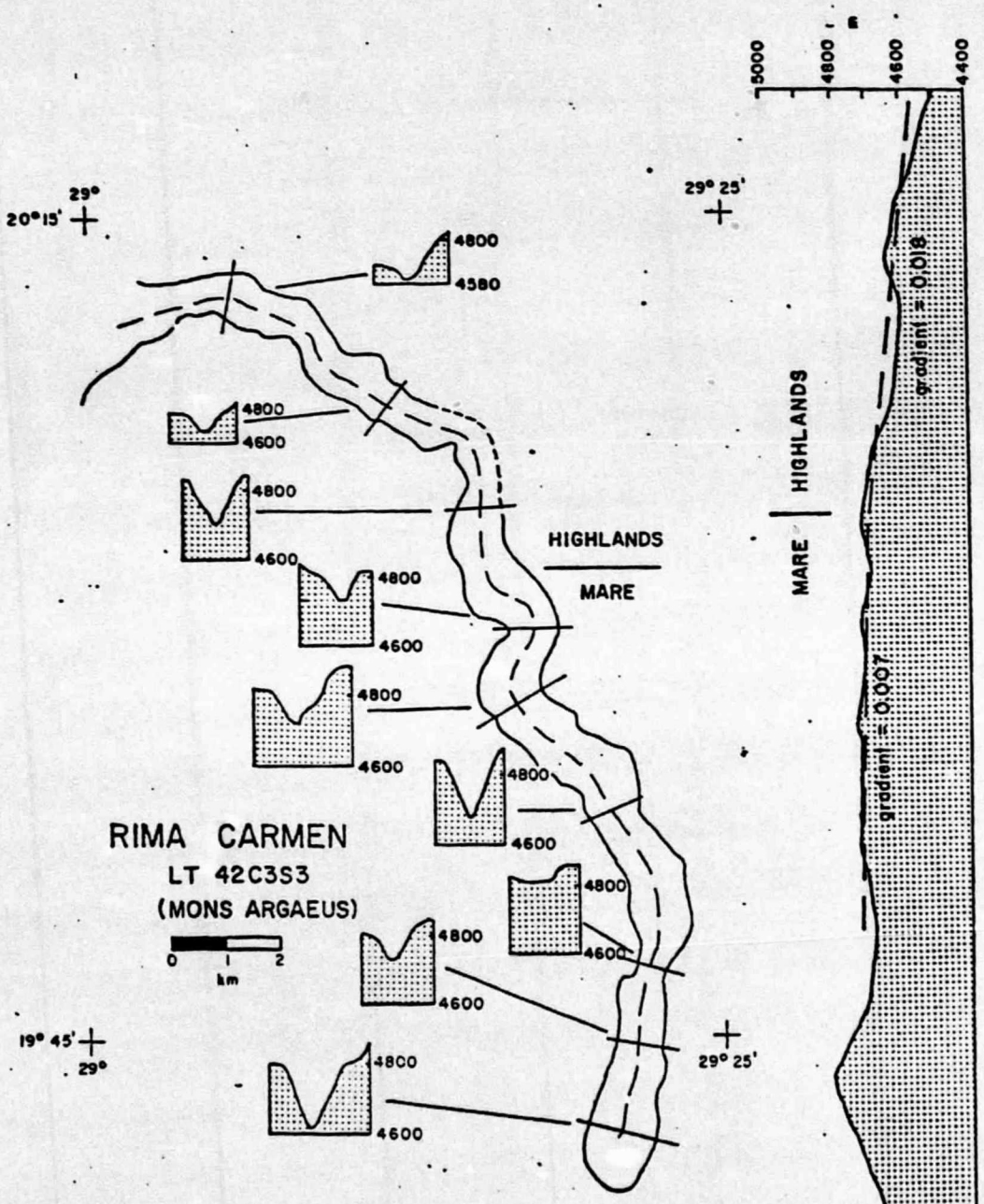

Figure 32. Cross-sections and longitudinal section through Rima Carmen. Although highly degraded, rille is deeper in the mare, and has a lower gradient in the mare than highlands. Photograph shown in Figure 30.

cation, 1976). Consequently, although post-basin uplift most likely occurred in the highland massifs, the uplift was not transmitted to the hummocky highlands in this area.

Several smaller sinuous rilles occur in a single mare unit (Im_2, Appendix 2) southwest of Mons Argaeus, where they slope from south to north, in accordance with the present dip (gradient = 0.014) of the mare surface. These rilles, although sinuous on a local scale, have an overall straight appearance, and are quasi-continuous for over 30 km. In terrestrial streams, low sinuousity can be caused by many factors, but is principally associated with a high gradient. As shown by Hulme (1973), lunar flows with low viscosity will have a high Reynolds Number, thus leading to turbulent flow and rille incision. The interplay of the thernodynamics and hydrodynamics of sinuous rille formation, however, is difficult to interpret because of modification of the original depth and slope. Also, comparisons with terrestrial streams are even more difficult because of order-of-magnitude increases in viscosity. Small linear rilles are also present in unit Im_2, and therefore, fractures may have helped to control the sinuousity of these rilles.

One 400 m wide sinuous rille occurs in the dark annulus northwest of Catena Littrow. Remnants of a depression are present on the crest of the ridge, but a smaller, fresh-appearing ridge has completely obscured the rille on the western flank. The rille apparently stops at the eastern edge of the ridge, and is not continuous in Imbrian mare (Im_1) to the east. Although the rille could be considered as an isolated example of volcanism associated with ridge formation, cross-cutting relations indicate that the ridge post-dates the rille, and

that the rille was formed solely in the bluish annulus material (EImb, Appendix 2).

Early, high Ti mare flooding in southeastern Serenitatis was therefore accompanied by incision of low viscosity lavas that flowed basinward. The discrepancy between highlands and mare ages at the 17 site, and analogous Orientale mare that is distinctly younger than the basin (Head, 1974b), indicate that these basalt lavas, although the oldest basalts sampled on the moon, were not the direct result of impact melting. The lavas may, however, be related indirectly to basin formation. Arkani-Hamed (1974a; 1974b) has proposed a model in which increased thermal insulation surrounding a major basin would cause the dominant heat (and magma) production to occur in the surrounding highlands. Evidence in southeastern Serenitatis and in Mare Imbrium (Boyce and Dial, 1975) supports early mare volcanism as originating peripheral to the basins, and these mare units may be the result of a thermal insulation mechanism.

Cones.

Late-Imbrian age explosive volcanic venting is represented by small cones and irregular collapse depressions aligned along a north-northwest line in dark annulus materials (Scott, 1973; Young and others, 1973). The northernmost area (Id, Plate 1) does not have a cone, but has an irregular depression in the center of the unit. These small patches of mare obscure, and therefore post-date, the small northwest-trending sinuous and linear rilles.

Topographic slopes on Osiris and Isis (Figs. 33 and 34) range from 7° to 12°, and are comparable to terrestrial basaltic cones in

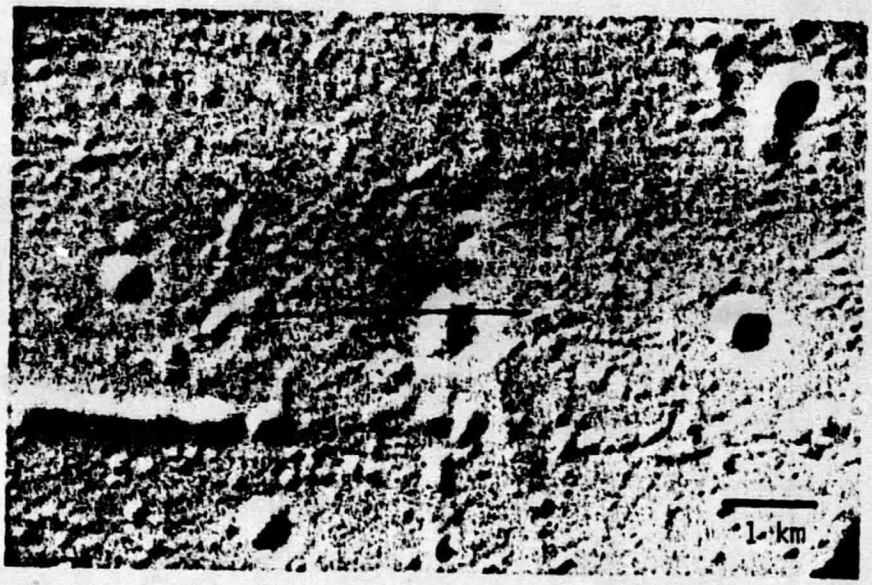

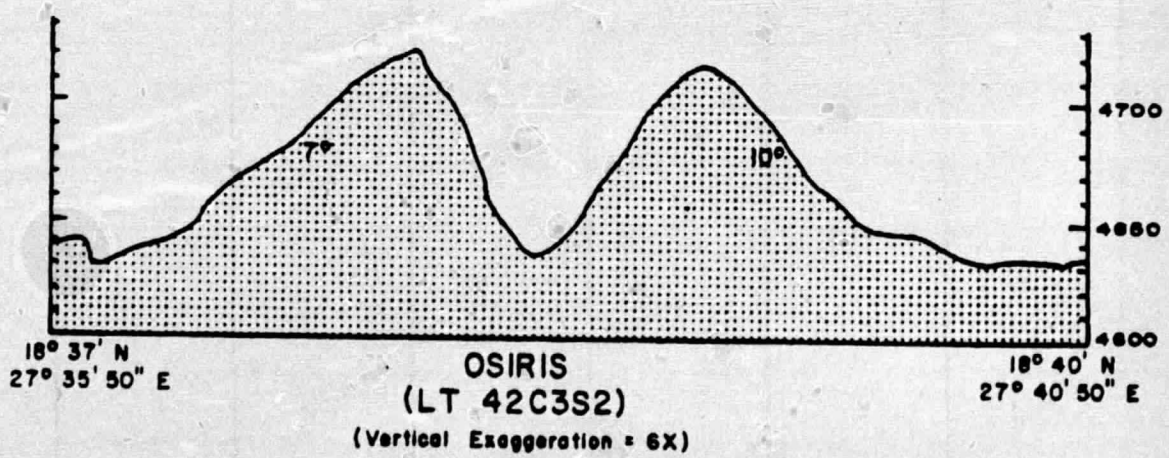

Figure 33. Photograph and section through Osiris; a small volcanic cone on the Serenitatis-Tranquillitatis border. Location is at intersection of two northwest-trending rilles and a collapse crater chain circumferential to Serenitatis. Elevations are in meters relative to 1730 km mean lunar radius (Apollo 17 panoramic Fr. 2317).

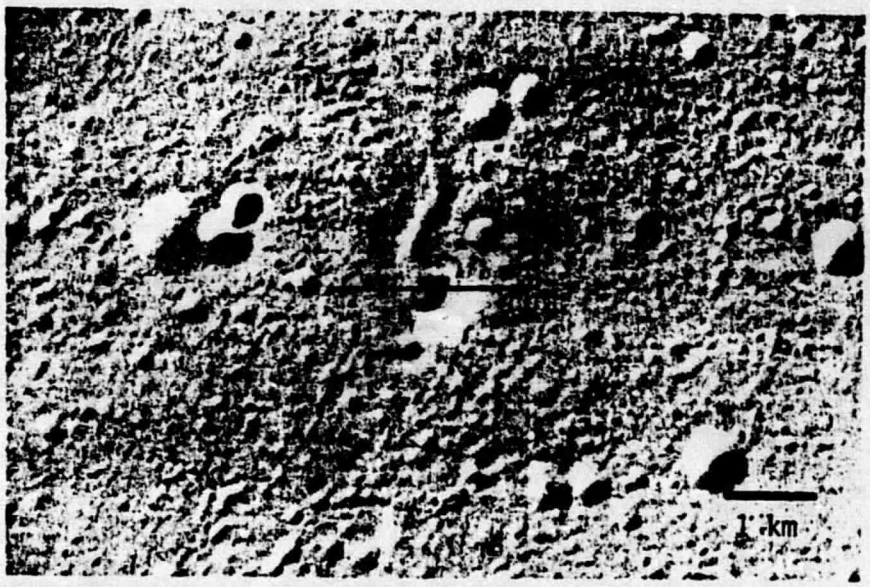

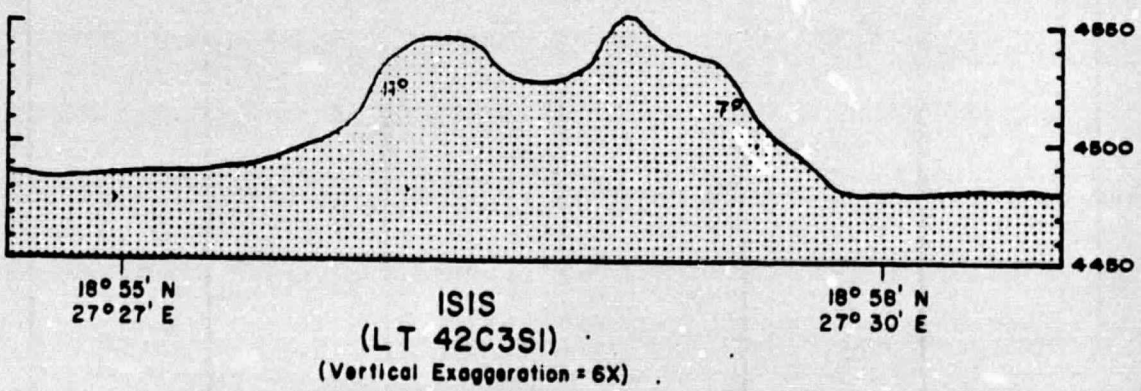

Figure 34. Isis, just north of Osiris, has a small sinuous rille that trends basinward (top of photo), indicating initial formation by lava. Low slopes on cone suggest a very low viscosity lava. Elevations are in meters relative to a 1730 km mean lunar radius (Apollo 17 panoramic Fr. 2317).

Iceland (Plate 30B in Green and Short, 1971). The morphologic similarity of these cones to terrestrial cinder cones prompted Scott (1973) and Eppler and Heiken (1975) to suggest a pyroclastic origin, as the rate of eruption can cause much different slope angles (McGetchin and others, 1974). A rille that breaches the northwestern edge of the summit crater of Isis (Fig. 34) suggests an origin by lava extrusion. However, blanketing of surrounding terrain and indistinct, gradational boundaries with surrounding mare are characteristic of a pyroclastic blanket. Consequently, the present available data favor initial construction of the landforms by extrusion, and possible later modification by a small amount of pyroclastic activity.

CHAPTER 5

SUMMARY

Geologic History

Pre-Imbrian.

Following the initial formation of the dominantly anorthositic lunar crust about 4.6 b.y. ago, the major events that affected the present day surface of southeastern Serenitatis were the giant impacts producing the Tranquillitatis, Serenitatis and Imbrium basins. A multiple impact origin for the Serenitatis basin is suggested by several means: 1) the gravity saddle in the middle part of the basin (Scott, 1974); 2) the irregular outline of the northern part of the basin; and 3) lineated terrain north of Littrow that is not radial to the center of the Serenitatis basin. An additional impact in the southern part of the basin is suggested by the outline of ridge systems and the small radius of curvature of an arcuate rille near Brackett. Impact melting and brecciation of the early anorthositic crust resulted in deposits of thick ejecta at the edge of the Serenitatis basin, in some cases retaining enough heat to form a cumulate texture (Jackson and others, 1975). In the massifs, remelting may have taken place within the ejecta. The sculptured hills (hilly and smooth terra) were more likely clumps of ballistic ejecta in which there was no reheating at the depositional site.

The high impact flux of pre-Imbrian time resulted in plains mater-

ials being derived primarily from neighboring highlands through secondary cratering, although some material may have been supplied in part by later, large basin formation.

Impact-induced deep fractures initially formed in the Taurus-Littrow area as a result of the southern Serenitatis impact(s). They consist of radial grabens and high-angle concentric normal faults dipping basinward. The deep fracture that later formed the "Lee-Lincoln" Scarp also may have formed at this time, although the offset at the surface indicates that the latest movement was downthrown to the east.

Imbrian Period.

Although it is likely that the Imbrium impact deposited some ejecta in southeastern Serenitatis, previous estimates have ranged from very thick (Short and Forman, 1972) to moderate (McGetchin and others, 1973) to negligible (Head, 1974a). Both sample information and the morphology of the massifs support the latter interpretation. Morphologically, the massifs resemble the fresh third ring of the Orientale basin, which argues against substantial amounts of Imbrium ejecta. The ages of Apollo 17 highland materials are distinct from Apollo 16 ages (probable Imbrium ejecta). Imbrium ejecta may, however, be present as a thin veneer on plains materials (e.g. within the crater Littrow).

The Imbrium impact may have affected the southeastern Serenitatis region another way. Scott and others (1972) and Head (1974a) suggested that the uplift of the massifs was due to reactivation of fractures radial to both Serenitatis and Imbrium. The present investigation does not refute these ideas. However, it may be possible that isostatic rise

of low density crust may provide additional means of vertical movement. The eastern dip of plains materials in the crater Littrow and nearby areas suggests at least 200-300 m (up to 700 m: Muehlberger, 1974) of differential uplift of the highlands. This value should be considered a minimum, however, because the northern highlands were subject to a regional rather than "massif-type" uplift.

Major depositional events of early Imbrian time were 1) repeated emplacement of relatively high Ti mare basalt and accompanying pyroclastics in the Taurus-Littrow area, and 2) concurrent development of the volcanic-type ridges through extrusion. Morphological characteristics of basalts in this area support an Arkani-Hamed (1973) type of model; that of initial mare basalts having their source at the periphery of the basin caused by thermal blanketing of the region by thick, hot ejecta. Subfloor basalts erupted through radial and concentric fissures; and flowed basinward. About 1.5 km of basalt was emplaced in the radial valleys, and the amount in the deeper basin is unknown, but ponding may have played a major factor (Young, 1975). Later, basalts of the dark annulus were deposited (3.7-3.8 b.y.), but these were thinner units of lower Ti content, totalling only 600-800 m thick.

Deformation associated with the downdropping of the central basin (stage 2 deformation of Muehlberger, 1974) was confined within the Imbrian Period. Arcuate rilles formed by stretching of the mare across the Serenitatis-Tranquillitatis boundary occured prior to deposition of the last two mare units of the dark annulus. Additional prominent arcuate and northeast-trending rilles in the dark mantle and hummocky highlands (Fossae Littrow) were also formed at this time, as grabens related to the subsidence of the basin during Imbrian mare emplacement.

Flooding of the rilles by later Eratosthenian-Imbrian mare indicates that formation of these rilles was also confined largely to Imbrian time. Estimates of the amount of downdropping of the central mare from ALSE suggest 500-600 m, but near Promontorium Acherusia (southwest of the map area), the mare outside the second ring is 1100 m higher than the dark annulus within the ring. This break in mare level becomes more subtle to the east, and finally, near Brackett, the slope of the dark annulus is gentle (1.8°). Arcuate rilles farther south of the dark annulus-central mare contact are continuous in highlands terra in the Promontorium Acherusia area, thus suggesting a deeper source for these rilles rather than a surface stretching of the mare crust, and they may be related to pre-Imbrian impacts in northern Tranquillitatis.

As noted by Muehlberger(1974), the slope of the dark annulus towards the basin was well established by the time of deposition of unit (Im_2, however, the present slope of the mare (gradient = 0.015; (LTO 42C3; Edition 2; February, 1975) was interpreted to be greater than the initial slope in that study. A comparison with Imbrium flows (Schaber, 1973a; 1973b) indicates that they occurred on gradients of about 0.003 (LTO 40A4), but subsequent ridge formation and associated tectonism (Schaber, 1973b) may have modified the original slope in that area. Therefore, although a small surface downwarping exists in the southeastern portion of the Eratosthenian-Imbrian mare, lack of arcuate rilles in both this unit, and the latest Imbrian dark annulus unit indicates that post-Imbrian downwarping of the basin was relatively minor.

Eratosthenian Period.

Towards the end of the Imbrian or beginning of Eratosthenian Periods (3.2 - 3.3 b.y.), emplacement of the last dark annulus unit (EImb) occurred. This mare unit is unique in that it compositionally resembles the dark annulus materials, but surface age-dating suggests a time of formation closer to that of the central mare (EIm). Although the unit may have formed as a discrete flow or flows originating within the Serenitatis basin, it is also possible that the unit represents a zone of vertical mixing between the dark annulus and central mare. Studies of the basin-wide distribution and characteristics of the unit will help explain its origin.

During early to middle Eratosthenian time, radial and concentric arches and ridges of the central mare formed, most likely as folds and faults in surface basalt units above deeper, impact-induced fracture systems. Relatively minor subsidence of the eastern and southeastern parts of the basin was accompanied by the formation of the sharper, north-trending rilles north of Clerke. Uplift of the massifs and highland areas near Littrow may have aided in providing the E-W tension necessary for rille formation.

At the end of the Eratosthenian Period, the large impacts producing Plinius (south of the map area) and Dawes took place. These impacts excavated highland material from beneath the dark annulus basalts, and obscured stratigraphic relations within the annulus.

Copernican Period.

Primary and secondary cratering continued to modify the southeastern Serenitatis region throughout the Copernican Period, and the only

major event of that period was the emplacement of the light mantle near the Apollo 17 site. Both Howard (1973) and Head (1975) have presented arguments supporting an avalanche mode of formation for the mantle, while Lucchitta (1975b) has supported an origin by ejecta from secondary craters of Tycho. With the lack of a cushioning atmosphere and effective means of transport, it seems more likely that the light mantle was formed by ballistic secondary ejecta rather than some sort of debris flow phenomenon.

Conclusions

Stratigraphy.

Results of correlations among earth-based and orbital geochemical data, lunar sample information, and Apollo photographs are summarized in the geologic map of southeastern Serenitatis (Plate 1). In addition, the following observations have been made as a result of this study:

1) Imbrian-age dark annulus materials surrounding the central Serenitatis basin are made up of three main units, and are composed of basalt with a high TiO_2 percent (7-8%). Apollo Lunar Sounder and X-ray Fluorescence data both indicate a total thickness of 600-800 m.

2) Extension of topographic slopes and Lunar Sounder data indicate that the dark annulus materials continue beneath the central mare at a depth of about 1 km.

3) The age sequence of mare basalts is paralleled by a corresponding decrease in the Ti content. Crater-age dating indicates deposition in two major episodes; Imbrian-age mare has a high Ti content (7-8%), whereas Eratosthenian-Imbrian mare varies from 2% to 8% Ti.

4) Precision crater size-frequency analysis coupled with crater-age dating determinations provide a valuable means of objectively defining a D_L value. The minimum counting area for age determinations that are compatible with visual estimates is 200 km^2.

Eratosthenian-Imbrian Boundary. The mapping of mare units outside the Imbrian basin has been impeded by the lack of agreement on both the absolute and relative age of the base of the Eratosthenian Period. As noted by Wilhelms (1970, p. 23), the type area (the crater Eratosthenes) is not well suited for age determinations because it is obscured by rays from Copernicus. The top of the Imbrian Period has also been informally regarded as the top of the mare material between Eratosthenes and Archimedes (Wilhelms, 1970, p. 36). In addition, Mutch (1972, p. 353) puts the Eratosthenian-Imbrian boundary at 3.2 b.y.; El-Baz (1975) at 3.3 b.y.; and Head (1976) at 3.0 b.y.

The use of the D_L method of relative age dating provides one solution to the problem, but not all lunar stratigraphers agree where to define the D_L boundary. Data of the present study indicate D_L values of Eratosthenes that range from 200 to 280 m, corresponding to absolute ages of from 3.0 to 3.5 b.y. Consequently, it is doubtful that the boundary can be defined very accurately from the crater Eratosthenes. A widespread class of mare basalts (D_L values from 200 to 260 m: Boyce, 1975) have ages that approximate that of Eratosthenes, and it is doubtful that many of these units have superposition relations that will allow separation into the Eratosthenian or Imbrian Periods. Later analysis and crater studies of the eastern Imbrium area may slightly change the range of D_L values associated with mare near Eratosthenes, and it is therefore suggested that future age assignments be supplemented by values of D_L where possible.

Structure.

Aided by the stratigraphic sequence of highland and mare units, the

structural features of southeastern Serenitatis have been separated into those that were impact-produced and those that were related to later basin deformation. At present, the following conclusions can be drawn:

1) The revised ring structure of the southern Serenitatis basin (Wolfe and Reed, 1976) is supported by the present mapping, although topographic considerations indicate a more complex basin than would be suggested by analogy with Orientale.

2) The arcuate graben rilles of the dark annulus materials formed entirely within the Imbrian Period, as evidenced by superposition relations among the basalt units. N-S oriented linear rilles north of Clerke probably formed in late Imbrian to early Eratosthenian time, and may be related to uplift of the eastern rim of the basin.

3) No single origin was found that would account for all the morphologic features of mare ridges and arches. Within the map area, they have most likely originated as surface folds and faults above deeper, impact-induced fractures, flow fronts, and small volcanic extrusions.

4) The location and morphology of small surficial volcanic features suggests that in the southeastern Serenitatis region, early basaltic flooding originated peripheral to the basin, and then flowed inwards towards the basin.

5) The slight shoulder in the Serenitatis mascon (Figure 14-3 in Sjogren and others, 1973) may be explained by the trough in the southeastern part of the Serenitatis basin, and resultant ponding of early mare basalts.

6) Photogeologic data of the present study support the theory that

the lunar mantle has become increasingly viscous with time (Phillips and others, 1976), and further suggest that most of the deep crustal response was confined to Imbrian time.

APPENDIX I

ORBITAL IMAGERY OF SOUTHEASTERN SERENITATIS

Two Lunar Orbiter and two Apollo orbital spacecraft have provided a total of 589 frames of southeastern Mare Serenitatis, or about 2.5% of the total lunar orbital imagery. Together with earth-based photography from the Consolidated Lunar Atlas (Kuiper and others, 1967), this imagery provides an excellent data base for geologic mapping of southeastern Serenitatis. Sun elevation varies from near-terminator on Apollo's 8 and 17 to almost 90° on Apollo 15 photographs. In addition to the frames listed here, there is also 16 mm movie film of the descent and ascent of the Apollo 17 lunar module from the Taurus-Littrow valley.

Earth-Based Photographs

N 5818	C 2499
C 687	C 2544
C 2202	C 1487

Lunar Orbiter Imagery

Orbiter IV (high resolution)	Orbiter V (med. and high resolution)
78H2	66
78H3	67
85H2	68
85H3	69
	70

Apollo 8

AS 8-13-2334 through 2351

Apollo 15

Mapping Camera Frames

0390 - 0400	1516 - 1524
0562 - 0572	1652 - 1661
0832 - 0841	1794 - 1803
0969 - 0979	1930 - 1940
1110 - 1121	2026 - 2033
1400 - 1410	2140 - 2145

Panoramic Camera Frames (forward frame numbers)

9286 - 9310

9546 - 9572

9860 - 9884

Hasselblad Camera Frames

81 - 10908	88 - 11990
81 - 10909	88 - 11991
81 - 10945	91 - 12390
87 - 11695	91 - 12398
87 - 11696	91 - 12399
87 - 11704 through 11714	94 - 12800 through 12809
	94 - 12845 through 12847

Apollo 17

Mapping Camera Frames

0304 - 0313	0444 - 0453

Apollo 17 Mapping Camera Frames (continued)

0593 - 0603
0791 - 0800
0936 - 0944
1216 - 1225
1497 - 1510
1653 - 1661
1800 - 1809
2084 - 1093
2247 - 2256
2408 - 2415
1683 - 1693
2877 - 2886

Panoramic Camera Frames (forward frame numbers)

2305 - 2329
2476 - 2768 (no stereo pairs for last 4 frames)
2891 - 2900 (no stereo pairs)
3010 - 3035 (no stereo pairs for last 4 frames)

Hasselblad Camera Frames

139 - 21277 through 21282
147 - 22464 through 22467
148 - 22770
149 - 22874 through 22876
150 - 23000 through 23027
150 - 23059 through 23069
151 - 23217
151 - 23218
151 - 23250 through 23255
151 - 23262 through 23264
153 - 23486 through 23495
153 - 23498
153 - 23501 through 23503
153 - 23509
153 - 23510
154 - 23602 through 23612
154 - 23615
154 - 23618 through 23623
154 - 23626
154 - 23627

Nikon Camera Frames

159 - 23923 through 23927

APPENDIX II

DESCRIPTION OF MAP UNITS

Crater Materials

Cc_1 - Cc_3 Crater materials

Undifferentiated materials of 1 - 5 km craters, including crater floor, slope and rim materials. Cc_1 craters are most subdued with no sharp distinction between interior slope and floor, and have a subdued rim. Cc_2 craters are sharper, the floor is partly visible, and the limits of ejecta are more distinct from surrounding terrain; in the central mare and parts of the dark annulus (EIm and EImb), they have bright rims. Cc_3 craters have distinct floors, fresh appearing rims and ejecta patterns, and may exhibit bright rays.

Primary impact craters of Copernican age; Cc_1 craters are oldest, and Cc_3 craters are the youngest (classification after Trask, 1971).

Csc Satellitic crater materials

Undifferentiated materials (including crater floor, wall and rim materials) of small (less than 3 km) craters and aligned groups of craters that have irregular rims and asymmetric ejecta patterns. Usually associated with bright rays.

Satellitic impact craters resulting from secondaries of Coper-

nican-age craters. North to northeast orientation of many of the craters suggests an origin from the craters Menelaus (southwest of map area) and possibly Tycho (much farther southwest of map area).

Ccl Crater cluster material

Irregular groups of small (less than 3 km) craters that show no prominent alignment; individual craters have symmetric rims and ejecta patterns. Craters have subdued rims and smooth slopes where superposed on dark mantle material (Imd).

Possible secondary impact craters formed by ballistic ejecta from distant craters. Clusters near Apollo 17 site may have originated from Tycho (Lucchitta, 1975b).

Ccf Crater floor

Low, rounded, small hills (about 1 km diameter) and intervening smooth surface on the floor of the 10 km crater Fabbroni.

Shock melted and brecciated rock produced by impact; may include talus from interior wall of crater (Ccw).

Ccw Crater wall

Smooth, high albedo interior walls of craters greater than 5 km.

Shocked and brecciated rock produced by impact; high albedo typical of steep, mass-wasted slopes.

Cce Crater ejecta

Radially textured, hummocky to smooth material surrounding 7

and 10 km craters Clerke and Fabbroni. Material has slightly higher albedo than surrounding terrain, and subdues adjacent topography.

Radial ejecta from early Copernican-age impact craters.

Ec Crater materials

Undifferentiated crater floor, wall and ejecta of subdued craters with indistinct rims and ejecta gradational with surrounding terrain.

Primary impact craters of Eratosthenian age (classification after Trask, 1971).

Esc Satellitic crater materials

Undifferentiated materials of small (less than 3 km) craters and aligned groups of craters with irregular rims and asymmetric ejecta patterns. More degraded appearance than Copernican craters (Csc).

Secondary impact craters and deposits of Eratosthenian age.

Ecf Crater floor material

Dark, swirled material in the floor of Dawes with numerous ridges and gullies concentric to crater wall; abundant 15 - 20 m blocks on surface.

Mixture of impact breccias, slumped wall material (Ecw) and possible impact melt (Dawes is assigned a late Eratosthenian age on the basis of visual albedo of ejecta).

Ecw Crater wall material

High albedo, interior crater wall material of Dawes and Plinius in southwest portion of map area. Interior rim of Dawes exhibits a dark band in the upper 300 m of its rim.

Brecciated basalts and highland materials (in Plinius) produced by impact.

Ece Crater ejecta

Hummocky to radially lineated material surrounding craters larger than 5 km. Color composite photographs indicate a very blue color on the eastern side of Dawes, and reddish to the west of Dawes and surrounding Plinius.

Impact-modified basalt (blue) and highland material (reddish) ejected from Eratosthenian-age craters.

Ic Crater material

Undifferentiated rim and floor deposits of highly degraded craters in highland regions. Rim materials merge with surrounding terrain, and have numerous superposed craters.

Primary impact craters of Imbrian age (classification after Trask, 1971).

Icf Crater floor material

Low albedo, hummocky to smooth material on floor of Vitruvius and 9 km crater at southern margin of map. Vitruvius appears partially covered by dark mantle, and contains N-S and E-W trending troughs 1-2 km wide.

Floor of Imbrian impact crater; floor of Vitruvius is possibly volcanically modified and covered by later pyroclastic deposits.

Icw Crater wall material

Interior slope of Vitruvius and smaller crater; albedo higher than surrounding crater units; includes hummocky material at base of slope in Vitruvius.

Slumped and faulted interior wall and talus deposits of Imbrian age impact craters.

Ice Crater rim material

Rim material of Vitruvius and extremely degraded rims of two smaller craters; numerous superposed smaller craters and irregular rim crest for Vitruvius.

Partially slumped and faulted rim of Imbrian age impact craters.

Terra Materials

Cb Bright mantle

Small (about 25 km^2) patch of very high albedo material that partially subdues local topography. Has serrate northern margin and is bounded on the south by a massif (pItm).

Samples from Apollo 17 indicate deposition between 15 and 95 m.y. ago (Reed and Wolfe, 1975). Unit is composed of anorthositic gabbro from the massif, emplaced predominantly as ejecta from secondary craters (Lucchitta, 1975b).

Imp Mare or plains material

Smooth material with both albedo and crater density intermediate between mare and plains materials; occurs at boundary of hilly terra and mare units.

Either basaltic mare material or local ejecta. May be a mixture of these lithologies.

IpIp Plains material

Smooth, cratered surface that fills depressions and older craters; similar to mare material, but has a higher visual albedo and occurs in topographically higher areas. Material in Littrow crater and depression to the south slopes gently (1.2°- 1.4°) to the east. May be subdued by darker material in some areas.

Mixture of local impact ejecta and possibly old mare material.

May contain or be covered by small amount of fine Imbrium ejecta.

IpIhs Hilly and smooth terra

Smooth, rounded hills and intervening patches of cratered terra. Albedo and color data similar to hilly terra unit (IpIh), and unit is differentiated on the basis of higher crater density than mare or plains units, and lower topographic position than hilly terra.

Ejecta predominantly from the Serenitatis excavation, with lower smooth areas filled in by ejecta from local impacts. Most likely a mixture of hummocky Serenitatis ejecta and plains material.

IpIh Hilly terra

Low, round to slightly angular, grooved and hummocky hills with a highly cratered surface east and northeast of massifs (pItm). Individual hills generally 2-5 km in diameter. May be masked by darker material in the Littrow area. Visual albedo intermediate (0.10 - 0.11; Pohn and others, 1970) and unit is reddish on color composite photographs. Unit has higher Al/Si ratio (0.90 - 1.00; Andre and others, 1975) than adjacent dark mare to the west.

Breccias of anorthositic-gabbro composition (Rhodes and others, 1974) emplaced mainly as a result of the Serenitatis impacts. Some amount of Imbrium ejecta may be present, but has not been identified in Apollo 17 samples (Reed and Wolfe, 1975).

pItm Terra massifs

High (4500 - 7000 m) rugged mountains in the Taurus-Littrow

area coincident with the third ring of the southern Serenitatis basin. Mountains have smooth, high albedo slopes at angles of 25° - 30°. Numerous boulders present on slopes and at their bases. Both spectral reflectance data and color composite photographs show enhancement in the red region of the visible spectrum. Gradational boundaries with hilly unit (Iplh).

Large, essentially coherent blocks of norite breccia and anorthositic gabbro (Rhodes and others, 1974) emplaced at about 3.95 - 4.05 b.y. as a result of the impact(s) that produced the southern Serenitatis basin. Blockiness and freshness of slopes indicate that later activity has modified original characteristics of the massifs.

Mare Materials

Imd Dark mantle material

Low visual albedo, dark blue-grey (El-Baz and Evans, 1973) material at southeast edge of Serenitatis basin, occupying valleys between highland massifs (pItm). Material is very blue spectrally, and is a poor radar (3.8 cm) reflector (Pieters and others, 1973). Superposed craters are extremely subdued, and small, fresh-appearing craters have no bright haloes except for those adjacent to the highlands. Contains numerous arcuate, and a few small sinuous rilles.

Major mare unit sampled on Apollo 17; returned samples and geologic investigation of the landing site indicate a relatively thick (15 - 30 m) layer of mixed orange and black glassy spheres and basaltic regolith. This unit overlies Ti-rich basalt similar to that of the Apollo 11 site (Cooper and others, 1974; Muehlberger and others, 1973). Deposited as basalt flows at 3.7 - 3.9 b.y. (Tera and others, 1974a), and subsequent pyroclastics possibly extending as young as 3.5 b.y. (Tera and Wasserburg, 1976).

Im_1 Mare basalt

Smooth, northwest-sloping dark blue-gray (El-Baz and Evans, 1973) unit forming major part of dark annulus at boundary between Mare Serenitatis and Mare Tranquillitatis. Color difference photographs indicate a blue color similar to that of Mare Tranquilli-

tatis. Visual albedo (0.085 - 0.096) not as low as dark mantle, but is lower than mare material of central Serenitatis. Numerous rilles and circular depressions are aligned in an arc to the southern Serenitatis basin. Topographically higher than other mare units of the Serenitatis basin except for dark mantle material (Imd).

Relatively high Ti (7-8%) basalt; on the basis of crater morphology dating, unit is slightly younger (3.7-3.8 b.y.) than the basaltic material of the dark mantle.

Im_2 Mare basalt

Smooth plain of material sloping more gently than unit Im_1 towards the Serenitatis basin. Slightly higher visual albedo and less blue than Im_1, but continues as part of dark blue-grey annulus surrounding Mare Serenitatis. Numerous slightly sinuous to straight rilles approximately 300-500 m across trend downslope into the basin.

Extrusive basalts, most likely originating in Tranquillitatis. Unit occupies shallow valley between Dawes and Mons Argaeus.

Im_3 Mare basalt

Smooth, dark blue grey patch of material with lobate north edge abutting against the more widespread dark annulus of Mare Serenitatis (EImb). Surface has slightly higher visual albedo than units Im_1 or Im_2, and is slightly less blue on color composite photographs. Scarp at northeast boundary shows that this unit is topographically higher than Im_2, and appears to be embayed by EImb. Contains no rilles, and has a slightly lower crater density than

Im_1 or Im_2, although crater frequency is obscured by Dawes ejecta. Surface is very smooth and slopes gently northward to the lowest part of the Serenitatis mare floor. Southernmost relations are obscured by ejecta from Dawes.

Latest Imbrian age volcanic flow; flooded arcuate rilles and flowed downslope into Mare Serenitatis. Probably is the result of a local extrusive volcanic episode of a limited amount of basalt.

Imt_1 Mare basalt

Smooth dark material similar to Im units, but has slightly lower visual albedo (0.085-0.096) and appears slightly redder on color composite photographs. Unit is bounded on the north by a northeast trending, relatively straight scarp. Contains numerous north to northwest trending straight rilles.

High Ti (7-8%; Johnson and others, 1975) Imbrian age basalt. Superposition relations with Unit Im_2 suggest a slightly younger age, although crater age dating indicates an Imbrian age (Boyce and others, 1974).

Imt_2 Mare basalt

Smooth material west of Vitruvius; similar to unit Imt_1, but has lower visual albedo (0.090 - 0.102), and is topographically higher. Differentiated from Imt_1 primarily on albedo; boundary with Imt_1 very gradational.

Imbrian age mare basalt with slightly higher Ti content than Imt_1; blanketed northeast of Vitruvius by dark mantle (Imd)unit.

Id Domical mare

Three small, finely textured patches of smooth, dark material that occur southwest of Mons Argaeus along a north-northwest line. Two of the areas have small, dark domes with summit depressions, and the northernmost area contains a slightly irregular depression. Material subdues northwest-trending rilles of unit Im_2. Visual albedo and color similar to Im_2.

Local volcanic cinder cones and probable pyroclastic deposits originating from a fissure radial to Mare Serenitatis (Scott, 1973). Unit is younger than Im_2, but relationship with Im_3 is not clear.

EIm Mare basalt

Relatively high visual albedo, smooth plain occupying central part of Mare Serenitatis. Color composite photographs show a dominant red color. Higher radar reflectivity than dark annulus at both 3.8 and 70 cm (Thompson and others, 1974); and characterized as a tan-grey color by orbital observations (El-Baz and Evans, 1973). Embays darker mare materials north of Mons Argaeus.

Major extensive basalt of central Mare Serenitatis; most likely a basalt of low Ti (2-3%; Pieters and McCord, 1975). Crater morphology dating indicates an age equal to, or slightly younger than Eratosthenes.

EImb Mare basalt

Innermost ring of dark annulus material at edge of the central mare. Unit is 10-30 km wide, has lower visual albedo (0.085-0.090)

than central mare, and appears blue in color composite photographs.

Crater morphology dating methods indicate that this unit is the same age as the central mare (Eratosthenian to Imbrian), but color data (Pieters and McCord, 1975) suggest a higher Ti content than unit EIm. Interpreted as either vertical mixture of EIm and Im basalts, or separate lava flow unit originating in the interior of the basin.

REFERENCES

Adams, J. B., Pieters, C., and McCord, T. B., 1974, Orange glass: Evidence for regional deposits of pyroclastic origin on the moon, in Proceedings of the Fifth Lunar Science Conference: Geochim. et Cosmochim. Acta, Suppl. 5, v. 1, p. 171-186.

Adler, I., Trombka, J., Gerard, J., Schmadebeck, R., Lowman, P., Blodgett, H., Yiu, L., Eller, E., Lamothe, R., Gorenstein, P., Bjorkholm, P., Harris, B., and Gursky, H., 1972, X-ray fluorescence experiment: Apollo 15 Preliim. Sci. Rept., NASA SP-289, p. 17-1 - 17-7.

Adler, I., Trombka, J. I., Lowman, P., Schmadebeck, R., Blodget, H., Eller, E., Yiu, L., Lamothe, R., Osswald, G., Gerard, J., Gorenstein, P., Bjorkholm, P., Gursky, H., Harris, B., Arnold, J., Metzger, A., and Reedy, R., 1973, Apollo 15 and 16 results of the integrated geochemical experiment: The Moon, v. 7, p. 487-504.

Andre, C. G., Hallam, M. E., Weidner, J. R., Podwysocki, M. H., Philpotts, J. A., Clark, P. E., and Adler, I., 1975, Correlation of Al/Si X-ray fluorescence data with other remote sensing data from the Taurus-Littrow area, in Proceedings of the Sixth Lunar Science Conference: Geochim. et Cosmochim. Acta, Suppl. 6, v. 3, p. 2739-2748.

Arkani-Hamed, J., 1973, On the thermal history of the moon: The Moon, v. 6, p. 380-383.

———, 1974a, Effect of a giant impact on the thermal evolution of the moon: The Moon, v. 9, p. 183-209.

———, 1974b, Lunar mascons as consequences of giant impacts: The Moon, v. 10, p. 307-322.

Bailey, N. G., and Ulrich, G. E., eds., 1975, Apollo 17 voice transcript pertaining to the geology of the landing site, Flagstaff, Ariz., U. S. Geol. Survey, 361p.

Baldwin, R. B., 1963, The measure of the moon, Chicago, Univ. Chicago Press, 488p.

Bence, A. E., Delano, J. W., Papike, J. J., and Cameron, K. L., 1974, Petrology of the highlands massifs at Taurus-Littrow: An analysis of the 2-4 mm soil fraction, in Proceedings of the Fifth Lunar Science Conference: Geochim. et Cosmochim. Acta, Suppl. 5, v. 1, p. 785-827.

Bowin, C., Simon, B., and Wollenhaupt, W. R., 1975, Mascons: A two-body solution: Jour. Geophys. Research, v. 80, p. 4947-4955.

Boyce, J. M., and Dial, A. L. Jr., 1973, Relative ages of some near-side mare units based on Apollo 17 metric photographs: Apollo 17 Prelim. Sci. Rept., NASA SP-330, p. 29-26 - 29-28.

Boyce, J. M., Dial, A. L., and Soderblom, L. A., 1974, Ages of the lunar nearside light plains and maria, in Proceedings of the Fifth Lunar Science Conference: Geochim. et Cosmochim. Acta, Suppl. 5, v. 1, p. 11-23.

Boyce, J. M., and Dial, A. L. Jr., 1975, Relative ages of flow units in Mare Imbrium and Sinus Iridum, in Proceedings of the Sixth Lunar Science Conference: Geochim. et Cosmochim. Acta, Suppl. 6, v. 3, p. 2585-2595.

Boyce, J. M., 1975, Chronology of the major flow units in the western nearside maria (abs.), in Origins of Mare Basalts: Houston, Texas, Lunar Science Institute, p. 11-14.

———, 1976, Relative ages of flow units in the lunar nearside maria (abs.), in Lunar Science VII, Houston, Texas, Lunar Science Institute, p. 85-87.

Brown, W. E. Jr., 1972, Lunar subsurface exploration with coherent radar: The Moon, v. 4, p. 113-127.

Brown, W. E. Jr., Adams, G. F., Eggleton, R. E., Jackson, P., Jordan, R., Kobrick, M., Peeples, W. J., Phillips, R. J., Porcello, L. J., Schaber, G., Sill, W. R., Thompson, T. W., Ward, S. H., and Zelenka, J. S., 1974, Elevation profiles of the moon, in Proceedings of the Fifth Lunar Science Conference: Geochim. et Cosmochim. Acta, Suppl. 5, v. 3, p. 3037-3048.

Bryan, W. B., 1973, Wrinkle-ridges as deformed surface crust on ponded mare lava, in Proceedings of the Fourth Lunar Science Conference: Geochim. et Cosmochim. Acta, Suppl. 4, v. 1, p. 93-106.

Burns, A. A., 1969, Diffuse component of lunar radar echoes: Jour. Geophys. Research, v. 74, p. 6553-6566.

Carr, M. H., 1966, Geologic map of the Mare Serenitatis region of the moon: U. S. Geol. Survey Misc. Inv. Map I-489.

Carr, M. H., Howard, K. A., and El-Baz, F., 1971, Geologic maps of the Apennine-Hadley region of the moon: U. S. Geol. Survey Misc. Inv. Map I-733.

Carr, M. H., 1972, Sketch map of the region around candidate Littrow Apollo landing sites: Apollo 15 Prelim. Sci. Rept., NASA SP-289, p. 25-63 - 25-65.

Casella, C. J., 1976, Evolution of the lunar fracture network: Geol. Soc. America Bull., v. 87, p. 226-234.

Charette, M. P., McCord, T. B., Pieters, C., and Adams, J. B., 1974, Application of remote spectral reflectance measurements to lunar geology classification and determination of Titanium content of lunar soils: Jour. Geophys. Research, v. 79, p. 1605-1613.

Charette, M. P., Adams, J. B., Soderblom, L. A., Gaffey, M. J., and McCord, T. B., 1976, Age-color relationships in the lunar highlands (abs.), in Lunar Science VII: Houston, Texas, Lunar Science Institute, p. 132-134.

Cooper, M. R., Kovach, R. L., and Watkins, J. S., 1974, Lunar near-surface structure: Rev. Geophys. Space Phys., v. 12, p. 291-308.

DeHon, R. A., 1975, An isopach map of eastern mare basalts (abs.), in Origins of Mare Basalts: Houston, Texas, Lunar Science Institute, p. 29-31.

———, 1976, Geologic structure of the eastern mare basins (abs.), in Lunar Science VII: Houston, Texas, Lunar Science Institute, p. 184-186.

El-Baz, F., 1972, The cinder field of the Taurus Mountains: Apollo 15 Prelim. Sci. Rept., NASA SP-289, p. 25-66 - 25-71.

El-Baz, F. and Evans, R. E., 1973, Observations of Mare Serenitatis from lunar orbit and their interpretation, in Proceedings of the Fourth Lunar Science Conference: Geochim. et Cosmochim. Acta, Suppl. 4, v. 1, p. 139-147.

Eppler, D., and Heiken, G., 1975, Lunar crater chains of non-impact origin, in Proceedings of the Sixth Lunar Science Conference: Geochim. et Cosmochim. Acta, Suppl. 6, v. 3, p. 2571-2583.

Fastie, W. G., Feldman, P. D., Henry, R. C., Moos, H. W., Barth, C. A., Thomas, G. E., Lillie, C. F. and Donahue, M., 1973, Ultraviolet spectrometer experiment: Apollo 17 Prelim. Sci. Rept., NASA SP-330, p. 23-1 - 23-10.

Greeley, R., and Gault, D. E., 1970, Precision size-frequency distribution of craters for 12 selected areas of the lunar surface: The Moon, v. 2, p. 10-77.

Green, J., and Short, N. M., eds., 1971, Volcanic landforms and surface features; A photographic atlas and glossary: New York, Springer-Verlag, 519p.

Hartmann, W. K., and Wood, C. A., 1971, Moon: Origin and evolution of multi-ring basins: The Moon, v. 3, p. 3-78.

Hartmann, W. K., 1972, Paleocratering of the moon: Review of post-Apollo data: Astrophys. and Space Science, v. 17, p. 48-64.

———, 1973, Ancient lunar mega-regolith and subsurface structure: Icarus, v. 18, p. 634-636.

Head, J. W., 1974a, Morphology and structure of the Taurus-Littrow highlands (Apollo 17): Evidence for their Origin and Evolution: The Moon, v. 9, p. 355-395.

———, 1974b, Orientale multi-ringed basin interior and implications for the petrogenesis of lunar highland samples: The Moon, v. 11, p. 327-356.

———, 1975, Processes of lunar crater degradation: Changes in style with geologic time: The Moon, v. 12, p. 299-329.

Heiken, G. H., McKay, D. S., and Brown, R. W., 1974, Lunar deposits of possible pyroclastic origin: Geochim. et Cosmochim. Acta, v. 38, p. 1703-1718.

Hinthorne, J. R., and Conrad, R. L., 1976, Comparison of Pb-Pb with Argon ages in highlands fragment 78503, 13, A (abs.), in Lunar Science VII: Houston, Texas, Lunar Science Institute, p. 373-375.

Hodges, C. A., 1973, Mare ridges and lava lakes: Apollo 17 Prelim. Sci. Rept., NASA SP-330, p. 31-12 - 31-21.

Howard, K. A., 1973, Avalanche mode of motion: Implications from lunar examples: Science, v. 180, p. 1052-1055.

Howard, K. A., and Muehlberger, 1973, Lunar thrust faults in the Taurus Littrow region: Apollo 17 Prelim. Sci. Rept., NASA SP-330, p. 31-22 - 31-25.

Howard, K. A., Carr, M. H., and Muehlberger, W. R., 1973, Basalt stratigraphy of southern Mare Serenitatis: Apollo 17 Prelim. Sci. Rept., NASA SP-330, p. 29-1 - 29-12.

Howard, K. A., Wilhelms, D. E., and Scott, D. H., 1974, Lunar basin formation and highland stratigraphy: Rev. Geophys. and Space Phys., v. 12, p. 309-327.

Hubbert, M. K., 1951, Mechanical basis for certain familiar geologic structures: Geol. Soc. America Bull., v. 62, p. 355-372.

Hulme, G., 1973, Turbulent lava flow and the formation of lunar sinuous rilles: Modern Geology, v. 4, p. 107-117.

Jackson, E. D., Sutton, R. L. and Wilshire, H. G., 1975, Structure and petrology of a cumulus norite boulder sampled by Apollo 17 in Taurus Littrow valley, the moon: Geol. Soc. America Bull., v. 86, p. 433-442.

Jessberger, E., Kirsten, T., and Standacher, T., 1976, Ages of plutonic clasts in consortium breccia 73215 (abs.), in Lunar Science VII: Houston, Texas, Lunar Science Institute, p.431-433.

Johnson, T. V., Matson, D. L., Phillips, R. J., and Saunders, R. S., 1975, Vidicon spectral imaging: Color enhancement and digital maps, in Proceedings of the Sixth Lunar Science Conference: Geochim. et Cosmochim. Acta, Suppl. 6, v. 3, p. 2677-2688.

Killpack, T. J., 1975, Apollo 17 specular power monitor data - Passive mode: M. S. Thesis, Univ. Utah, Salt Lake City, 237 p.

Kirsten, T., Horn, P. and Heymann, D., 1973, Chronology of the Taurus-Littrow region I: Ages of two major rock types from the Apollo 17 site: Earth Planet. Sci. Letters, v. 20, p. 125-130.

Kirsten, T. and Horn, P., 1974, Chronology of the Taurus-Littrow region III: Ages of mare basalts and highlands breccias and some remarks about the interpretation of lunar highland rock ages, in Proceedings of the Fifth Lunar Science Conference: Geochim. et Cosmochim. Acta, Suppl. 5., v. 2, p. 1451-1475.

Kobrick, M., 1976, Lunar shape and topography from the Apollo Lunar Sounder (abs.), in Lunar Science VII: Houston, Texas, Lunar Science Institute, p. 454-456.

Kopal, Z., and Carder, R. W., 1974, Mapping of the moon: Past and Present: Dordrecht, Netherlands, Reidel Publishing Co., 237p.

Kuiper, G. P., Whitaker, E. A., Strom, R. G., Fountain, J. W., and Larson, S. M., 1967, Consolidated lunar atlas, Suppl. 3 and 4 to the USAF photographic lunar atlas: Ariz. Univ. Lunar and Planetary Lab. Contr., No. 4, 24p., 226 photographs.

LSPET (Lunar Sample Preliminary Examination Team), 1973, Preliminary examination of lunar samples: Apollo 17 Prelim. Sci. Rept., NASA SP-330, p. 7-1 - 7-46.

Lucchitta, B. K., 1973, Geologic setting of the dark mantling material in the Taurus-Littrow region of the moon: Apollo 17 Prelim. Sci. Rept., NASA SP-330, p. 29-13 - 29-25.

Lucchitta, B. K., and Schmitt, H. H., 1974, Orange material in the Sulpicius Gallus Formation at the southwestern edge of Mare Serenitatis, in Proceedings of the Fifth Lunar Science Conference: Geochim. et Cosmochim. Acta, Suppl. 5, v. 1, p. 223-234.

Lucchitta, B. K., 1975a, Dark mantles on the moon, A review (abs.), in Origins of Mare Basalts: Houston, Texas, Lunar Science Institute, p. 104-106.

——, 1975b, Tycho and the Apollo 17 landing site (abs.): EOS, v. 56, p. 389.

Lucchitta, B. K., and Sanchez, A. G., 1975, Crater studies in the Apollo 17 region, in Proceedings of the Sixth Lunar Science Conference: Geochim. et Cosmochim. Acta, Suppl. 6, v. 3, p. 2427-2441.

Lucchitta, B. K., 1976, Analysis of scarps on the rim of Mare Serenitatis (abs.), in Lunar Science VII: Houston, Texas, Lunar Science Institute, p. 507-508.

Lucke, R. L., Henry, R. C., and Fastie, W. G., 1974, Far-ultraviolet mapping from Apollo 17 (abs.), in Lunar Science V: Houston, Texas, Lunar Science Institute, p. 469-471.

MacDonald, G. A., 1972, Volcanoes: Englewood Cliffs, New Jersey, Prentice-Hall, Inc., 510p.

Maxwell, T. A., El-Baz, F., and Ward, S. H., 1975, Distribution, morphology and origin of ridges and arches in Mare Serenitatis: Geol. Soc. America Bull., v. 86, p. 1273-1278.

May, T. W., Peeples, W. J., Maxwell, T., Sill, W. R., Ward, S. H., Phillips, R. J., Jordan, R., and Abbott, E., 1976, Subsurface layering in Maria Serenitatis and Crisium: Apollo lunar sounder results (abs.), in Lunar Science VII: Houston, Texas, Lunar Science Institute, p. 540-542.

McCord, T. B., Charette, M. P., Johnson, T. V., Lebofsky, L. A., Pieters, C., and Adams, J. B., 1972, Lunar spectral types: Jour. Geophys. Research, v. 77, p.1349-1359.

McCord, T. B., and Adams, J. B., 1973, Progress in remote optical analysis of lunar surface composition: The Moon, v. 7, p. 453-474.

McCord, T. B., Pieters, C., and Feierberg, M. F., 1976, Spectral reflectance maps of the lunar frontside (abs.), in Lunar Science VII: Houston, Texas, Lunar Science Institute, p.512-514.

McGetchin, T. R., Settle, M., and Head, J. W., 1973, Radial thickness variation in impact crater ejecta: Implications from lunar basin deposits: Earth Planet. Sci. Letters, v. 20, p. 226-236.

McGetchin, T. R., Settle, M., and Chouet, B. A., 1974, Cinder cone growth modeled after Northeast Crater, Mount Etna, Sicily: Jour. Geophys. Research, v. 79, p. 3257-3272.

McGill, G. E., 1971, Attitude of fractures bounding straight and arcuate lunar rilles: Icarus, v. 4, p. 53-58.

Melosh, J., 1976, The mechanical stability of very large craters (abs.), in Lunar Science VII: Houston, Texas, Lunar Science Institute, p. 549-551.

Metzger, A. E., Trombka, J. I., Reedy, R. C., and Arnold, J. R., 1974, Element concentrations from lunar orbital gamma-ray measurements, in Proceedings of the Fifth Lunar Science Conference: Geochim. et Cosmochim. Acta, Suppl. 5, v. 2, p. 1067-1078.

Moore, H. J., Hodges, C. A., and Scott, D. H., 1974, Multiringed basins - Illustrated by Orientale and associated features, in Proceedings of the Fifth Lunar Science Conference: Geochim. et Cosmochim. Acta, Suppl. 5, v. 1, p. 71-100.

Muehlberger, W. R., Batson, R. M., Cernan, E. A., Freeman, V. L., Hait, M. H., Holt, H. E., Howard, K. A., Jackson, E. D., Larson, K. B., Reed, V. S., Rennilson, J. J., Schmitt, H. H., Scott, D. H., Sutton, R. L., Stuart-Alexander, D., Swann, G. A., Trask, N. J., Ulrich, G. E., Wilshire, H. G., and Wolfe, E. W., 1973, Preliminary geologic investigation of the Apollo 17 landing site: Apollo 17 Prelim. Sci. Rept., NASA SP-330, p. 6-1 - 6-91.

Muehlberger, W. R., 1974, Structural history of southeastern Mare Serenitatis and adjacent highlands, in Proceedings of the Fifth Lunar Science Conference: Geochim. et Cosmochim. Acta, Suppl. 5, v. 1, p. 101-110.

Muller, P. M., and Sjogren, W. R., 1968, Mascons: Lunar mass concentrations: Science, v. 167, p. 680-684.

Mutch, T. A., 1972, Geology of the moon: A stratigraphic view: Princeton, Princeton Univ. Press, 324p. (second ed.).

Nunes, P. D., Tatsumoto, M., and Unruh, D. M., 1974, U-Th-Pb systematics of some Apollo 17 lunar samples and implications for a lunar basin excavation chronology, in Proceedings of the Fifth Lunar Science Conference: Geochim. et Cosmochim. Acta, Suppl. 5, v. 2, p. 1487-1514.

Nyquist, L. E., Bansal, B. M., Wiesman, H., and Jahn, B. M., 1974, Taurus-Littrow chronology: Some constraints on early lunar crustal development, in Proceedings of the Fifth Lunar Science Conference: Geochim. et Cosmochim. Acta, Suppl. 5, v. 2, p. 1515-1539.

Oberbeck, V. R., 1975, The role of ballistic erosion and sedimentation in lunar stratigraphy: Rev. Geophys. and Space Phys., v. 13, p. 337-362.

Oberbeck, V. R., Horz, F., and Morrison, R. H., 1975, On the origin of the lunar smooth-plains: The Moon, v. 12, p. 19-54.

Olhoeft, V. R., and Strangway, D. W., 1975, Dielectric properties of the first 100 meters of the moon: Earth Planet. Sci. Letters, v. 24, p. 394-404.

Papanastassiou, D. A., and Wasserburg, G. J., 1976, Early lunar differentiates and lunar initial $^{87}Sr/^{86}Sr$ (abs.), in Lunar Science VII: Houston, Texas, Lunar Science Institute, p. 665-667.

Peeples, W. J., Sill, W. R., May, T. W., Ward, S. H., Phillips, R. J., and Jordan, R. L., 1976, Orbital radar evidence for lunar subsurface layering in Maria Serenitatis and Crisium: Preprint, submitted to Jour. Geophys. Research.

Phillips, R. J., Conel, J. E., Abbott, E. A., Sjogren, W. L., and Morton, J. B., 1972, Mascons: Progress toward a unique solution for mass distribution: Jour. Geophys. Research, v. 77, p. 7106-7114.

Phillips, R. J., Adams, G. F., Brown, W. E. Jr., Eggleton, R. E., Jackson, P., Jordan, R., Linlor, W. I., Peeples, W. J., Porcello, L. J., Ryu, J., Schaber, G., Sill, W. R., Thompson, T. W., Ward, S. H., and Zelenka, J. S., 1973, Apollo lunar sounder experiment: Apollo 17 Prelim. Sci. Rept., NASA SP-330, p. 22-1 - 22-26.

Phillips, R. J., Abbott, E. A., Conel, J. E., Johnson, T. V., and Saunders, R. S., 1976, Isostatic adjustment of craters in lunar history (abs.), in Lunar Science VII: Houston, Texas, Lunar Science Institute, p. 688-690.

Pieters, C., McCord, T. B., Zisk, S., and Adams, J. B., 1973, Lunar black spots and the nature of the Apollo 17 landing area: Jour. Geophys. Research, v. 78, p. 5867-5875.

Pieters, C., and McCord, T. B., 1975, Classification and distribution of lunar mare basalt types (abs.), in Origins of Mare Basalts: Houston, Texas, Lunar Science Institute, p. 125-129.

Podwysocki, M. H., Weidner, J. R., Andre, C. G., Bickel, A. L., Liu, R. S., Adler, I., and Trombka, J. I., 1974, The application of trend surface analysis to a portion of the Apollo 15 X-ray fluorescence data, in Proceedings of the Fifth Lunar Science Conference: Geochim. et Cosmochim. Acta, Suppl. 5, v. 3, p. 3017-3024.

Pohn, H. A., and Offield, T. W., 1970, Lunar crater morphology and relative age determination of lunar geologic units - Part 1. Classification: U. S. Geol. Sruvey Prof. Paper 700-C, p. C153-C162.

Pohn, H. A., 1971, Geologic map of the Lansberg P region of the moon: U. S. Geol. Survey Misc. Inv. Map I-627.

Pohn, H. A., and Wildey, R. L., 1970, A photoelectric-photographic study of the normal albedo of the moon: U. S. Geol. Survey Prof. Paper 599-E, p. E1-E20.

Pohn, H. A., Wildey, R. L., and Sutton, G. E., 1970, Albedo map of the moon: in U. S. Geol. Survey Prof. Paper 599-E, Plate 1.

Porcello, L. J., Jordan, R. L., Zelenka, J. S., Adams, G. F., Phillips, R. J., Brown, W. E. Jr., Ward, S. H., and Jackson, P. L., 1974, The Apollo lunar sounder radar system: Proc. Inst. Electrical and Electronics Engineers, v. 62, p. 769-783.

Reed, V. S., and Wolfe, E. W., 1975, Origin of the Taurus-Littrow massifs, in Proceedings of the Sixth Lunar Science Conference: Geochim. et Cosmochim. Acta, Suppl. 6, v. 3, p. 2443-2461.

Reedy, R. C., Bielefeld, M. J., Trombka, J. I., Metzger, A. E., and Arnold, J. R., 1975, Intermare and intramare comparisons of element concentrations determined by orbital gamma-ray spectroscopy (abs.), in Origins of Mare Basalts: Houston, Texas, Lunar Science Institute, p. 130-134.

Rhodes, J. M., Rodgers, K. V., Shih, C., Bansal, B. M., Nyquist, L. E., Wiesmann, H., and Hubbard, N. J., 1974, The relationship between geology and soil chemistry at the Apollo 17 landing site, in Proceedings of the Fifth Lunar Science Conference: Geochim. et Cosmochim. Acta, Suppl. 5, v. 2, p. 1097-1117.

Roedder, E., and Weiblen, P. W., 1973, Apollo 17 "orange soil" and meteorite impact on liquid lava: Nature, v. 244, p. 210-212.

Schaber, G. G., 1973a, Eratosthenian volcanism in Mare Imbrium: Source of the youngest lava flows: Apollo 17 Prelim. Sci. Rept., NASA SP-330, p. 30-17 - 30-25.

———, 1973b, Lava flows in Mare Imbrium: Geologic evaluation from Apollo orbital photography, in Proceedings of the Fourth Lunar Science Conference: Geochim. et Cosmochim. Acta, Suppl. 4, v. 1, p. 73-92.

Schaeffer, O. A., and Husain, L., 1974, Chronology of lunar basin formation, in Proceedings of the Fifth Lunar Science Conference: Geochim. et Cosmochim. Acta, Suppl. 5, v. 2, p. 1541-1555.

Schmitt, H. H., 1974, Lunar mare color provinces as observed on Apollo 17: Geology, v. 2, p. 55-56.

Scott, D. H., 1972, Geologic map of the Eudoxus quadrangle of the moon: U. S. Geol. Survey Misc. Inv. Map I-705.

Scot , D. H., and Pohn, H. A., 1972, Geologic map of the Macrobius of the moon: U. S. Geol. Survey Misc. Inv. Map I-799.

Scott, D. H., Lucchitta, B. K., and Carr, M. H., 1972, Geologic maps of the Taurus-Littrow region of the moon: U. S. Geol. Survey Misc. Inv. Map I-800, Sheet 1, 1:250,000; Sheet 2, 1:50,000.

Scott, D. H., 1973, Mare Serenitatis cinder cones and terrestrial analogs: Apollo 17 Prelim. Sci. Rept., NASA SP-330, p. 30-7 - 30-8.

——, 1974, The geologic significance of some lunar gravity anomalies, in Proceedings of the Fifth Lunar Science Conference: Geochim. et Cosmochim. Acta., Suppl. 5, v. 3, p. 3025-3036.

Scott, D. H., Diaz, J. M., and Watkins, J. A., 1975, The geologic evaluation and regional synthesis of metric and panoramic photographs, in Proceedings of the Sixth Lunar Science Conference: Geochim. et Cosmochim. Acta, Suppl. 6, v. 3, p. 2531-2540.

Shoemaker, E. M., and Hackman, R. J., 1962, Stratigraphic basis for a lunar time scale, in Kopal, Z., and Mikhailov, Z. K., eds., The Moon, Symposium 14 of the Internat. Astron. Union: London, Academic Press, p. 289-300.

Shoemaker, E. M., Hackman, R. J., and Eggleton, R. E., 1962, Interplanetary correlation of geologic time, in Advances in the Astronautical Sciences, v. 8: New York, Plenum Press, p. 70-89.

Short, N. M., and Forman, M. L., 1972, Thickness of impact crater ejecta on the lunar surface: Modern Geology, v. 3, p. 69-91.

Simonds, C. H., 1975, Thermal regimes in impact melts and the petrology of the Apollo 17 station 6 boulder, in Proceedings of the Sixth Lunar Science Conference: Geochim. et Cosmochim. Acta, Suppl. 6, v. 1, p. 641-672.

Sjogren, W. L., Muller, P. M., and Wollenhaupt, W. R., 1972, S-band transponder experiment: Apollo 16 Prelim. Sci. Rept., NASA SP-315, p. 24-1 - 24-7.

Sjogren, W. L., Wollenhaupt, W. R., and Wimberly, R. N., 1973, S-band transponder experiment: Apollo 17 Prelim. Sci. Rept., NASA SP-330, p. 14-1 - 14-4.

Sjogren, W. L., Wimberly, R. N., and Wollenhaupt, W. R., 1974, Lunar gravity: Apollo 17: The Moon, v. 11, p. 41-52.

Sjogren, W. L. and Wollenhaupt, W. R., 1976, Lunar global figure from mare surface elevations: The Moon, v. 15, p. 143-154.

Soderblom, L. A., 1970, The distribution and ages of regional lithologies in the lunar maria: Ph. D. Dissertation, Calif. Inst. Technology, Pasadena, 139p.

Soderblom, L. A., and Lebofsky, L. A., 1972, Technique for rapid determination of relative ages of lunar areas from orbital photography: Jour. Geophys. Research, v. 77, p. 279-296.

Strain, P., and El-Baz, F., 1975, Sinuous rilles of the Harbinger Mountains region of the moon (abs.), in Lunar Science VI: Houston, Texas, Lunar Science Institute, p. 786-788.

Strom, R. G., 1964, Analysis of lunar lineaments, I: Tectonic maps of the moon: Comm. Lunar and Planetary Lab, v. 2, p. 205-216.

———, 1972, Lunar mare ridges, rings and volcanic ring complexes: Modern Geology, v. 2, p. 133-137.

Stuart-Alexander, D. E., and Howard, K. A., 1970, Lunar maria and circular basins - A review: Icarus, v. 12, p. 440-456.

Tera, F., Papanastassiou, D. A., and Wasserburg, G. J., 1974a, Isotopic evidence for a terminal lunar cataclysm: Earth Planet. Sci. Letters, v. 22, p. 1-21.

———, 1974b, The lunar time scale and a summary of isotopic evidence for a terminal lunar cataclysm (abs.), in Lunar Science V: Houston, Texas, Lunar Science Institute, p. 792-794.

Tera, F., and Wasserburg, G. J., 1976, Lunar ball games and other sports (abs.), in Lunar Science VII: Houston, Texas, Lunar Science Institute, p. 858-860.

Thompson, T. W., Howard, K. A., Shorthill, R. W., Tyler, G. L., Zisk, S. H., Whitaker, E. A., Schaber, G. G., and Moore, H. J., 1973, Remote sensing of Mare Serenitatis: Apollo 17 Prelim. Sci. Rept., NASA SP-330, p. 33-3 - 33-9.

Thompson, T. W., Shorthill, R. W., Whitaker, E. A., and Zisk, E. A., 1974, Mare Serenitatis: A preliminary definition of surface units by remote observations: The Moon, v. 9, p. 89-96.

Thompson, T. W., 1974, Atlas of lunar radar maps at 70 cm wavelength: The Moon, v. 10, p. 51-85.

Trask, N. J., 1971, Geologic comparison of mare materials in the lunar equatorial belt, including Apollo 11 and Apollo 12 landing sites: U. S. Geol. Survey Prof. Paper 750-D, p. D138-D144.

Trombka, J. I., Arnold, J. R., Reedy, R. C., Peterson, L. E., and Metzger, A. E., 1973, Some correlations between measurements by the Apollo gamma-ray spectrometer and other lunar observations, in Proceedings of the Fourth Lunar Science Conference: Geochim. et Cosmochim. Acta, Suppl. 4, v. 3, p. 2847-2853.

Ward, S. H., El-Baz, F., Maxwell, T. A., Peeples, W. J., and Sill, W. R., 1973, Radar descriptions of lunar surface features (abs.): Abstracts with Programs, Geol. Soc. America Ann. Mtng., p. 855.

Whitaker, E. A., 1966, The surface of the moon, in Hess, W. N., Menzel, D. H., and O'Keefe, J. A., eds., The nature of the lunar surface: Proceedings of the 1965 IAU-NASA Symposium: Baltimore, Johns Hopkins, p. 79-98.

Whitaker, E. A., 1972a, Lunar color boundaries and their relationship to topographic features: A preliminary survey: The Moon, v. 4, p. 348-355.

———, 1972b, Mare Imbrium lava flows and their relationship to color boundaries: Apollo 15 Prelim. Sci. Rept., NASA SP-289, p. 25-83 - 25-84.

Wilhelms, D. E., and McCauley, J. F., 1971, Geologic map of the near side of the moon: U. S. Geol. Survey Misc. Inv. Map I-703, Scale 1:1,000,000.

Wise, D. U., and Yates, M. T., 1970, Mascons as structural relief on a lunar 'moho': Jour. Geophys. Research, v. 75, p. 261-268.

Wolfe, E. W., Lucchitta, B. K., Reed, V. S., Ulrich, G. E., and Sanchez, A. G., 1975, Geology of the Taurus-Littrow valley floor, in Proceedings of the Sixth Lunar Science Conference: Geochim. et Cosmochim. Acta, Suppl. 6, v. 3, p. 2463-2482.

Wolfe, E. W., and Reed, V. S., 1976, Geology of the massifs at the Apollo 17 landing site: Jour. Research, U. S. Geol. Survey, v. 4, p. 171-180.

Young, R. A., Brennan, W. J., Wolfe, R. W., and Nichols, D. J., 1973, Analysis of lunar mare geology from Apollo photography, in Proceedings of the Fourth Lunar Science Conference: Geochim. et Cosmochim. Acta, Suppl. 4, v. 1, p. 57-71.

Young, R. A., Brennan, W. J., and Nichols, D. J., 1974, Problems in the interpretation of lunar mare stratigraphy and relative ages indicated by ejecta from small impact craters, in Proceedings of the Fifth Lunar Science Conference: Geochim. et Cosmochim. Acta, Suppl. 5, v. 1, p. 159-170.

Young, R. A., 1975, Mare crater size-frequency distributions: Implications for relative surface ages and regolith development, in Proceedings of the Sixth Lunar Science Conference: Geochim. et Cosmochim. Acta, Suppl. 6, v. 3, p. 2645-2662.

Young, R. A., 1976, Evidence for a shallow regional subsurface discontinuity in southern Mare Serenitatis (abs.), in Lunar Science VII: Houston, Texas, Lunar Science Institute, p. 959-961.

Zisk, S. H., 1970, Radar atlas of the moon: Haystack Observatory, limited circulation.

VITA

Name	Theodore Allen Maxwell
Birthplace	[redacted]
Birthdate	[redacted]
High School	Henry James Memorial High School Simsbury, Connecticut
College 1967-1971	Franklin and Marshall College Lancaster, Pennsylvania
University 1971-1976	University of Utah Salt Lake City, Utah
Degrees 1971 1973	 A.B., Franklin and Marshall College M.S., University of Utah
Professional Organizations	American Geophysical Union Geological Society of America Society of Economic Paleontologists and Mineralogists
Professional Experience	NSF-URP grant, 1970, Franklin and Marshall College; NASA Fellowship Trainee, 1972-1973, University of Utah; Graduate Research Assistant, 1973-1975, University of Utah; Visiting Graduate Fellow, 1976, Lunar Science Institute; Geologist, 1976-present, National Air and Space Museum, Smithsonian Institution